AN ABSTRACT OF THE THESIS OF

Ching-Hsiu Tsai for the degree of Doctor of Philosophy in Genetics presented on February 23, 1993. Title: Characterization of the Role of the 3' Noncoding Region of Turnip Yellow Mosaic Virus RNA

Abstract approved by: Redacted for Privacy

Theo W. Dreher

Turnip yellow mosaic virus (TYMV) is a monopartite positive strand RNA virus whose 6.3 kb genome possesses a 5' m^7GpppG cap structure. The most distinctive feature of the 3' noncoding region is a tRNA-like structure to which valine can be bound enzymatically. A second feature is a potential pseudoknot immediately upstream of the tRNA-like structure. Nucleotide substitutions were introduced into the anticodon loop of the tRNA-like structure and the potential pseudoknot of TYMV RNA to characterize the roles of the 3' noncoding region.

To fully understand the specificity of TYMV RNA valylation and its implication in viral RNA replication, the valylation identity elements recognized in TYMV RNA by wheat germ valyl-tRNA synthetase were determined in *in vitro* aminoacylation experiments. Three nucleotides were identified as major determinants of TYMV RNA valylation. In descending order of contribution to valine identity, these are the middle nucleotide of the anticodon (A56), the 3' anticodon nucleotide (C55), and the 3'-most anticodon loop nucleotide (C53).

Mutant RNAs with substitutions in the anticodon loop were used to investigate the relationship between the *in vitro* valylation of viral RNAs and their *in vivo* replication in Chinese cabbage protoplasts and plants. Only those mutants capable of efficient and complete valylation showed efficient replication in protoplasts and gave rise to systemic symptoms in the whole plants. The observed correlation between *in vitro* valylation and replication *in vivo* was strengthened by the fortuitous isolation of a second-site suppressor mutant. The C57→U57 mutation suppressed both the poor valylation and poor replication in protoplasts resulting from the C55→A55 mutation. These results suggest that the valylation of TYMV RNA *in vivo* is a requisite for its efficient replication.

Experiments were performed to assess whether aminoacylation specifically by valine is required. A potential role for histidylation of TYMV RNA previously suggested by *in vitro* studies with yeast histidyl-tRNA synthetase, was not supported by studies with the wheat germ enzyme. No significant histidylation was found, and TYMV RNA appears to be specifically chargeable by valine in higher plant cells. The replacement of valine by methionine was studied with two mutant RNAs that were deficient in valylation but could be fully charged with methionine by wheat germ methionyl-tRNA

synthetase. The very poor replication of these mutants in protoplasts suggests that the requirement for valylation is specific.

Second site suppressor studies, valuable in clarifying the role of valylation, also provided evidence that a pseudoknot immediately upstream of the tRNA-like structure plays an important role in TYMV replication. Two structural features, the tRNA-like structure and the upstream pseudoknot, are thus important functional elements of the 3' noncoding region of TYMV RNA.

Characterization of the Role of the 3′ Noncoding Region of Turnip Yellow Mosaic Virus RNA

by

Ching-Hsiu Tsai

A THESIS

submitted to

Oregon State University

in partial fulfillment of

the requirements for the

degree of

Doctor of Philosophy

Completed February 23, 1993

Commencement June 1993

APPROVED:

Redacted for Privacy

Professor of Agricultural Chemistry/ Genetics Program in charge of major.

Redacted for Privacy

Director of Genetics Program.

Redacted for Privacy

Dean of Graduate School.

Date thesis is presented February 23, 1993

Prepared by Redacted for privacy

ACKNOWLEDGEMENTS

I would like to express my sincere gratitude to my major advisor Dr. Theo Dreher, who gave me the opportunity to study in his laboratory, and whose support, encouragement and guidance made this research a very valuable educational experience. The most valuable lessons I learned from him are not only how to perform experiments successfully but also how to be a good scientist, how to think logically, how to treat people with kindness and respect. He is not only a good advisor as well as a good friend.

Many thanks go to the colleagues in the laboratory, Dr. Connie Bozarth, Kay Bransom, and Dr. John Weiland, for help in experimental design and discussions about the research.

With sincere appreciation, I would like thank Drs. Henry Schaup, Jo-Ann Leong, John Hays, and Jim Baggett for their suggestions as well as for serving on my committee.

Special thanks go to my loving wife, Gene (Chung-Ying), for her warm love, encouragement, and patience during the years of my graduate studies. Without her inspiration and support, this work would have taken far longer. Especially, she dedicates herself to take good care of our two lovely children, Mimi (Wong-Mi) and Michelle (Wong-Hann).

Finally, I would also like to thank my mother for her concern at a distance from the other side of the earth.

TABLE OF CONTENTS

LIST OF FIGURES

LIST OF APPENDICES FIGURES

LIST OF TABLES

LIST OF APPENDICES TABLES

PREFACE

An edited version of Chapter II of this thesis has been published by Dreher *et al.* (1992) (Biochemistry 31:9183-9189). DNA clone mpT7YSma (wild-type) and its derivatives: TY-G56, TY-U56, TY-C54, TY-G4 and TY-C4 were constructed in collaboration with Drs. C. Florentz and R. Giegé (Strasbourg, France). The rest of the eighteen mutants were constructed by Ching-Hsiu Tsai and Dr. Dreher.

Chapter III has been published by Tsai and Dreher (1991) (J. Virol. 65:3060-3067). However, Table III-1 in this thesis is updated, to include the two extra mutants TYMC-U53 and TYMC-U54, and more refined kinetic data describing the valylation properties. A mistake (TYMC-U53 should be TYMC-G96/U53) that occurred in the published paper has also been corrected in the thesis.

Chapter IV has been published by Tsai and Dreher (1992) (J. Virol. 66:5190-5199). Tobacco mosaic virus U2 and U5 strains used in Chapter V in the thesis were kind gifts from Dr. J. A. Dodds. Purified yeast histidyl-tRNA synthetase was a kind gift from Dr. C. Florentz and R. Giegé (Strasbourg, France).

An edited version of Appendix I has been published by Tsai and Dreher (1993) (BioTechniques 14:58-61). Appendix II of this thesis has been accepted to be published in Molecular Plant-Microbe Interactions (MPMI).

Characterization of the Role of the 3′ Noncoding Region of Turnip Yellow Mosaic Virus RNA

INTRODUCTION

Although it was not realized at the time, the first signs of virus infection in plants were observed as early as the Seventeenth Century in tulip flowers that exhibited the color breaking phenotype. The causal agent, tulip breaking potyvirus, was not identified until much later. The first indication of an entirely new class of pathogenic agents came towards the end of the Nineteenth Century, when A. E. Mayer and M. W. Beijerinck showed that the agent causing mosaic disease in tobacco plants was filterable and thus due neither to a micro-organism nor to nutritional imbalance. It was demonstrated that the disease could be artificially transmitted through the injection of sap from sick plants with capillary glass needles, and by the beginning of this century, the term virus (originally *contagium vivum fluidum*) came into general use. It was not until the 1930's, with the application of chemical and biophysical techniques, that the nature of viruses was clarified; most of the early work was done with tobacco mosaic virus (TMV; Waterson and Wilkinson, 1978; Bos, 1983).

Turnip yellow mosaic virus (TYMV) belongs to the tymoviruses, which have single-stranded, monopartite ribonucleic acids (RNA) genomes with icosahedral particles (van Regenmortel, 1989). TYMV is one of the best characterized plant viruses regarding its replication cytology and enzymology (Bové and Bové, 1985; Matthews, 1991). Nevertheless, many details concerning the mechanism of viral RNA replication are lacking. A distinctive feature of the TYMV genome is the presence of a tRNA-like structure in the 3′ noncoding region. For brome mosaic virus, an analogous feature has been shown to function as the promoter controlling (-) strand synthesis. The experiments of this thesis were designed to elucidate the roles of the 3′ tRNA-like structure noncoding region of TYMV RNA, with emphasis on the possible role of valylation in its replication.

The thesis contains five chapters, followed by Conclusions, Bibliography and Appendices. The first chapter is a literature review that summarizes the published information relevant to the experiments described in the following chapters. This review includes four sections: (1) a description of our present understanding of TYMV, its structure, genetics and replication; (2) a description of the properties and discussion of the possible functions of plant viral tRNA-like structures; (3) a survey of the occurrence and functions of pseudoknots in the 3′ noncoding regions of plant viral RNAs and in other RNAs; (4) a review of our knowledge of the identity determinants of various tRNA species.

To fully understand the characteristics of the valylatability of TYMV RNA, short transcripts containing the tRNA-like structure were used to study the specificity of valylation. Chapter II describes three major valylation identity determinants found in TYMV RNA. This was studied because a knowledge of the valine identity determinants would permit the design of TYMV RNAs that lacked

valine charging, and that could be used to study the relationship between valylation and replication. In chapter III, evidence is given that the *in vitro* valylation of TYMV RNA is correlated with its *in vivo* replication. An advantage of using an error-prone viral replication system is that a mutant with a poor replication rate can be suppressed by naturally introducing a second mutation to give rise to a fitter and more successfully replicating variant. In chapter IV, this approach has been explored to study the role of the 3′ noncoding region of TYMV RNA. A pseudoknot in the region immediately upstream of the tRNA-like structure appears to play an important role in TYMV replication.

To address whether aminoacylation specifically by valine is required for TYMV replication, experiments assessing the mischarging of TYMV RNA mutants were conducted. Chapter V deals with the mischarging activities of those mutants with degraded valine identity. The perspectives and implications of mischarging with high levels of methionine of two such mutants that replicated poorly are discussed. Based on the results from chapter II to chapter V, the specificity of TYMV RNA aminoacylation and the relationship to replication is discussed in the Conclusions.

Two appendices comprise the last part of the thesis. Appendix I mentions a useful polymerase chain reaction technique which can be applied to make correct 3′ ends of transcripts. In our studies, we use this technique to generate the correct 3′-CCA_{OH} ends of tRNAs and short transcripts derived from TYMV RNA for *in vitro* aminoacylation studies. Appendix II reports that a single nucleotide substitution resulting in one amino acid substitution in the TYMV movement protein enhances viral yields and causes more severe symptoms in Chinese cabbage plants. It was hoped that this TYMV mutant would facilitate future studies on TYMV replication due to the enhanced levels of viral products in infected plants.

CHAPTER I Literature Review

I. Turnip Yellow Mosaic Virus

A. General Virology

Turnip yellow mosaic virus (TYMV), the type member of the tymovirus group, was first reported by Markham and Smith in 1946 as one of the causal agents of diseases on cruciferous plants. The symptoms produced by TYMV on turnip are a bright yellow and green mottling, while on Chinese cabbage there is brilliant white, yellow or green mottling that shows a variegation rather than a mosaic pattern (Markham and Smith 1946; 1949). There are currently 21 viruses, collected worldwide, classified in the tymovirus group (Francki *et al.*, 1985; Hirth and Givord, 1988; Matthews, 1991).

The host range of TYMV is relatively narrow and confined to Cruciferae (many species susceptible by mechanical inoculation) and one species in each of two related families: *Reseda odorata* in the Resedaceae and *Cleome spinosa* in the Capparidaceae (Markham and Smith, 1949). Other tymoviruses have broader host ranges, e.g. okra mosaic virus (OkMV) can be transmitted to plants belonging to 23 families (Hirth and Givord, 1988). TYMV is transmitted in the field by members of the *Phyllotreta* and *Psylliodes* genera of flea beetles (Markham and Smith, 1949; Fulton *et al.*, 1980). The mustard beetle (*Phaedon cochleariae*) and its larvae can also transmit the viruses (Matthews, 1980).

B. The Virus Particle

TYMV is an RNA-containing icosahedral plant virus 28-29 nm in diameter. It is built of 180 somewhat banana-shaped identical protein subunits clustered into 20 hexamers and 12 pentamers (Finch and Klug, 1966). The triangulation number (T) is 3. TYMV has one of the more stable particles among the icosahedral viruses. There are strong protein-protein interactions in the virion, as evidenced by the existence of stable empty protein shells (Matthews, 1991). Besides the 20 kDa virus-encoded coat (capsid) protein (Peter *et al.*, 1972; Pleij *et al.*, 1976), virion particles contain RNA and polyamines (Matthews, 1980). Encapsidated RNA is a mixture of TYMV RNAs ranging from 0.7 to 6 kb in length, as originally observed after separation by sucrose gradient centrifugation (Pleij *et al.*, 1976). *In vitro* translation of these RNAs in a wheat germ cell-free system reveals that the infectious c. 6 kb-long RNA does not program the synthesis of the coat protein. Efficient production of the TYMV coat protein is observed only when the 0.7 kb subgenomic RNA (which is also encapsidated) is used as translation template (Pleij *et al.*, 1976; Mellema *et al.*, 1979). It is currently believed that the only functional mRNAs involved in TYMV gene expression are the genomic RNA and coat protein

subgenomic RNA. No other 3'-coterminal subgenomic RNAs have been detected, and the remaining virion RNAs, which are predominantly N-coterminal (Mellema *et al.*, 1979) fragmented RNAs, are thought to represent nonfunctional degradation products.

The TYMV coat protein has been completely sequenced (Peter *et al.*, 1972). It has a molecular weight of 20,133 Dalton, and consists of 189 amino acid residues. The N-terminal amino acid is an acetylated methionine residue. Twenty of the 189 amino acids are proline residues, about half of which are clustered in Pro-X-Y-Pro, Pro-X-Pro-Y-Pro or Pro-Pro sequences. No X-ray crystallography data on the structure of the TYMV coat protein or virion exist.

Polyamines have been reported in preparations of TYMV (Johnson and Markham, 1962) and identified as 1% spermidine and 0.4% spermine (as % of virus weight), with small amounts of putrescine and cadaverine also present (Beer and Kosuge, 1970; Cohen and Greenberg, 1981). The polyamines interact with viral RNA rather than with the protein coat, since the empty protein shell contains fewer than five molecules of spermidine per particle. The spermidine contents of virus preparations are in the range of 200-700 molecules per virion, sufficient to neutralize approximately 20% to 36% of the viral RNA-phosphates (Torget *et al.*, 1979). During TYMV infections on Chinese cabbage, a TYMV propagation host, there are significant increases in the levels of S-adenosylmethionine (the precursor of spermine and spermidine), and polyamines (spermidine, spermine and putrescine) in the leaves (Torget *et al.*, 1979; Cohen *et al.*, 1981; 1985). Using radioactive tracers to study the incorporation of polyamines into TYMV virions, it has been demonstrated that the newly formed virus particles contain predominantly newly synthesized spermidine and spermine. However, inhibition of spermidine synthesis by dicyclohexylamine leads to incorporation of preexisting spermidine and increased amounts of newly made spermine into assembling virus particles. Thus, in spite of spermidine depletion, the positive charge contributed by polyamines to the virus is somewhat conserved (Balint and Cohen, 1985a; 1985b).

Spermidine has been shown to stabilize tRNA molecules (Sakai and Cohen, 1976) and condense MS2 RNA (Leipold, 1977). It has been proposed that polyamines serve to produce a compact and stable RNA structure within the TYMV virus particle (Mitra and Kaesberg, 1965; Jonard *et al.*, 1972). During the purification of the TYMV RNA components by cesium chloride gradient centrifugation, the major component B_{1a} is converted to a higher buoyant density component B_{2a}. It has been demonstrated that the formation of the component B_{2a} is due to a loss of polyvalent cations like spermidine from the virion RNA. The isolation of the B_{2a} component is usually accompanied by RNA degradation which may result from some degree of conformational change in the virion RNA that leads to increased sensitivity to ribonuclease (Noort *et al.*, 1982). For Belladonna mottle tymovirus (BDMV), it has been shown that the stability of the virion at alkaline pH can be attributed to the presence of 90 to 140 molecules of spermidine, 20 to 50 molecules of putrescine and 500 to 900 calcium ions in each virus particle (Savithri *et al.*, 1987). However, the polyamines can be easily exchanged with other cations

by dialyzing against high concentration of salts such as potassium or cesium chloride, resulting in a loss of particle stability.

Another role of polyamines is proposed to involve a regulatory function, based on the results from *in vitro* translation. Polyamines increased translational initiation rates for polyphenylalanine synthesis from polyU in bacterial lysates (Igarashi *et al.*, 1977) and translational yield from polyU in rabbit reticulocyte lysates (Snyder and Edwards, 1991); viral protein synthesis from MS2 bacteriophage RNA was also increased (Algranati and Goldenberg, 1977). In wheat germ extracts, polyamines were found to be important in optimizing the synthesis of full-length proteins encoded by alfalfa mosaic virus RNAs and globin mRNA, either by preventing the premature termination of translation or by inhibiting product degradation (Thang *et al.*, 1976; Hunter *et al.*, 1977). Polyamines have also been shown to enhance the suppression *in vitro* of termination codons (Morch and Benicourt, 1980; Santos *et al.*, 1990).

There have been no studies reported on the RNA-protein interaction in encapsidation. The coat protein binding site on TYMV RNA still remains unknown.

C. Genome Structure, Organization and Function

All the members in the tymovirus group have positive sense RNA genomes ranging between 6.0 and 6.4 kilobases (kb) in length, and have characteristically high cytosine (35-40%) and low guanine (15-17%) contents. The RNA genomes of five tymovirus members have been sequenced: TYMV (Morch *et al.*, 1988; Keese *et al.*, 1989; Dreher and Bransom, 1992), eggplant mosaic virus (Osorio-Keese *et al.*, 1989), ononis yellow mosaic virus (Ding *et al.*, 1989), kennedya yellow mosaic virus (Ding *et al.*, 1990a) and erysimum latent virus (Srifah *et al.*, 1992). TYMV has a 6318-nucleotide-long genomic RNA (6319 nucleotides in TYMV Club Lake isolate, Keese *et al.*, 1989), which possesses a 5′ m^7GpppG cap structure (Briand *et al.*, 1978) and a tRNA-like structure at the 3′ end (Rietveld *et al.*, 1983) to which a valine can be bound enzymatically (Pinck *et al.*, 1970).

The TYMV genome encodes three major open reading frames (ORFs) (Fig. I-1): ORF-69 initiates at nucleotide 88 and encodes a 69 kDa protein; ORF-206 initiates at nucleotide 95 and encodes a 206 kDa protein, which can be read through to produce a 221 kDa protein; ORF-CP, located in the 3′ region of the genome, encodes the 20 kDa coat protein that is expressed from a subgenomic RNA.

TYMV has very compact coding. ORF-69 almost completely overlaps ORF-206, which is separated from ORF-CP with only a very short intergenic region. Readthrough of the ORF-206 amber termination codon extends the ORF to overlap the ORF-CP. Computer-assisted alignments of predicted amino acid sequences have identified three domains within ORF-206 that share sequence similarities with coding regions of other positive stranded RNA viruses (Fig. I-2). In the N-terminal region of ORF-206, the segment encoded by the amino acids 58-219 shows a distant sequence relationship with

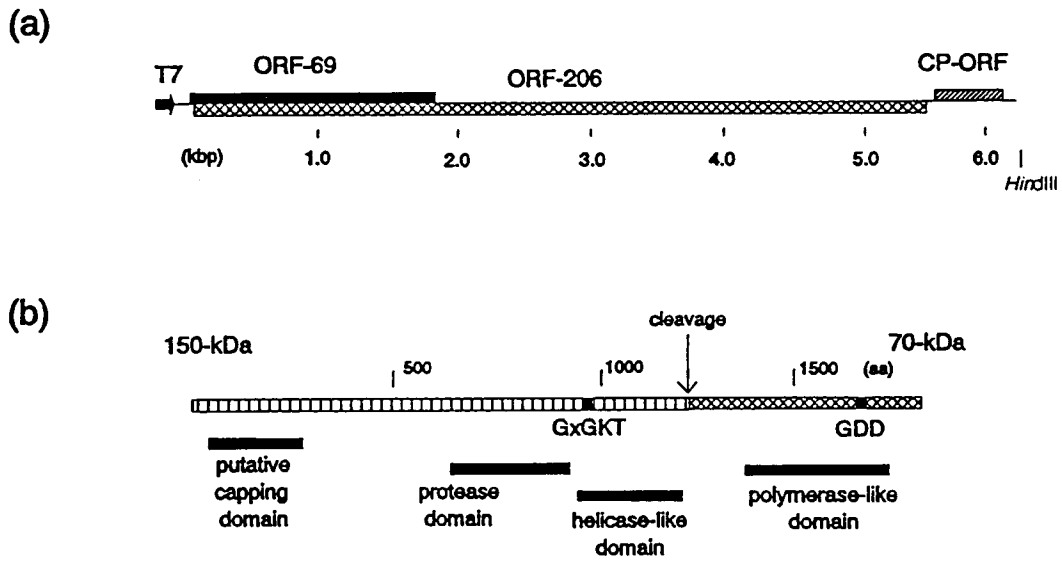

Figure I-1. The TYMV genome and its expression. (a) Diagram of the cDNA insert of pTYPC, which can be transcribed with T7 RNA polymerase after linearization at the *Hind*III site, yielding infectious genomic transcripts. The major open reading frames encoded by TYMV are shown. (b) The expression of ORF-206. The 150 kDa and 70 kDa products arise by cleavage of the precursor 206 kDa protein at the indicated position. Domains with sequences conserved among many positive strand RNA viruses are indicated with their presumptive activities: capping (methyltransferase), helicase, polymerase. The protease domain has been mapped experimentally (Bransom *et al.*, 1991).

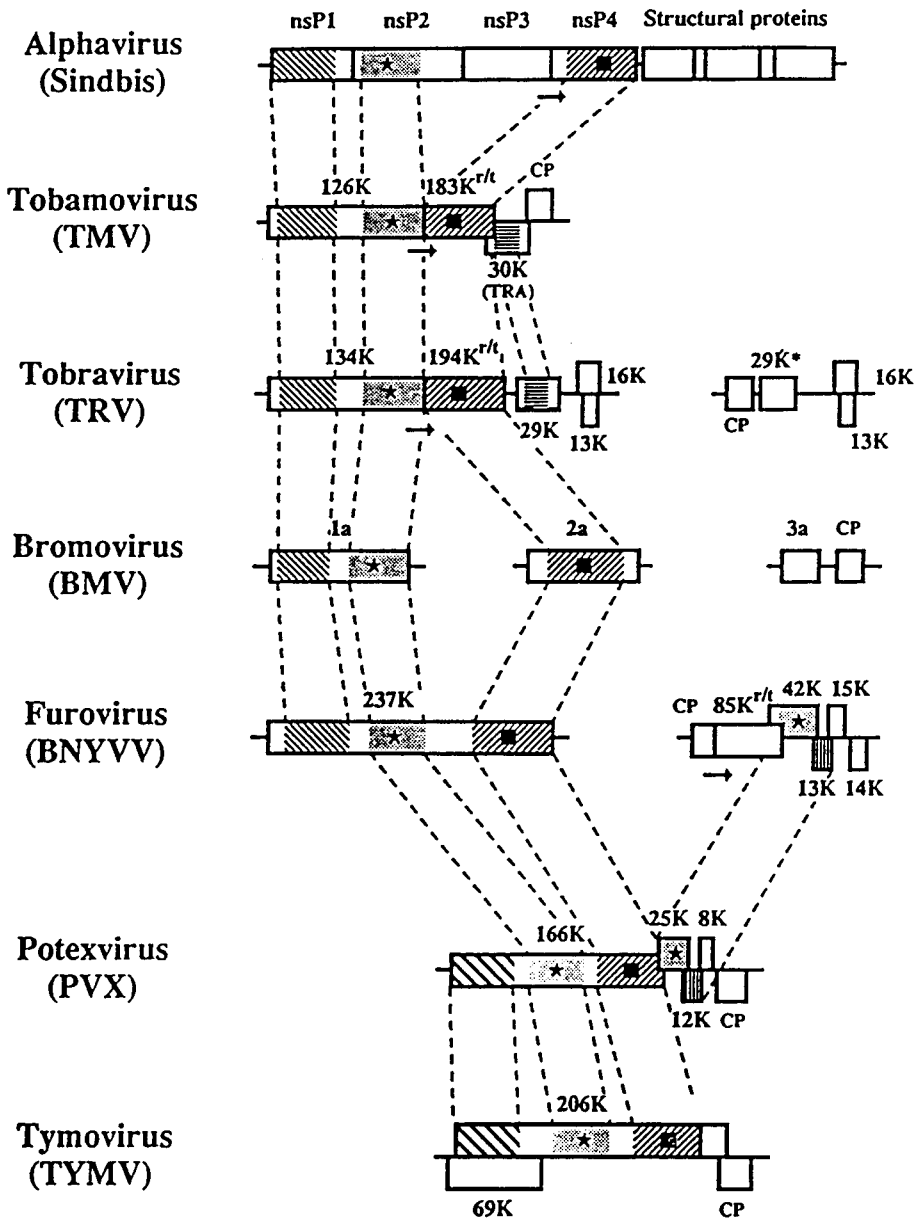

Figure I-2. Comparison of the genomes of Sindbis virus and some alpha-like plant viruses. TMV, tobacco mosaic virus; TRV, tobacco rattle virus; BMV, brome mosaic virus; BNYVV, beet necrotic yellow vein virus; PVX, potato virus X; TYMV, turnip yellow mosaic virus. Coding regions in the genomes are indicated as open bars; regions of amino acid sequence homology in the gene products are indicated by similar shading. Other notations: CP, coat protein; TRA, movement (transport) protein; ★, GXGKT, nucleotide binding sequence motif; ■, GDD, RNA-dependent RNA polymerase domain; →, leaky termination codon; r/t, readthrough protein (taken from Goldbach *et al.*, 1991)

nsP1 of Sindbis virus (Rozanov *et al.*, 1992), which has methyltransferase activity and is involved in 5' cap synthesis (Mi and Stollar, 1991). A second domain encoded by amino acids 973-1204 and surrounding the putative nucleotide binding fold element, Gly-Cys-Gly-Lys-Thr (GCGKT), shares sequence similarity with a broader family of nucleic acid helicases (Habili and Symons, 1989; Gorbalenya and Koonin, 1989). The homologous protein from plum pox potyvirus has been shown to possess double-stranded RNA-dependent ATPase and helicase activities (Laín *et al.*, 1991; 1990). In the C-terminal region of ORF-206, the third conserved domain encoded by amino acids 1496 to 1728 is related to RNA-dependent RNA polymerases with the core sequence Gly-Asp-Asp (GDD) (Kamer and Argos, 1984; Argos, 1988; Koonin, 1991). The association of this core sequence with RNA-dependent RNA polymerase activity has been biochemically proven only in the case of poliovirus (Jablonski *et al.*, 1991). No functional tests on the biochemical properties of the nonstructural proteins encoded by TYMV have been reported.

Studies on the role of the TYMV gene products was made accessible by construction of an infectious cDNA clone pTYMC (Weiland and Dreher, 1989). Capped TYMC transcripts made *in vitro* had 20-40% the specific infectivity of virion RNA when inoculated into protoplasts, and produced systemic symptoms indistinguishable from those of the original Strasbourg isolate when inoculated onto Chinese cabbage (*Brassica pekinensis* cv. Wong Bok or Spring A1), turnip (*Brassica rapa* cv. Just Right) and *Arabidopsis thaliana* (ecotype Bencheim) plants. The roles of ORF-69 and ORF-206 were investigated using site-directed mutagenesis to inactivate initiation codons and create premature termination codons. Constructs in which ORF-69 expression was interrupted replicated normally in protoplasts, but failed to infect Chinese cabbage plants systemically. These results suggested that the 69 kDa protein was involved in permitting the cell-to-cell spread of the virus (Bozarth *et al.*, 1992).

Use of constructs interfering specifically with ORF-206 expression has shown that the expression of ORF-206 is essential for RNA replication (Weiland and Dreher, 1989). The expression of both active helicase-like and polymerase-like domains is required for TYMV replication, since TYMC transcripts carrying a single amino acid change in the putative nucleotide-binding fold or one in the polymerase GDD core sequence failed to replicate (Weiland, 1992; Weiland and Dreher, 1993). The putative helicase and polymerase domains appear on separate mature proteins, the 150 kDa and 70 kDa proteins, that arise proteolytically from the N-terminal and C-terminal regions, respectively, of the ORF-206 product. This maturation is catalyzed by a viral protease encoded immediately upstream of the helicase-like coding region of ORF-206 (Bransom *et al.*, 1991).

Genetic complementation experiments using defective RNAs with substitutions or in-frame deletion mutations located in the 150 kDa or 70 kDa coding regions have shown that there are limitations on the function *in trans* of the essential domains. The defective RNAs, which were incapable of independent replication, were coinoculated to turnip protoplasts with helper genomes or with a second, potentially complementing defective RNA. In most cases, the *trans*-replication of

defective RNAs was inefficient, more so for RNAs encoding a defective 150 kDa protein than for those encoding a defective 70 kDa protein. In contrast, a defective RNA with a deletion of most of the 70 kDa coding region (and encoding a functional 150 kDa protein) was able to replicate efficiently *in trans*. When coinoculated with a helper genome lacking most of the coat protein gene, this defective RNA and the helper RNA accumulated to comparable levels, 10% of wild-type (Weiland, 1992; Weiland and Dreher, 1993). When coinoculated with a second defective RNA carrying a mutation in the putative nucleotide binding element of the 150 kDa protein, the combined accumulation in turnip protoplasts of defective genomic RNAs was about half that of genomic RNA in wild-type infections. Further, this combination of defective genomes replicated systemically in turnip plants, remaining stable for 5 serial passages, and thus constituting a novel bipartite form of TYMV (Weiland, 1992). The defective RNA with the mutation in the 70 kDa coding region accumulated to levels 10-fold higher than the coreplicating RNA encoding a defective 150 kDa protein. The above results have been interpreted in support of a model (Fig. I-3) in which the 150 kDa and 70 kDa proteins form a complex *in cis* that interacts preferentially with the (-) strand promoter elements of the RNA from which these proteins were made. Thus, TYMV RNA replication is predominantly *cis*-preferential; this can be avoided when a 150 kDa/70 kDa complex cannot form *in cis*, e.g. in the case of the defective RNA with the large deletion in the 70 kDa coding region (Weiland and Dreher, 1993). *Cis*-preferential replication would probably enhance the establishment of an infection, by facilitating the assembly of replication complexes when the components are present at low concentration early in infection.

Coat protein is translated from a subgenomic RNA, and the expression is not essential for viral genome replication. A genome with a deletion of two-thirds of ORF-CP was able to replicate in protoplasts and induce normal chlorotic local lesions on the inoculated leaves, but failed to induce systemic symptoms (Weiland, 1992). These results suggest that the coat protein is important for long distance movement, but is nonessential for cell-to-cell spread.

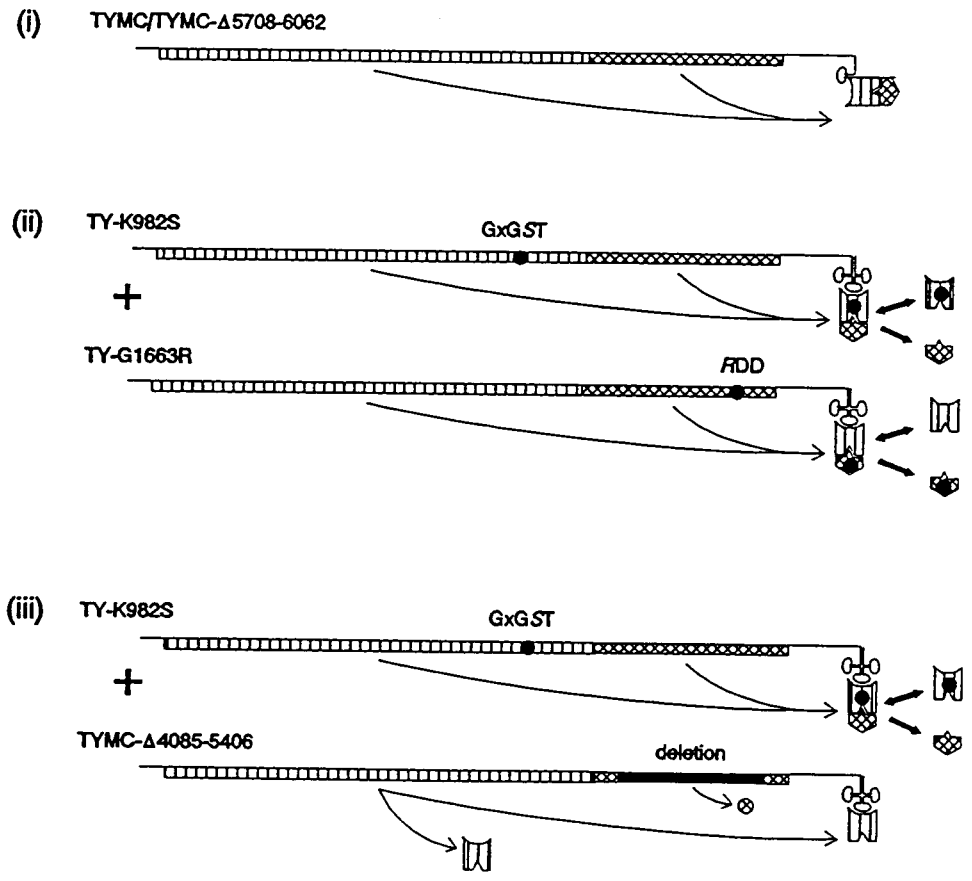

Figure I-3. A model of *cis*-preferential replication of TYMV RNAs. The proposed interactions between the 150 kDa and 70 kDa proteins that result in *cis*-preferential replication. (i) Formation of a stable, productive complex *in cis* on replication-proficient RNAs. (ii) Two defective RNAs that mutually complement inefficiently (replication = 1% relative to TYMC) due to the trapping of mutant proteins in relatively stable complexes that form *in cis*. (iii) Two defective RNAs whose very efficient mutual complementation (replication = 50% relative to TYMC) is proposed to result from the inability of a complex to form *in cis* on one of the RNAs, due to the large deletion in the 70 kDa protein (Weiland and Dreher, 1993).

D. Replication

The typical infection cycle of (+)-sense RNA viruses such as TYMV comprises the processes of viral entry and uncoating, translation of the viral genomic RNAs, replicase complex formation, (-)-sense RNA synthesis, (+)-sense genomic RNA synthesis, subgenomic RNA synthesis, coat protein translation, virion assembly and export of viral genomes to adjacent cells.

a. Virus Uncoating

Using radioactive tracers, it was demonstrated that the TYMV uncoating process takes place within 45 sec after inoculation, with at least 80-90% of uncoating occurring in the epidermis (Matthews, 1985). The release of TYMV RNA from the virion has been studied using freeze-thawing as a model for the physiological process, resulting in the suggestion that RNA is released through a hole that forms in the icosahedral particle (Katouzian-Safadi and Berthet-Colominas, 1983; Katouzian-Safadi and Haenni, 1986; Adrian *et al.*, 1992). This hole was estimated to correspond to the loss of some five to nine coat protein subunits, perhaps representing the loss of one or two capsomeres or faces from the icosahedron (Katouzian-Safadi and Berthet-Colominas, 1983). Recent studies in which uncoating and release of the genomic RNA were visualized by cryo-electron microscopy (Adrian *et al.*, 1992) have supported the earlier studies based on physical methods (Katouzian-Safadi and Berthet-Colominas, 1983). It is not certain, however, how the above observations relate to the physiological events immediately following inoculation. For several viruses, there is evidence for ribosome-dependent cotranslational disassembly, for instance for the rod-shaped TMV (Wilson, 1984; Shaw *et al.*, 1986; Turner *et al.*, 1987), and for the spherical viruses southern bean mosaic virus (Brisco *et al.*, 1985), BMV (Brisco *et al.*, 1986) and Semliki Forest virus (Singh and Helenius, 1992). At present, it is neither clear whether ribosomes are involved in TYMV uncoating, nor if ribosome-dependent uncoating could result in initial loss of one or two capsomeres as observed in the model studies described above.

b. Expression and Function of Essential Replication Genes

The released genomic RNA can serve as a messenger RNA for translation. The mature essential nonstructural proteins (150 kDa and 70 kDa proteins) are presumed to then associate with host factor(s) to form a replication complex (replicase) for (-)-sense RNA synthesis using genomic RNA as a template. The laboratory of Dr. J. M. Bové conducted studies on the TYMV replicase during the 1970's and early 1980's. A partially purified replicase preparation from TYMV-infected Chinese cabbage was demonstrated to possess (-)-strand synthesis activity when supplied with (+)-sense RNA

templates (Mouches *et al.*, 1974). Other activities, such as (+)-sense genomic and subgenomic RNA synthesis, were not reported. Two major protein bands with apparent molecular weight 115 kDa and 45 kDa were present in the replicase preparations (Mouches *et al.*, 1984). An antiserum raised against the 115 kDa protein cross-reacted with radiolabelled TYMV translation products, indicating a viral origin for this protein (Candresse *et al.*, 1986). However, the origin of a 115 kDa viral protein is not clear from our current understanding of the gene expression of TYMV (Fig. I-1), and it remains to be determined whether this replicase protein is a specific or nonspecific product (i.e. degradation product) of TYMV gene expression. The form in which the domains shown genetically to be essential (i.e. the putative helicase and polymerase domains) appear in the replicase is also unclear from Bové's studies. Immunological experiments indicated that the 45 kDa protein present in replicase preparations was of host origin: no immunological cross-reactivity could be demonstrated between TYMV translation products and the 45 kDa replicase protein, and antiserum raised against the entire replicase preparation was able to detect a 45 kDa protein in uninfected host cell extracts. Antibodies against the 115 kDa protein partially inhibited replicase activity, suggesting that the 115 kDa protein is involved in TYMV (-)-sense RNA synthesis (Candresse *et al.*, 1986).

Significant progress has been made in understanding the replicases of a small number of other positive strand viruses. The replicase isolated from *E. coli* infected with bacteriophage Qß comprises three host encoded subunits — EF-Tu, EF-Ts and ribosomal protein S1 — and one viral encoded subunit, the polymerase (Blumenthal and Carmichael, 1979). The replicase isolated from plants infected with cucumber mosaic virus (CMV) exhibits two virus encoded subunits, identified as the translation products of RNA 1 and RNA 2, and one host encoded subunit (Hays and Buck, 1990). RNA 1 encodes a protein with methyltransferase-like and helicase-like domains, while RNA 2 encodes a protein with a polymerase-like domain (Habili and Symons, 1989). The CMV replicase preparation is able to carry out the complete replication of CMV genomes, including the synthesis of (+)-sense and (-)-sense RNAs corresponding to RNAs 1, 2, and 3, and subgenomic RNA 4. This replicase preparation has also been shown to be capable of the complete replication of the 334 nucleotide-long R satellite RNA of CMV (Hays *et al.*, 1992). As suggested for the TYMV replicase, both of the Qß and CMV replicases appear to contain viral and host subunits.

c. Promoters controlling (+), (-) and subgenomic RNA synthesis.

Because new strand synthesis initiates opposite the 3'-noncoding regions of RNA viral genomes, it was long suspected that these regions contained the promoters controlling (-)-strand RNA synthesis. Direct evidence was first obtained with BMV, by studying *in vitro* the biochemical properties of the BMV replicase complex. A BMV RNA fragment containing the 3'-terminal 134 nucleotides is the shortest fragment capable of forming the core of the BMV tRNA-like structure (Fig. I-4B; refer section

IIB). This fragment also is the shortest fragment that serves efficiently as a template for (-)-strand synthesis *in vitro* (Miller *et al.*, 1986). The BMV tRNA-like structure present in the 3' noncoding region can thus be considered to function as the promoter of (-)-strand synthesis. Results of experiments studying the replication of deleted genomes (French and Ahlquist, 1987) and of genomes carrying mutations in the 3' tRNA-like structure (Dreher *et al.*, 1988b) have corroborated the validity of the *in vitro* replicase studies. The implications of the overlap of promoter function and tRNA mimicry are discussed in section IIB. Minus-strand promoters have been poorly characterized for other positive strand RNA viruses.

With TYMV, an *in vitro* replication system has been used to study the role of the tRNA-like structure in replication. Short 3' fragments derived from TYMV RNA that contained the complete 3' tRNA-like structure (Morch *et al.*, 1987) or only the acceptor stem (38-nucleotides long, Gargouri-Bouzid *et al.*, 1991; 42-nucleotides long, P. Georgel, unpublished observations) were copied *in vitro* by a replicase preparation made from Chinese cabbage plants infected with TYMV. Such RNAs were also able to act as competitors of TYMV RNA copying *in vitro* (Morch *et al.*, 1987; Gargouri-Bouzid *et al.*, 1991; P. Georgel, unpublished observations). However, the validity of the TYMV *in vitro* replication system has not been established by correlation of results obtained *in vitro* and *in vivo*.

Minus-sense genomic RNAs serve as templates for the transcription of both (+)-sense genomic RNA and of subgenomic mRNA. Subgenomic mRNAs are produced by viruses in order to express genes not accessible on the genomic RNA. In the case of TYMV, coat protein is expressed from a subgenomic RNA, which is produced late in infection. The mechanism for producing subgenomic RNA was first revealed by Miller *et al.* (1985), who used *in vitro* replication studies to show that BMV subgenomic RNA 4 arises by internal initiation on the (-)-strand of genomic RNA 3. The sequences involved in subgenomic promoter function have been defined both *in vitro* (Marsh *et al.*, 1988) and *in vivo* (French and Ahlquist, 1988), and mapped to the intergenic region immediately upstream of the subgenomic initiation site. The evidence from other positive strand viruses supports the synthesis of subgenomic RNA by internal initiation controlled by promoters situated near the RNA initiation site (Goldbach, 1987; Levis *et al.*, 1990). The TYMV subgenomic promoter has not been studied experimentally, but two sequences conserved among several tymoviruses — one closely upstream of the coat protein ORF and thought to overlap the RNA initiation site, and a second 7-8 nucleotides further upstream, referred to as the "tymobox" (Ding *et al.*, 1990b) — are potential subgenomic promoter elements. The studies on the replication of BMV (Pogue and Hall, 1992) and polio virus (Andino *et al.*, 1990) indicates that the secondary structure of the 5' noncoding region of (+)-sense genomic RNA may play a role in (+)-sense RNA synthesis.

Positive strand synthesis involves the synthesis of RNAs with 5' caps. The mechanism of cap addition has not been elucidated for any positive strand RNA virus, although recent studies have made some progress in identifying the domains of essential proteins that are involved in cap synthesis (see

Section IC). The synthesis of the (+)-sense strands of the aminoacylatable plant viruses appears in addition to require the post-transcriptional addition of a 3'-A residue to provide a complete 3'-CCA_{OH} terminus. Host (CTP, ATP):tRNA nucleotidyltransferase (NTase) is thought to be responsible for this addition. Mature TYMV virion RNA lacks the adenosine residue at the 3'-terminus (Silberklang *et al.*, 1977; Briand *et al.*, 1977), but TYMV RNAs become valylated during infection, suggesting the addition of the 3'-A *in vivo* by host NTase. The posttranscriptional addition of the 3'-terminal adenosine by NTase is also indicated for BMV RNAs, since this residue has no complement in the (-) strand template and is not present in double-stranded replicative form RNAs (Miller *et al.*, 1986).

d. TYMV Replication and Assembly are Associated with Chloroplast Membranes

As is typical for positive strand RNA viruses, TYMV replication is associated with host cell membranes. Electron microscope observations of infected tissues have shown that small peripheral vesicles form along the chloroplast surface by invagination of both chloroplast membranes (Francki *et al.*, 1985; Matthews, 1991), triggering an aggregation and swelling of the chloroplasts to form a polyplast (Hatta and Matthews, 1974). The vesicles contain fibrillar osmiophilic material with the expected appearance of nucleic acid (Francki, 1987), while freeze-etch studies have suggested the presence of stockpiles of pentameric and hexameric clusters of coat protein subunits on the chloroplast membrane surrounding the vesicles. Ultrahistochemical experiments support the localization of TYMV RNA replication at the chloroplast periphery. In immunocytochemical labelling experiments, antiserum raised against the 115 kDa protein present in TYMV replicase preparations was associated with chloroplast membranes and labelled the junctions between chloroplasts in the polyplast (Garnier *et al.*, 1986). It was also shown, by high resolution autoradiography detection of [^{3}H]uridine incorporated in the presence of actinomycin D, that TYMV RNA synthesis is associated with the chloroplast periphery (Garnier *et al.*, 1980). Based on the above observations, Matthews (1981) has proposed that RNAs synthesized within the vesicles emerge through the vesicle neck, and virus assembly is initiated by interaction with the coat protein clusters present outside each vesicle.

II. tRNA-like Structures in Viral Genomes

A. Properties of the tRNA-like Structures

In 1970, it was demonstrated that the 3′ end of the TYMV genome can be aminoacylated with valine to form a covalent ester linkage like that of charged tRNA (Pinck *et al.*, 1970; Yot *et al.*, 1970). Since then, the genomic RNA molecules from several viruses have been shown to share some characteristics with tRNA and to interact with tRNA-specific proteins, in particular aminoacyl-tRNA synthetases. Genomic RNAs from five different plant virus groups can accept a specific amino acid at their 3′ end (Table I-1). Tymoviral RNAs can be charged with valine, tobamoviral RNAs with histidine (except the cowpea strain of TMV, CcTMV, which accepts valine), and the RNAs from bromoviruses, cucumoviruses and hordeiviruses can be charged with tyrosine. Additionally, the RNAs from the plant tobraviruses are substrates for adenylation by (CTP, ATP):tRNA nucleotidyl-transferase, although they fail to accept any amino acid (van Belkum *et al.*, 1987a).

These findings imply that the above plant viral RNA molecules contain tRNA-like structures at their 3′ termini that mimic the tertiary structures of tRNAs. The existence of such structures has been verified for most of the above viral RNAs experimentally using chemical modification and enzymatic digestion studies (e.g. Florentz *et al.*, 1982; Rietveld *et al.*, 1983; Mans *et al.*, 1991; Florentz and Giegé, 1993), and for TYMV RNA by computer modelling studies (Dumas *et al.*, 1987). In all cases, the analogue of the tRNA aminoacyl acceptor arm is characterized by a special construction called RNA pseudoknotting (Pleij *et al.*, 1985; 1989; 1990). Of the viral RNAs, the proposed conformation of the tRNA-like structure from TYMV most closely resembles the overall L-conformation of canonical tRNAs (Rietveld *et al.*, 1982). To date, no viral tRNA-like structures have been solved, for instance by X-ray crystallography or nuclear magnetic resonance.

a. The TYMV tRNA-like structure

The evidence from structural probing using nucleases and chemicals shows that the 3′ 82 nucleotides of TYMV RNA are able to fold into a tRNA-like structure with an L-shaped tertiary conformation (Rietveld *et al.*, 1983; Dumas *et al.*, 1987; Fig. I-4A). A number of features are analogous to tRNAs: the 3′-CCA terminus, the 12 base pair amino acid acceptor arm, seven-membered loops that are analogous to the T and anticodon loops, and the anticodon itself. Primary sequences contain little resemblance to cellular $tRNA^{Val}$ molecules, however. The anticodon loop comprises the sequence 59-CCCACAC-53, which is similar to those of $tRNA^{Val}$ from lupine (Barciszewska and Jones, 1987) and to a $tRNA^{Val}$ gene from *Arabidopsis thaliana* (Gokhman and Zamir, 1990) [anticodon loops CUIACAC and CTAACAC, respectively; anticodons underlined, I is inosine]. Unlike tRNAs, no

Table I-1. Properties of tRNA-like structures at the 3′ end of plant viral RNAs.[a]			
Virus	**Virus group**	**aaRS**	**NTase**
turnip yellow mosaic virus (TYMV)	tymovirus	ValRS	+
tobacco mosaic virus (TMV)	tobamovirus	HisRS	+
cowpea strain of TMV (CcTMV)[b]	tobamovirus	ValRS	+
tobacco rattle virus (TRV)	tobravirus	-[c]	+
brome mosaic virus (BMV)	bromovirus	TyrRS	+
cucumber mosaic virus (CMV)	cucumovirus	TyrRS	+
barley stripe mosaic virus (BSMV)	hordeivirus	TyrRS	?[d]

a. References of this table are from Mans *et al.* (1991) and therein.

b. The only member of tobamoviruses that charges valine.

c. Can not be aminoacylated.

d. Not known.

modified nucleotides have been reported as constituents of the tRNA-like structure (Silberklang *et al.*, 1977; Briand *et al.*, 1977).

TYMV RNA can be specifically recognized by several tRNA-associating proteins such as (CTP, ATP):tRNA nucleotidyltransferase (NTase) from *E. coli* (Joshi *et al.*, 1982a), valyl-tRNA synthetase (ValRS) from wheat germ (Dreher *et al.*, 1988), yeast (Giegé *et al.*, 1978), and *E. coli* (Pinck *et al.*, 1970; Joshi *et al.*, 1982a), and by elongation factors EF-Tu from *E. coli* (Joshi *et al.*, 1984) or EF-1α from wheat germ (Joshi *et al.*, 1986). Detailed comparisons between TYMV RNA and $tRNA^{Val}$ have shown that TYMV RNA is a remarkably efficient tRNA mimic. The affinity of valylated TYMV RNA for wheat germ EF-1α is comparable to that of yeast Val-$tRNA^{Val}$ EF-Tu (Joshi *et al.*, 1986). The valylation of TYMV virion RNA by yeast ValRS is significantly less efficient than that of yeast $tRNA^{Val}$ (K_M's of 400 nM and 120 nM, respectively, and V_{max}/K_M 20-fold less for TYMV RNA than $tRNA^{Val}$), but far superior to the mischarging of non-cognate tRNAs (V_{max}/K_M 500- to 5000-fold higher; Giegé *et al.*, 1978).

Accurate kinetic parameters are hard to determine for virion RNA, because of uncertainty concerning the concentration of 3′ ends; the valylation properties of short RNA transcripts derived from TYMV RNA containing the 3′ tRNA-like structure have been studied (Dreher *et al.*, 1988a; Mans *et al.*, 1990; Florentz *et al.*, 1991), but have not been critically compared to tRNAs. Transcripts containing as few as 84 viral 3′ nucleotides were valylated with close to optimal efficiency with wheat germ ValRS (Mans *et al.*, 1990), but even short heterologous 5′ nucleotides are able to introduce alternative foldings into the tRNA-like structure, resulting in decreased valylation (Dreher *et al.*, 1988a; Mans *et al.*, 1990). Yeast $tRNA^{Val}$ and 258-nucleotide-long TYMV RNA transcripts both had a K_M of 210 nM when valylated by yeast ValRS (Florentz *et al.*, 1991) when compared directly (V_{max} values not reported). Further, a nonvalylating TYMV RNA mutant (anticodon mutation CAC→CUC; TY-U56) was a competitive inhibitor of $tRNA^{Val}$ valylation (Florentz *et al.*, 1991). The results reported by Florentz *et al.* (1991) suggest that the kinetic parameters for the valylation of TYMV RNA and $tRNA^{Val}$ are not as different as suggested by the earlier study of Giegé *et al.* (1978), who did not have access to a molecularly homogeneous preparation of viral RNA. This conclusion is supported by the finding that TYMV RNAs can be adenylated and consequently valylated *in vivo* after microinjection into *Xenopus laevis* oocytes (Joshi *et al.*, 1978), and that a portion of TYMV RNAs are valylated during replication in Chinese cabbage leaves (Joshi *et al.*, 1983).

Although TYMV RNA is a good substrate for valylation *in vitro* with ValRS from different sources as described above, charging with other amino acids has also been reported. Short 3′ TYMV transcripts 264 nucleotides long were charged by yeast HisRS to a level 0.25 mol his/mol RNA, with a specificity constant V_{max}/K_M 100-fold lower as compared to an unmodified yeast $tRNA^{His}$ transcript (Rudinger *et al.*, 1992b). Even more efficient histidine charging was observed for mutants TY-56 and

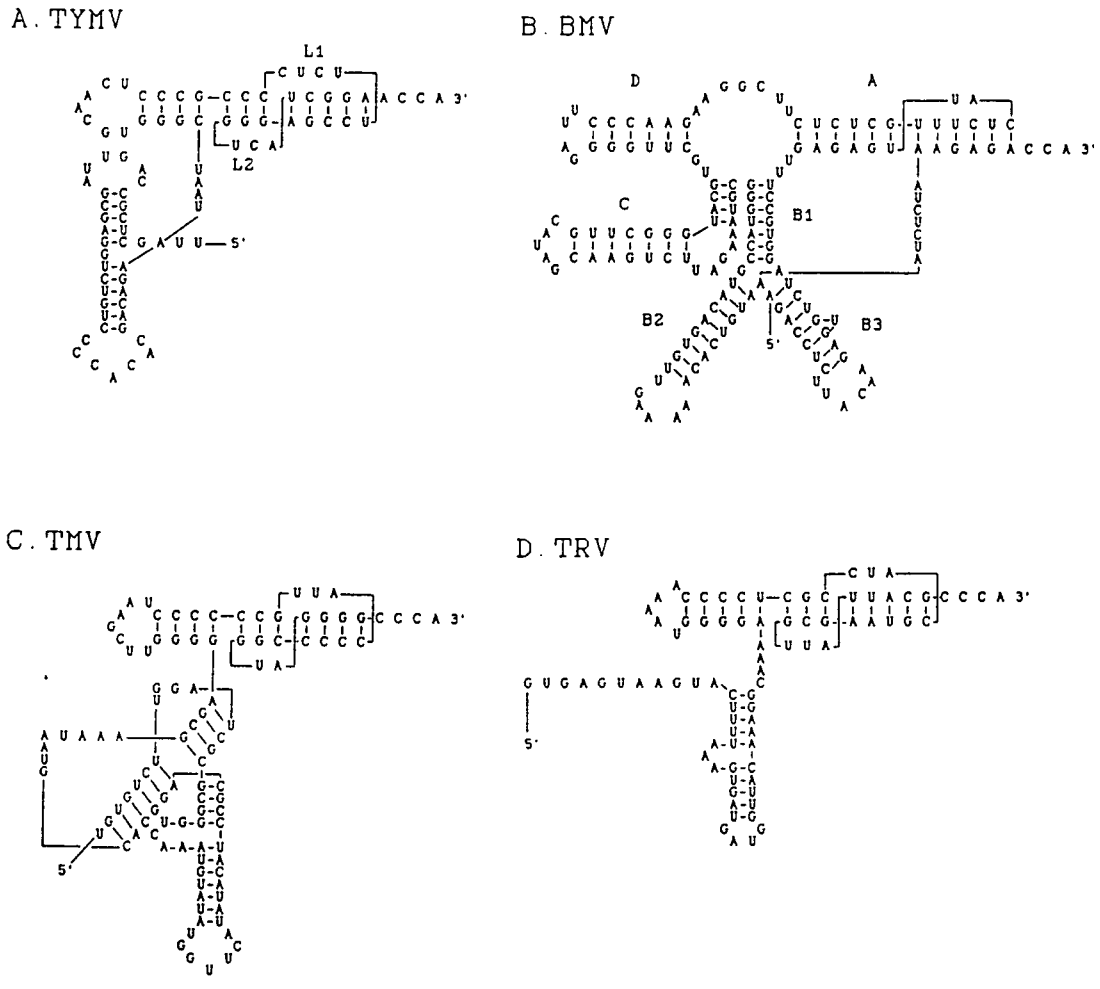

Figure I-4. The diagrams present the tRNA-like structures of: A. TYMV, turnip yellow mosaic virus; L1, pseudoknot loop 1; L2, pseudoknot loop 2. B. BMV, brome mosaic virus, arms identified by letters A to D (Perret *et al.*, 1989). C. TMV, tobacco mosaic virus (Rietveld *et al.*, 1984). D. TRV, tobacco rattle virus (van Belkum *et al.*, 1987a).

TY-U56 (Fig. I-5), mutations in the middle A56 position of the anticodon (which has been identified as a major determinant of TYMV RNA valylation by yeast ValRS; Florentz *et al.*, 1991; see Section IVC). Still shorter transcripts containing only the tRNA-like structure (TY-Alu) were also very efficiently histidylated (Rudinger *et al.*, 1992b). TY-G56, TY-U56 and TY-Alu were charged to levels 0.85, 0.95 and 0.85 mol his/ mol RNA, respectively, and had V_{max}/K_M values 22, 20 and 5-fold lower than that of the $tRNA^{His}$ transcript, respectively. Significantly, even fully modified yeast $tRNA^{Val}$ was a moderately good substrate for the yeast HisRS, charging to a level 0.3 mol his/mol RNA with V_{max}/K_M 250-fold lower than for the $tRNA^{His}$ transcript (Rudinger *et al.*, 1992b). The virological significance of these observations is unclear, and the occurrence of TYMV RNA histidylation by a higher plant HisRS needs to be investigated. However, the observed level of $tRNA^{Val}$ mischarging is high compared to other examples of mischarging (Giegé *et al.*, 1978), suggesting that the conditions of the *in vitro* histidylations may have made the HisRS unusually active in mischarging.

The charging with other amino acids of several tymoviral RNAs by a mixture of *E. coli* aminoacyl-tRNA synthetases has been reported (van Belkum *et al.*, 1987b). However, in that particular experiment involving competitive charging with all amino acids present, TYMV RNA accepted almost as much leucine as valine. This is contrary to previously conducted similar experiments, which detected only valine charging (Pinck *et al.*, 1970). It appears possible that the viral RNA preparations used by van Belkum *et al.* (1987b) were contaminated with tRNAs. All of the tymoviral RNAs that they tested contain tRNA-like structures similar to that of TYMV RNA (van Belkum *et al.*, 1987b). In all cases, the CACAC sequence of the anticodon loop is conserved. A similar tRNA-like structure is also present at the 3' end of the valylatable RNA from CcTMV (Beachy *et al.*, 1976; Meshi *et al.*, 1981; Rietveld *et al.*, 1984), suggesting that this viral RNA is a recombinant that arose from a cell with a tobamovirus and tymovirus dual infection. Although the tRNA-like structure of CcTMV RNA resembles that of the tymoviruses, it can apparently be only partially valylated with yeast ValRS (c. 6-21%; Beachy *et al.*, 1976).

b. The tRNA-like structures of other viruses

The structural model proposed by Rietveld *et al.* (1984) for the histidylatable tRNA-like structure of tobacco mosaic virus (TMV) (Fig. I-4C) is based on both chemical and enzymatic structural mapping and on phylogenetic evidence. As for the TYMV tRNA-like structure, the aminoacyl acceptor stem contains a pseudoknot and is a close analogue of that from tRNAs. In TMV RNA, this similarity extends to the presence of a UUCG sequence in the T-loop analogue, corresponding to the invariant TΨC(G/A) of tRNAs. The 105 nucleotide-long TMV 3' tRNA-like structure contains a putative anticodon arm with bulge loops on the long hairpin. In this long anticodon arm histidine anticodon triplet (GUG) occurs in most tobamoviral RNAs, with an asparagine anticodon

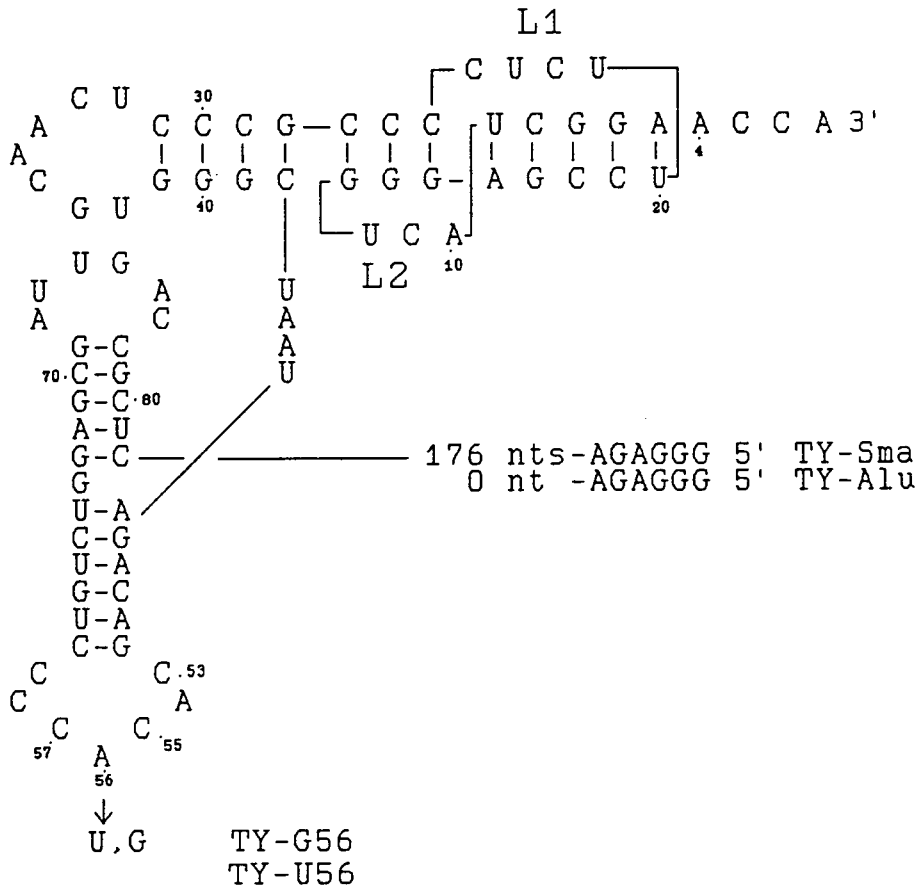

Figure I-5. Structural folding of the 3' region of TYMV RNA that is involved in valylation. TY-Sma is the wild-type transcript containing 258 nucleotides of TYMV RNA and 6 non-viral nucleotides 5'-GGGAGA (Dreher *et al.*, 1988). TY-Alu is a shorter wild-type transcript containing only the tRNA-like structure (82 nucleotides) and 6 non-viral nucleotides. An alternative folding of TY-Alu has been demonstrated (Mans *et al.*, 1990; Fig. V-1 in this thesis). TY-G56 and TY-U56 are the mutant transcripts derived from the TY-Sma with mutations at position 56 as indicated.

(GUU) present in some members (Rietveld *et al.*, 1984; García-Arenal, 1988; reviewed by Mans *et al.*, 1991). One of the bulges of the anticodon arm is well conserved among different tobamoviral RNAs, and is involved in the formation of a second pseudoknot that is integral to the tRNA-like structure. This results in a structure significantly more complex than that of TYMV RNA and tRNAs. *In vitro* histidylation studies showed that virion RNAs can be charged with histidine to a level of only 0.4 mol/mol (Öberg and Philipson, 1972; Carriquiry and Litvak, 1974). This level of charging is significantly below that of the valylatable and tyrosylatable plant viral RNAs, which can typically be fully charged. Unlike TYMV RNA, tobamoviral virion RNAs have complete 3'-CCA termini; no histidine bound to the RNA in the virion has been reported, but this may be due to spontaneous deacylation. TMV RNA lacking the 3' A residue is a substrate for adenylation by nucleotidyltransferase; studies on the interaction between TMV RNA and this enzyme indicate an interaction with the UUCG sequence in the T-loop analogue (Hegg *et al.*, 1990).

The bromoviruses and cucumoviruses are multipartite viruses that encapsidate three genomic RNAs and one subgenomic RNA (RNA 4). The 3' end sequences of RNAs 1, 2, 3 and 4 from bromoviruses and cucumber mosaic virus exhibit similar proposed structures (Joshi *et al.*, 1983; Rietveld *et al.*, 1983), although there is only modest sequence similarity (Ahlquist *et al.*, 1981). Like TMV RNA, the virion RNAs of these viruses terminate in 3'-CCA, yet appear not to be aminoacylated in the capsid. Also as for TMV RNA, the aminoacyl acceptor arm is built around a pseudoknot, and the UUCG sequence is present in the T-loop analogue. The remainder of the tRNA-like structure is even more complex than that of TMV, however, and the structural components that are analogous to the anticodon domain were only revealed after mutagenic structure/function studies (refer section IIB) and footprinting studies on the interaction between the tRNA-like structure and yeast tyrosyl-tRNA synthetase (Perret *et al.*, 1989). These studies resulted in a model in which the anticodon-analogous domain of BMV RNA is an inverted Y-shaped complex of three short stems, with no analogue of the anticodon loop or triplet present. In addition, an extra stem/loop exists within the tRNA-like structure (arm D, Fig. I-4B). Despite the complexity of the BMV tRNA-like structure and its deviation from the L-shaped tRNA conformation, BMV RNA mimics certain properties of $tRNA^{Tyr}$ very efficiently (see section IIB).

Barley stripe mosaic virus (BSMV) is the type member of the hordeivirus group. The 3' end of BSMV RNAs can be aminoacylated with tyrosine *in vitro* (Agranovsky *et al.*, 1981) and *in vivo* (Loesch-Fries and Hall, 1982). The proposed tRNA-like structure belongs to the bromo-/cucumo-virus family, and is most similar to that of broad bean mosaic bromovirus (BBMV), which lacks arm D (Ahlquist *et al.*, 1981; Boykov *et al.*, 1981; Joshi *et al.*, 1983; Kozlov *et al.*, 1984).

The genome of tobacco rattle tobravirus (TRV) consists of RNA 1 and RNA 2, which have similar 3' ends. Chemical and enzymatic mapping shows that the 3' terminal 140 nucleotides of TRV RNA (PSG strain) has an aminoacyl acceptor arm with a pseudoknot structure similar to that of

tymoviral and tobamoviral RNAs (Fig. I-4D) (van Belkum *et al.*, 1987a). However, the RNA does not appear to form a classical anticodon domain as in tRNAs or tymoviral RNAs. The inability to aminoacylate these RNAs, as described previously, may thus be due to the absence of a canonical anticodon domain, although the presence of such a domain is not in all cases a prerequisite for aminoacylation, e.g. a minihelix comprising the T-arm/acceptor-arm half of $tRNA^{Ala}$ can be charged with alanine efficiently by alanine-tRNA synthetase (Francklyn and Schimmel, 1989).

Since the elongation factors EF-Tu and EF-Ts are subunits of the replicase of the *E. coli* RNA phage Qß, the existence of a tRNA-like structure at the 3′ end of the Qß genome was suspected (Blumenthal *et al.*, 1972). Further, an interaction between the 3′ end of coliphage RNAs with RNase P (Guerrier-Takada *et al.*, 1988) and (CTP, ATP):tRNA nucleotidyltransferase (Prochiantz *et al.*, 1975) has been reported, although attempts to aminoacylate bacteriophage RNAs have not been successful (Prochiantz *et al.*, 1975; Hall, 1979). The 3′ noncoding regions of coliphage RNAs have been found to possess extensive structural features, and a structural model with some elements of a tRNA-like structure has been proposed. Chemical modification and enzymatic mapping studies with MS2 RNA have supported such structures (Adhin *et al.*, 1990). The only region resembling tRNA is a 12-basepair-helix corresponding to the aminoacyl acceptor arm, with a single-stranded -CCCA 3′-terminus (Fig. I-6). The overall similarity with tRNA is thus low, but the existence of a structure analogous to the T/acceptor domain and the observation of adenylation activity with 3′-CCC termini by NTase agrees with the known interaction of this enzyme with the equivalent domain in tRNA (Spacciapoli *et al.*, 1989).

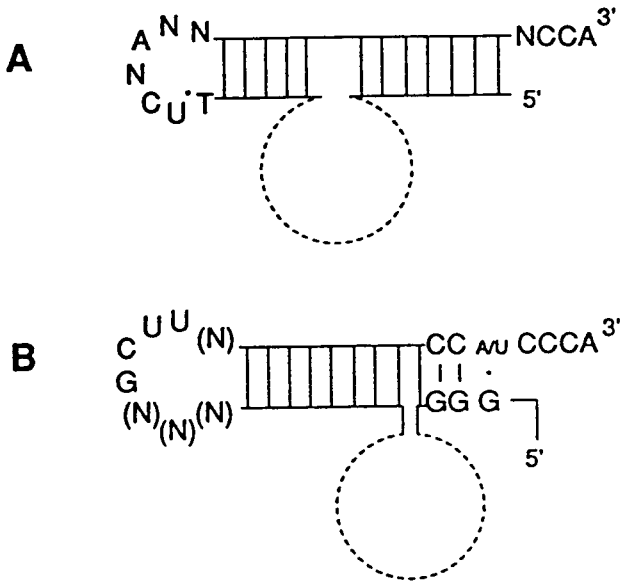

Figure I-6. Secondary structure homology between the 3′ end of bacteriophage RNA and tRNA. A. Classical aminoacyl acceptor domain of tRNA in which the T stem in stacked upon the aminoacyl acceptor stem. The dashed line represents the D stem/anticodon domain. B. Putative aminoacyl acceptor domain at the 3′ end of RNA coliphage (Adhin *et al.*, 1990). The dashed line represents the variable region of about 35 nucleotides. (N) represents nucleotides not found in all phage RNAs (taken from Mans *et al.*, 1991).

B. Possible Functions of Viral tRNA-like Structures

a. A Possible Role Regarding Translation

Possible functions for viral tRNA-like structures have been proposed since their discovery (Hall, 1979; Haenni *et al.*, 1982; Florentz *et al.*, 1984; Dreher and Hall, 1988a; Mans *et al.*, 1991). Based on efficient aminoacylation of the tRNA-like structure *in vitro* (Giegé *et al.*, 1978) and *in vivo* (Joshi *et al.*, 1978; Joshi *et al.*, 1982a; Loesh-Fries and Hall, 1982), as well as the interactions with several factors involved in protein synthesis, the viral tRNA-like structures have been proposed to function as amino acid donors to the ribosome-dependent protein synthesis system. The possibility that tyrosine could be donated from BMV RNA to a nascent peptide was examined in a wheat germ cell-free translation system. However, only trace amounts of [^{3}H]tyrosine were incorporated into acid precipitable form when [^{3}H]tyrosylated BMV RNA was supplied as the donor of activated amino acid substrate (Chen and Hall, 1973). It was therefore concluded that BMV RNA is unlikely to be an amino acid donor involved in peptide chain elongation. Similar conclusions were reported from experiments with valylated eggplant mosaic tymovirus (EMV) and wheat germ extracts (Hall *et al.*, 1979).

A second role at the translational level for tRNA-like structures has been proposed. By virtue of the ability to bind the elongation factor EF-1α, it was suggested that the viral RNA might be able to bind to ribosomes more efficiently than other mRNAs. The viral RNA may even be able to dislodge host mRNA from ribosomes and beneficially position the viral RNA for binding to the newly released ribosomal subunits. Such processes might be expected to assist in the competition with cellular mRNAs for translation (Hall, 1979), but such roles for the viral tRNA-like structures have not received any supporting evidence to date.

Since several viral RNA genomes show complementarity between the 5′ and 3′ terminal sequences (Fig. I-7), and there is experimental evidence for a circular form of TYMV RNA from light scattering measurements (Strazielle *et al.*, 1965), this property has been proposed to play a regulatory role in the viral life cycle (Florentz *et al.*, 1984). In this model, the viral RNA exists in equilibrium between the circular and linear forms. The ORF-206 initiation codon in the 5′ region of the RNA is proposed to be involved in base-pairing with the 3′ complementary sequence and thus to be inaccessible for ribosomes. It was proposed that the remaining secondary structure of the 3′-terminal sequences would permit the binding of valyl-tRNA synthetase, which might then shift the equilibrium toward the linear form in which the initiation codon is available for translation. According to this proposal, the aminoacylation of the tRNA-like structure is not necessarily a requirement, since synthetase binding to the RNA would suffice.

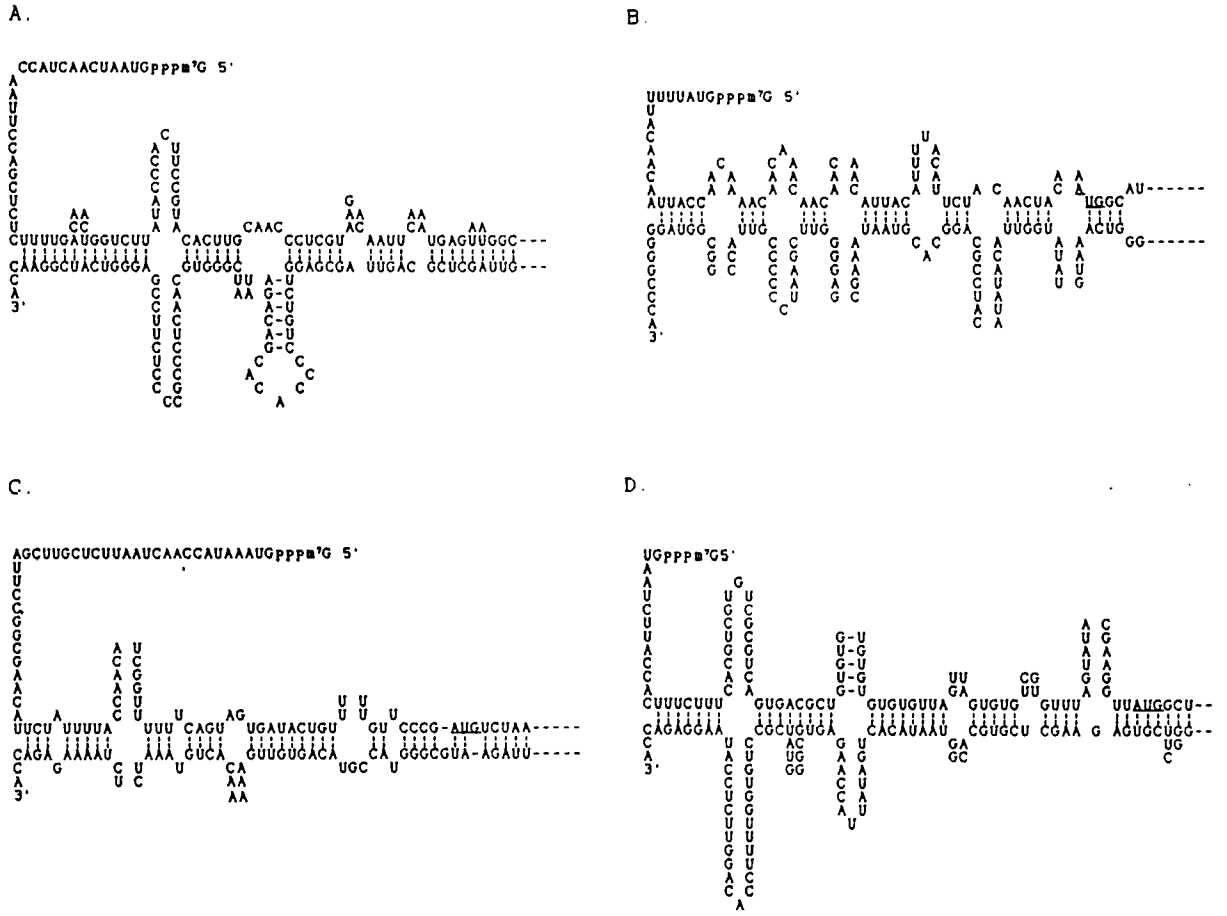

Figure I-7. Structural models of base-pairings between the 5'- and 3'-ends of: A. TYMV, turnip yellow mosaic virus. B. TMV, tobacco mosaic virus. C. BMV, brome mosaic virus (RNA 3). D. CMV, cucumber mosaic virus (Q strain, RNA 3) (taken from Florentz *et al.*, 1984).

b. A Possible Role Regarding Telomere Function

NTase is an enzyme involved in for tRNA maturation, producing functional 3'-CCA_{OH} termini. This enzyme also plays an important role in maintaining the intactness of the 3'-termini of mature tRNAs; these termini are normally subjected to nuclease attack and undergo constant turnover (Deutscher, 1982). Studies with BMV suggest that the 3' termini of viral RNAs undergo a similar turnover *in vivo* (Rao *et al.*, 1989). These studies made use of the finding from *in vitro* replication studies that the *de novo* initiation of (-)-sense RNAs on (+)-sense templates occurs opposite the penultimate 3'-C residue with the insertion of a G residue (Miller *et al.*, 1986). Further analysis of the initiation site using templates after stepwise removal of 3'-terminal nucleotides showed that initiation was unaffected by the removal of the terminal A, but drastically decreased by removal of further residues (Miller *et al.*, 1986). These results suggested that the maintenance of terminal nucleotides is critical for (-)-sense RNA initiation and thus infectivity. In order to assess the importance of 3'-end turnover during infection, the infectivities of four mutants of BMV RNA3 with single or double mutations of the last two nucleotides in the 3'-CCA_{OH} terminus of the tRNA-like structure were tested *in vivo*. All four mutants were deficient with respect to aminoacylation and replication *in vitro* (Dreher *et al.*, 1984), yet replicated with kinetics almost indistinguishable from wild-type in barley protoplasts and plants (Rao *et al.*, 1989). The mutant sequences at the 3' ends of the inoculum RNAs were all restored to wild-type sequence in the progeny.

These results support the existence of active 3' end turnover *in vivo*, presumably utilizing host NTase to repair incomplete termini. Such repair is crucial in retaining intact genomes capable of replication. In this regard, the function of NTase is analogous to that of telomere terminal transferase or telomerase (Rao *et al.*, 1989), which adds tandem repeats at the ends of eukaryotic chromosomal DNAs (Blackburn, 1990). The substrate for NTase, the tRNA-like structure, can thus be considered to function as the telomere of the viral linear RNA genome.

As discussed in Section IC, NTase is thought to play a second role during replication, that of providing the 3'-A residue to complete the 3'-CCA terminus, thus making the genomic RNAs aminoacylatable.

c. Role as Promoters of (-) Strand Synthesis

Experiments mapping (-)-strand promoter activity to the 3' tRNA-like structures of BMV and TYMV were mentioned in Section ID. The implications of the coincidence between sequences involved in (-) strand promotion and tRNA mimicry have been investigated with BMV, where (-) strand promoter activity, tyrosylation and NTase-dependent 3'-adenylation (of 3'-CC termini) coincide in the same 134-nucleotide-long tRNA-like fragment. An extensive mutational analysis studied the

relationships between promoter activity, tyrosylation, 3′-adenylation *in vitro* and the integrity of the tRNA-like structure. Disruption of the tRNA-like structure, by introducing helix-disrupting substitutions into the pseudoknot of the aminoacyl acceptor stem, resulted in loss of all three *in vitro* activities. These activities were rescued by compensating secondary mutations that permitted a pseudoknot similar to that in wild-type RNA to form (Dreher and Hall, 1988b; 1988c). Thus, promoter function and tRNA mimicry depend on the overall tertiary conformation of the 3′ region.

The precise ways in which tRNA-like structures might promote (-)-strand synthesis have not been determined. Further, it has not been clearly resolved whether aminoacylation is critical in promoter function. This question was probed by the mutagenic studies of BMV RNA mentioned above. Although some sequences important for (-)-strand synthesis, tyrosylation and adenylation overlapped, additional sequence requirements were different for each property. Thus, a number of mutants with defects in specific activities were obtained. These mutations were introduced into BMV RNA 3 transcripts, which were co-inoculated onto barley protoplasts with wild-type RNAs 1 and 2. Recall that BMV RNAs 1 and 2 encode all the essential proteins and are able to support the replication *in trans* of RNA 3.

In order to understand the relationship between replication and tyrosylation, the BMV RNA 3 mutants which were inefficiently tyrosylated *in vitro*, were analyzed as *trans*-replication substrates *in vivo*, using barley protoplasts and plants (Dreher *et al.*, 1989). The *in vivo* replication levels were found to be correlated with (-)-strand promoter activity determined *in vitro*, rather than with tyrosylation or adenylation properties. Mutants B3-Δ5′ and B3-5′AGA, which were specifically defective in tyrosylation *in vitro* (initial tyrosylation rates 5% and 3% relative to wild-type; tyrosylation plateaus 19% and 17% of wild-type, respectively), replicated to levels 60-70% of wild-type *in vivo* (Dreher *et al.*, 1989). When present at the 3′ end of RNA 2 rather than RNA 3, the above mutations had different effects. The Δ5′ mutation acted as a *trans*-dominant inhibitor of the replication of all the BMV RNAs (Rao and Hall, 1991), as if the mutation were titrating an essential factor. The 5′-AGA mutation affected the level of RNA 2 only, and appears to have had a slightly more negative effect on RNA 2 replication than on RNA 3 when present on that RNA (Rao and Hall, 1991). The replication of variants of RNA 3 bearing two further mutants with adenylation defects were also studied *in vivo*. B3-ψGG, only 15% of whose progeny had correct (i.e. potentially tyrosylatable) 3′-CCA termini, replicated to 40% of wild-type (Dreher *et al.*, 1989). Only 5-10% of B3-5′PsK progeny had 3′-CCA ends, and these molecules were effectively non-tyrosylatable *in vitro* (Dreher and Hall, 1988c), yet the mutant RNA replicated without sequence alteration to 20% of wild-type levels (Dreher *et al.*, 1989). These results suggest that tyrosylation in BMV is not mandatory for replication.

Circumstantial evidence from two other viral systems supports the conclusion that aminoacylation is not crucial for replication. Among the cucumoviruses, which are closely related to BMV, cucumber mosaic cucumovirus (CMV) RNAs can be tyrosylated (Kohl and Hall, 1974), while

the RNAs of tomato aspermy cucumovirus (TAV) failed to be tyrosylated at any detectable levels, although the 3'-CC derivatives could be adenylated by NTase *in vitro* (Joshi and Haenni, 1986). Despite these differences in aminoacylatability, TAV RNA 3 could be replicated in the presence of co-inoculated CMV RNAs 1 and 2 (Rao and Francki, 1981). Thus, the CMV replicase is apparently able to replicate tyrosylatable and non-tyrosylatable RNAs to a comparable extent. Experiments with TMV showed that substituting the 3' tRNA-like structure with those from other histidylatable tobamoviral RNAs, from the valylatable CcTMV RNA and from the tyrosylatable BMV RNA did not prevent replication (Ishikawa *et al.*, 1988; 1991), suggesting that specific aminoacylation is not obligatory for TMV RNA replication. The tobamoviral RNAs differ from the bromoviral, CMV and tymoviral RNAs by their inefficient charging, which in itself suggests that aminoacylation may be less crucial in tobamoviral than in other systems.

Whether or not aminoacylation is crucial to the replication of the viral RNAs discussed above, the most likely explanation for the coincidence of tRNA-like structure and promoter is that proteins, presumably host proteins that are normally involved in tRNA metabolism or function, recognize the viral tRNA-like structures and become sequestered into replication complexes (Hall, 1979; Dreher and Hall, 1988a). The replicase of Qß bacteriophage remains a model for the plant viral replicases. Replicase obtained from Qß-infected *E. coli* cells is made up of two *E. coli* elongation factors, EF-Tu and EF-Ts, as subunits (Blumenthal *et al.*, 1972). The interactions *in vitro* of viral tRNA-like structures from BMV and TYMV with elongation factors have been mentioned above (Litvak *et al.*, 1973; Bastin and Hall, 1976; Joshi *et al.*, 1984; Joshi *et al.*, 1986). These results have led to the proposal that the plant viral tRNA-like structures interact with host elongation factor, which may then function as a factor in the replicase complex in viral replication. This function is not necessarily dependent on obligatory aminoacylation of the viral RNAs (elongation factors bind charged tRNAs far more readily than uncharged), since Qß RNA itself cannot be charged. Preliminary experimental results do not support EF-1α involvement in the plant viral replicases: EF-1α was not detected in the replicase preparation from Chinese cabbage plants infected with TYMV by either an enzyme-linked immunosorbent assay (Joshi *et al.*, 1986) or an immunoblotting assay (Pulikowska *et al.*, 1988). Biochemical characterization of the viral replicases will be needed to confirm these results, and decide whether other tRNA-associating host proteins act as replicase subunits.

C. Evolution

The tRNA-like structures at the 3' end of plant viral genomes have been suggested to represent living fossils retained from the early stages of evolution (Weiner and Maizels, 1987). These authors' genomic tag model invokes tRNA-like structures as key features in the evolution of RNA enzymes from the self-replicating RNA genomes that are postulated to have existed in archaic times. In the RNA

world, it was suggested, genomic RNA molecules had a special 3′-terminal tag that served both to identify the molecule as a substrate for the replicase (a catalytic RNA molecule) and to specify the initiation site for replication. RNA molecules lacking this tag would not be efficiently replicated and could not function as genomes. This hypothesized 3′ genomic tag was viewed as the prototypical tRNA-like structure (Weiner and Maizels, 1987). Derivatives of 3′-tagged genomes could be made by removal of the tRNA-like structure by cleavage (perhaps involving an enzyme such as the catalytic RNA of RNase P; Guerrier-Takada *et al.*, 1988; Pace and Smith, 1990), revealing enzyme activities previously constrained by the presence of the bulky genomic tag. The very 3′ end of the genomic tag ($-CCA_{OH}$) was postulated to serve as part of the telomere to prevent loss of genomic information from the linear genomes (Weiner and Maizels, 1987). This $-CCA_{OH}$-ended telomere might have been the ancestor (Weiner, 1988) of the telomeres found in modern DNA genomes, which contain end sequences based on the motif G_nT_m motif (Blackburn and Szostak, 1984; Blackburn, 1990). The genomic tag model as applied to viruses such as TYMV implies that the main functions of the tRNA-like structure are as (-)-strand promoter and telomere.

As an alternative to evolution of present-day tRNA-like structures in direct lineage from genomic tags present in the RNA world, it seems possible that viruses such as TYMV and all its elements evolved far more recently. Among present-day viruses, the involvement of tRNA-like properties or structures in viral RNA replication is a recurring theme. The retroviruses in eukaryotic cells use host tRNAs as primers in the initiation of genome replication by reverse transcriptase, which specifically binds the tRNA (Varmus, 1988; Kuiper and Lambowitz, 1988). Except that the tRNA is separated from the 3′ end of the (retroviral) genome, the strategy could be said to resemble the plant viral use of tRNA-like structures as (-) strand promoters. The replication machineries of other RNA viruses also apparently have an affinity for tRNA-like molecules, since defective interfering RNAs that include host tRNA sequences have been reported for both Sindbis alphavirus (Monroe and Schelsinger, 1983) and the phage Qß (Munishkin *et al.*, 1988).

Other observations linking the replication of RNA viruses to tRNA biology have been reported recently, suggesting that the eukaryotic virus replicase systems may have evolved from host RNA polymerase III (Marsh and Hall, 1987). Transfer RNAs and some small RNA molecules are transcribed by RNA polymerase III with the help of several transcription factors (Sprague, 1992); of interest, one of the factors has recently been discovered to be a tRNA (L. Young and K. Sprague, unpublished). The transcription factors assist in the recognition of two intragenic control regions (ICRs) that act as promoter elements directing transcription (Geiduschek and Tocchini-Valentini, 1988). In the tRNA gene promoters, these ICRs correspond to the sequences of the D- and T-loops. Although these ICR promoter sequences have not been found in viral 3′ tRNA-like structures, several viral RNAs harbor ICR-like sequences in their 5′ noncoding regions (Marsh and Hall, 1987; Marsh *et al.*, 1989). In BMV, these two ICRs (ICR1 and ICR2) are located at the very 5′ end of the genome and are present

in a stem-loop structure. Point mutations in the ICR2, which occurs in a loop (Pogue *et al.*, 1990), or mutations in the ICR1, which occurs in a stem region, that abolished stem formation resulted in impaired BMV RNA replication in protoplasts (Pogue and Hall, 1992).

III. RNA Pseudoknots

A. The Pseudoknots Present in Plant Virus RNAs

A pseudoknot is a structural element in an RNA molecule in which the nucleotides within a loop (hairpin loop, bulge loop, etc.) basepair with nucleotides outside that loop. According to this definition, 14 different types of pseudoknots can be formed in principle (Pleij and Bosch, 1989; Pleij, 1990). A survey of the literature shows that at least 10 types of these pseudoknots have been reported (Mans, 1991). Except for a B-pseudoknot in the tRNA-like structure of TMV, which involves basepairing with a bulge loop, the pseudoknots found in tRNA-like structures of plant viral RNAs belong to the H type in which nucleotides in a hairpin loop basepair with nucleotides in a nearby single-stranded region. The pseudoknots of the plant viral tRNA-like structures are important in constituting the amino acid acceptor arm of the tRNA-like structure (section II of this chapter). Pseudoknots have also been found in the region immediately upstream of the tRNA-like structures of several plant viral RNAs.

a. Pseudoknots in the tRNA-like Structures

The importance of the pseudoknots in the acceptor stems of viral tRNA-like structures has been tested. A three-base substitution that disrupted the base-pairing of the pseudoknot which is part of the proposed acceptor stem of BMV RNA was shown to simultaneously impair replication, aminoacylation and NTase-dependent adenylation activities *in vitro*. Compensatory changes designed to restore the pseudoknot were demonstrated to restore some or most of each of these functions (Dreher and Hall, 1988b; 1988c). Analysis of a series of mutations in the pseudoknot structure of TYMV RNA showed that disruption or distortion of the pseudoknot impairs valylation, assayed *in vitro* using a wheat germ extract (Mans *et al.*, 1992). The length of the 4-base-long loop 1 (Fig I-4A) could be varied between 2 and 8 nucleotides with little effect on valylation, but the complete removal of loop 1 resulted in a total loss of valylatability. Both the length and the sequence of loop 2 were shown to be important for maintaining the integrity of the pseudoknot and functional valylation. Stem 1, comprising three G:C basepairs, was important for efficient valylation: any base pairs besides C:G and any substitutions that disrupted base pairing were shown to impair valylation.

Pseudoknots are structural elements of relatively low stability (Wyatt *et al.*, 1990), whose conformations are responsive to varying solution conditions, such as alteration of Mg^{2+} levels (Rietveld *et al.*, 1983). As physiological conditions vary, the pseudoknot may be denatured; this transition may function as a molecular switch converting the tRNA-like structure between states that are active and

inactive in mimicking tRNA properties (Mans, 1991). This may play a role in regulating viral functions.

b. Pseudoknots Immediately Upstream of the tRNA-like Structure

Five pseudoknots are present in the 204 nucleotide-long 3′ noncoding region of TMV RNA (van Belkum *et al.*, 1985). Two of them are involved in the tRNA-like structure, the remaining three being located immediately upstream of the tRNA-like structure. The existence of these three consecutive H-type pseudoknots was proposed on the basis of chemical modification and enzymatic digestion, and was supported by comparisons with structures predicted for the RNAs from other tobamoviruses: TMV-L (tomato strain), CcTMV (cowpea strain), and CGMMV (watermelon strain or cucumber green mottle mosaic virus) (van Belkum *et al.*, 1985). Pseudoknots immediately upstream of the tRNA-like structure have also been found in BMV and TYMV (Pleij *et al.*, 1987).

To elucidate the biological functions of the upstream pseudoknot region in TMV RNA, several mutations were introduced into these three consecutive pseudoknots, including deletions and nucleotide substitutions; the replication activities of these mutant RNAs were tested in both tobacco plants and protoplasts (Takamatsu *et al.*, 1990). Deletion studies showed that the first pseudoknot (5′ pseudoknot) is dispensable for TMV replication. Extension of the deletion into the central pseudoknot region resulted in reduction in viral multiplication, accompanied by loss of development of mosaic symptoms on systemic tobacco plants. Cessation of viral replication was observed when the deletions disrupted the formation of the 3′ pseudoknot. Point mutations that destabilized the 3′ pseudoknot resulted in a loss or great reduction of viral replication, whereas complementary mutations restored the pseudoknot and restored TMV replication to nearly the wild-type level. Thus, the pseudoknot structure, rather than primary sequence, is required for TMV replication (Takamatsu *et al.*, 1990).

At present, the role of the upstream pseudoknots is unclear, but they may act as spacers that make the tRNA-like structure accessible at the surface of the folded viral RNA as elements bound by proteins necessary for viral function, or they may be involved in improving the stability of the viral RNA. Some evidence for the latter suggestion has been obtained for TMV. The entire 3′ noncoding region of TMV RNA, including the tRNA-like structure and upstream pseudoknot domain, has been tested as a functional replacement of the poly(A) tail of an mRNA in plant and animal cells. Like the poly(A) tail, the TMV 3′ noncoding region increased mRNA stability and translational efficiency when placed at the 3′ end of an mRNA (Gallie and Walbot, 1990). When the extended tertiary structure was dissected, the upstream pseudoknot domain was found to be largely responsible for increasing reporter gene (ß-glucuronidase, GUS) expression. However, the 3′-terminal tRNA-like structure was required for optimal function. Further studies showed that the contribution of the tRNA-like structure in potentiating mRNA expression was lost after removal of the 3′-terminal 6 nucleotides, which disrupted

the pseudoknot in the acceptor arm. The contribution of the 3' noncoding region to gene expression was decreased when the upstream pseudoknots and the downstream tRNA-like structure were separated by 5 nucleotides (Gallie *et al.*, 1991).

B. Occurrence and Function of Pseudoknots in Other RNAs

a. Pseudoknots Involved in Frameshifting

Frameshifting is a strategy of viral gene expression, in which a termination codon can be avoided and a fusion protein can be synthesized from two overlapping reading frames. The production of some retroviral *gag-pol* or *gag-pro-pol* fusion proteins has been demonstrated to involve frameshifting (Jacks *et al.*, 1988; Wilson *et al.*, 1988). Normally, termination occurs at the *gag* stop codon to yield virus core protein. However, as ribosomes enter the overlap region, a proportion of them shifts to the -1 frame, permitting the synthesis of a fusion protein; the viral reverse transcriptase (the *pol* gene product) is subsequently released by proteolytic cleavage. The frameshifting requires two elements in the mRNA, a "shifty" sequence at which the ribosome slips and an associated, downstream RNA secondary structure. In several instances, a pseudoknot is the key feature of this secondary structure, as demonstrated with compensatory mutations introduced into base-paired regions (e.g. Chomorro *et al.*, 1992).

Besides the retroviruses, avian infectious bronchitis coronavirus (IBV) has been found to use frameshifting to express the viral RNA-dependent RNA polymerase (Brierley *et al.*, 1987). IBV has a large, single-stranded, monopartite RNA genome with positive polarity. Two large open reading frames, F1 and F2, overlap by 42 nucleotides, with F2 in the -1 frame with respect to F1. A highly efficient -1 ribosomal frameshift (around 25-30%) suppresses the F1 termination codon (Brierley *et al.*, 1987). Deletion analysis defined an 86 nucleotide sequence encompassing the overlap region that was sufficient to allow frameshifting in a heterologous context (Brierley *et al.*, 1989). This element consists of a stem-loop downstream of the site of frameshifting and a sequence of 7 bases further downstream from the 3' end of the stem that are complementary to the hairpin loop, forming a pseudoknot structure. Mutations that disrupted either stems of the pseudoknot severely reduced frameshifting, while compensatory mutations that restored the pseudoknot also restored frameshifting (Brierley *et al.*, 1989).

The double-stranded RNA viruses of *Saccharomyces cereviseae*, L-A and L1, have genomes encoding two large ORFs overlapping by 134 and 129 bases, respectively. The first ORF encodes the capsid protein, and the second ORF which encodes the putative RNA-dependent RNA polymerase, has been demonstrated to be read via a -1 ribosomal frameshifting event. The RNA elements required for frameshifting were identified as both the shifty sequence and a downstream pseudoknot (Dinman *et al.*, 1991; Tzeng *et al.*, 1992).

b. Pseudoknots Involved in mRNA Regulation and Translation

Evidence from three systems indicates that pseudoknots can act as specific recognition elements for protein binding. The 5' region of the α operon mRNA in *E. coli* contains a pseudoknot which was proposed to be a translational suppressor recognition region. The existence of this pseudoknot structure was determined by probing with nucleases specific for single- or double-stranded RNA (Deckman and Draper, 1987). A systematic dissection of the structure using mutagenesis and suppressor binding experiments showed that this RNA contained an unusual "double pseudoknot" structure (Tang and Draper, 1989). Further, the repressor protein S4 was shown to bind to the pseudoknot (Tang and Draper, 1989). Likewise, translation of mRNA from the *E. coli rpsO* operon is repressed by ribosomal protein S15 by binding to a pseudoknot element in the 5' noncoding region (Philippe *et al.*, 1990). It was suggested that protein S15 interaction with the mRNA triggers and stabilizes the pseudoknot conformation. Finally, experiments with the single strand nucleic acid binding gene *32* protein of bacteriophage T4 suggest that a pseudoknot in gene *32* mRNA acts as the nucleation site for the highly cooperative binding of the gene *32* protein (McPheeters *et al.*, 1988); as in the examples above, this binding accomplishes autogenous translational repression (Gold, 1988).

The application of a procedure using sequential cycles of RNA binding to select for high affinity substrates (SELEX: systematic evolution of ligands by exponential enrichment) has supported the idea that proteins can specifically recognize and bind pseudoknot elements in RNAs. Starting with a randomized sequence variant of HIV-1 RNA and applying SELEX selection with HIV-1 reverse transcriptase binding, Tuerk *et al.* (1992) identified pseudoknots in all the high-binding-affinity RNAs selected. The binding may be physiologically relevant, since at least one of the RNA ligands was able to inhibit cDNA synthesis by HIV reverse transcriptase.

Pseudoknots have also been proposed to be involved in RNA splicing (Pleij, 1990), and have been identified in the RNase P catalytic RNA subunit, and in 16S ribosomal RNAs, although their roles in these RNAs are not understood (Pleij, 1990).

IV. Transfer RNA Identity

A. Background

Transfer RNA plays a crucial role in the translation of genetic information from nucleic acid to protein. Each tRNA can be charged with an amino acid by its cognate aminoacyl tRNA synthetase (aaRS). Through this process, the anticodon trinucleotides in the tRNA become associated with a specific amino acid in the form of a charged tRNA. After aminoacylation, there is no further proofing for correct charging; thus, the selection of the appropriate tRNAs by a given aaRS from the complex mixture present in cells is a key step in maintaining the fidelity of translation. The degeneracy of the genetic code, whereby more than one triplet codon corresponds to a given amino acid, requires that multiple tRNAs (isoacceptors) with the same amino acid specificity but with distinct anticodons are charged by the same aaRS. In the context of invariant bases and similar secondary and tertiary structures, aaRS's must be able to recognize a set of distinct elements in isoacceptor tRNAs that constitute the *identity determinants* (Normanly and Abelson, 1989; Hou *et al.*, 1989). Identity elements can be both positive and negative. Positive elements are the features in the tRNAs that the cognate aaRS can recognize directly, and the negative elements are the features that impede the recognition by other aaRSs (Normanly and Abelson, 1989). Typically, a small number of nucleotides constitute the major determinants of tRNA identity, although some other nucleotides are frequently needed for complete identity.

B. Defining the tRNA Identity

Three genetic approaches have been used to determine tRNA identity. In the first, the effects of modifying or replacing nucleotides in a tRNA directly by an enzymatic method *in vitro* were studied. The anticodon and the adjacent hypermodified nucleotide (residues 34-37) of yeast $tRNA^{Phe}$ (Bruce and Uhlenbeck, 1982a; 1982b), and (residues 33-35) of yeast $tRNA^{Tyr}$ (Bare and Uhlenbeck, 1985) were replaced with various oligoribonucleotides by a series of chemical cleavage, ribonuclease digestion and T4 RNA ligase manipulations. This approach permits the replacement of target nucleotides without altering the other (including hypermodified) residues, but is limited to defined segments of the tRNA, usually loop regions.

In the second approach, suppressor tRNAs with various mutations on are used to define tRNA identity *in vivo*, via testing the efficiency of suppression of a defined termination codon in a reporter protein (Normanly *et al.*, 1986). *E. coli* cells are transformed simultaneously with a plasmid expressing a synthetic suppressor tRNA and a plasmid carrying a reporter protein gene; the reporter gene has a specific nonsense codon that can be suppressed by the insertion of an amino acid under the

direction of the suppressor tRNA. The identity of the amino acid inserted by variants of the suppressor tRNA, can be assessed either by enzyme activity measurements or by direct amino acid sequencing. Thus, tRNA identity can be assayed in a proper physiological context, but there are two disadvantages of this approach. First, the anticodon of the tRNA is restricted, since it must decode one of the nonsense codons; limits this approach to the assay of identity determinants outside the anticodon. This limitation has been overcome to some degree by using a modified initiator tRNA and appropriately mutated initiation codon of the reporter gene in place of the suppressor tRNA and suppressible nonsense codon, respectively. Thus, various anticodons can be studied (Chattapadhyay *et al.*, 1990; Pallanck and Schulman, 1991). Second, since the interaction between the suppressor tRNA and aaRS can only be measured by the efficiency of suppression, the contribution of a particular element to identity cannot always be separated from other processes, e.g. tRNA transcription, modification, processing and acceptance by the ribosomes. This assay therefore does not simply represent the true efficiency of aminoacylation (Normanly and Abelson, 1989).

In the third approach, tRNA and their variants are synthesized *in vitro* from cloned genes under the control of the bacteriophage T7 promoter (Sampson and Uhlenbeck, 1988). These *in vitro* tRNA transcripts have the correct 3′ ends and usually the correct 5′ ends, but do not contain the hypermodified bases found in native tRNA. The characteristics of the aminoacylation can be directly quantified by determining the kinetic parameters, K_M for tRNA as substrate, and k_{cat} or V_{max}. The main advantage of this approach is the ability to alter sequences in virtually all parts of the tRNA molecule, and to assess their involvement in identity determination. The main disadvantage is the absence of modified bases. In most cases, this does not have a large influence on the kinetic parameters K_M and k_{cat} (e.g. Sampson and Uhlenbeck, 1988), but there is evidence that fully unmodified tRNAs are more liable to be mischarged by another aaRS (Perret *et al.*, 1990).

Three strategies have been used to test the significance of particular identity determinants. The most common strategy is a subtractive one, in which selected mutations in a test tRNA are made in order to determine the effect of the mutation in degrading identity. The transplantation of identity is another common strategy, used to switch the identity of a given tRNA by changing as few nucleotides as possible, converting the molecule to a cognate tRNA in a non-cognate tRNA background (e.g. $tRNA^{Ala}$ transplanting by Hou and Schimmel, 1988; McClain and Foss, 1988; and $tRNA^{Met}$ and $tRNA^{Val}$ switching by Schulman and Pelka, 1988). The third strategy is to molecularly dissect a tRNA into pieces to delineate determinants for tRNA identity. Truncated RNAs such as the "minihelices" comprising the T-stem or "microhelices" comprising the acceptor stem alone, have been used to study the major identity determinants of $tRNA^{Ala}$ (Francklyn and Schimmel, 1989; Musier-Forsyth *et al.*, 1991).

Other approaches that describe the physical interaction between an aaRS and its cognate tRNA have been used to support the above approaches. Footprinting studies (e.g. Schatz *et al.*, 1991;

Rudinger *et al.*, 1992a) and X-ray crystallography of aaRS/ATP/tRNA co-crystals ((Rould *et al.*, 1989; 1991; Ruff *et al.*, 1991) help define the intimate contacts between aaRS and tRNA, which in many cases involve identity elements. The atomic resolution of X-ray crystallography can identify direct molecular contacts and the functional groups involved.

C. Identity Determinants of Valylatable RNAs

a. Identity determinants of *E. coli* $tRNA^{Val}$

Since an anticodon sequence directly links aminoacylation to the genetic code, this would be a logical site to specify the amino acid to be coupled to a tRNA. However, based on early studies of nonsense suppressors in *E. coli* derived from glutamine, leucine, serine and tyrosine tRNAs, which insert the "correct" amino acid in spite of single base changes in the anticodon, the anticodon could not be the sole determinant of tRNA specificity in all tRNAs. Nevertheless, significant reductions in the efficiency of aminoacylation of several *E. coli* tRNAs have been found to result from base changes in the anticodon, and it has been realized that the anticodon functions not only in translating the genetic code during protein synthesis, but also in specifying the identity for specific aminoacylation in at least some tRNAs, such as $tRNA^{Val}$, $tRNA^{Met}$ (Schulman and Pelka, 1988), and $tRNA^{Phe}$ (Bruce and Uhlenbeck, 1982a; 1982b).

The major determinants of $tRNA^{Val}$ in *E. coli* were first revealed in *in vitro* experiments, by switching the anticodons between $tRNA^{Met}$ and $tRNA^{Val}$ (Schulman and Pelka, 1988). An elongator $tRNA^{Met}$ transcript was a poor substrate for *E. coli* ValRS and had a V_{max}/K_M value 200,000-fold lower than that of a $tRNA^{Val}$ transcript. Replacement of the methionine CAU with the valine UAC anticodon converted $tRNA^{Met}$ into an efficient substrate for the *E. coli* ValRS and increased the V_{max}/K_M value by a factor of 20,000. Further dissection of this effect showed that the 3′ anticodon nucleotide C36 of $tRNA^{Val}$ plays an important role in conferring the specificity for valine acceptance to $tRNA^{Met}$ (Schulman and Pelka, 1988). An A35→G35 mutation introduced into the *E. coli* $tRNA^{Val}$ anticodon (converting it to an alanine anticodon UGC) resulted in a 10,000-fold decrease in the specificity of valylation relative to the $tRNA^{Val}$ transcript. The reverse experiment, "transplanting" the $tRNA^{Val}$ anticodon (UAC) to $tRNA^{Ala}$ (anticodon UGC) by a single nucleotide substitution, showed that the mutant $tRNA^{Ala/UAC}$ transcript had a V_{max}/K_M value for valylation only 5-fold less than that of the $tRNA^{Val/UAC}$ transcript (Tamura *et al.*, 1991). The results of these *in vitro* experiments indicate that both nucleotides A35 and C36 in the anticodon are the major determinants of $tRNA^{Val}$ identity.

The role of the anticodon in $tRNA^{Val}$ identity has not only been defined *in vitro*, but also explored *in vivo* using a modified initiator $tRNA^{fMet}$ bearing a $tRNA^{Val}$ anticodon (GAC). Valine was correctly inserted into protein, dependent on the supply of a GUC initiation codon complementary to

the anticodon of the initiator $tRNA^{fMet/GAC}$ (Chattapadhyay *et al.*, 1990). Mutations in the middle A35 and 3′ C36 nucleotides of the valine anticodon in the initiator $tRNA^{fMet/GAC}$ caused a 100- and 500-fold decreases relative to wild-type in valine insertion for the C35 and U35 mutants, respectively, and no valine insertion for the A36 and U36 mutants (Pallanck and Schulman, 1991).

Besides the anticodon, the discriminator base A73 was also shown to play a secondary role in determining *E. coli* $tRNA^{Val}$ identity. When A73 in $tRNA^{Val}$ was changed to C73, G73 or U73, the specificity of valine acceptance dropped, and V_{max}/K_M values were 5, 55 and 1000-fold lower than that of the wild-type $tRNA^{Val}$ transcript, respectively (Tamura *et al.*, 1991). A fluorine-19 nuclear magnetic resonance study comparing free and ValRS-complexed *E. coli* $tRNA^{Val}$ indicated that ValRS interacts with $tRNA^{Val}$ along the entire inside of the L-shaped molecule, from the acceptor stem to the anticodon (Chu and Horowitz, 1991). Thus, it is conceivable that other minor identity determinants will be found in the future.

Little is known of the valine identity determinants of $tRNA^{Val}$ from other sources. However, studies of the valylation of yeast $tRNA^{Val}$ that have used minihelices derived from the amino acid acceptor and anticodon arms also suggest the involvement of the discriminator base and the anticodon in identity determination in the yeast system. The amino acid acceptor minihelix could be valylated to levels 0.02 to 0.025 mol val/mol RNA by yeast ValRS, with a V_{max}/K_M value 600,000-fold lower than that of $tRNA^{Val}$. This valylation was abolished by the A73 → G73 substitution of the discriminator base, and could be stimulated to some degree by adding another minihelix representing the anticodon stem-loop (Frugier *et al.*, 1992). The latter stimulation was dependent on the presence of a correct valine anticodon (Frugier *et al.*, 1992).

b. Identity Determinants of TYMV RNA Recognized by Yeast ValRS

As described in section IIA in this chapter, the 258-nucleotide-long TYMV RNA transcript (TY-Sma; Fig. I-5) containing the entire 3′ tRNA-like structure has the same K_M (for RNA) of 210 nM as yeast $tRNA^{Val}$ when valylated by yeast ValRS (Florentz *et al.*, 1991). This similarity suggests that similar identity determinants are present in $tRNA^{Val}$ and TYMV RNA. Florentz *et al.* (1991) have investigated the identity elements recognized by yeast ValRS in TYMV RNA by introducing substitutions into the TY-Sma transcripts. Variants TY-G56 and TY-U56 with mutations of the middle nucleotide of the anticodon triplet were poorly valylated, and showed V_{max}/K_M values 18,000 and 28,000-fold lower than those of TY-Sma, respectively. These results are similar to those obtained by mutating the middle anticodon position of *E. coli* $tRNA^{Val}$ (A35 → G35; Tamura *et al.*, 1991), but the identity contribution of the 3′ anticodon nucleotide, found to be an important determinant of *E. coli* $tRNA^{Val}$ (Schulman and Pelka, 1988), was not explored in these studies (Florentz *et al.*, 1991).

Mutation of TYMV RNA nucleotide A4, analogue of the discriminator base A73 of $tRNA^{Val}$,

had an effect on valylation similar to that observed in *E. coli* $tRNA^{Val}$ (Tamura *et al.*, 1991). The V_{max}/K_M values for the valylation by yeast ValRS of variants TY-C4 and TY-G4 were decreased by a factor of 30 and 300, respectively, relative to TY-Sma (Florentz *et al.*, 1991). The above results support the suggestion that $tRNA^{Val}$ and TYMV RNA molecules share similar identity determinants.

D. Identity Profiles of Other tRNAS

a. Other tRNAs with Identity Determinants Located in the Anticodon

Besides $tRNA^{Val}$, identity determinants are found in the anticodons of several other tRNAs (Schulman, 1991). The tRNAs with the greatest concentration of identity in the anticodon nucleotides are $tRNA^{Val}$ (discussed above), $tRNA^{Met}$ and $tRNA^{Gln}$, all of which have been studied using *E. coli* tRNAs. For each of these, single substitutions in the anticodon have resulted in V_{max}/K_M decreases of about 10^5-fold (Schulman and Pelka, 1988; Jahn *et al.*, 1991). Methionine identity determinants have been studied by mutating the anticodon of $tRNA^{Met}$, and by transplanting the methionine anticodon nucleotides into $tRNA^{Val}$ (Schulman and Pelka, 1988), and into $tRNA^{Trp}$ (Schulman, 1991). All three anticodon nucleotides act as identity determinants (Schulman, 1991), but the "wobble" nucleotide C34 appears to be the most significant (Schulman and Pelka, 1984). The genetic elucidation of anticodon identity determinants in *E. coli* $tRNA^{Gln}$ (Jahn *et al.*, 1991) has been supported by X-ray crystallographic studies that have explained at the atomic level the recognition of anticodon nucleotides by GlnRS (Rould *et al.*, 1991). As with $tRNA^{Met}$, all three anticodon nucleotides are important identity elements (Jahn *et al.*, 1991). This appears to differ from the situation with $tRNA^{Val}$; the degeneracy of the genetic code, which results in 4 valine codons differing in the 3′ position, would suggest that the wobble (5′) position of $tRNA^{Val}$ is not a crucial identity determinant. This has not yet been tested experimentally.

Other tRNAs possess identity in their anticodons, but in addition possess major determinants in other parts of the tRNA. Even $tRNA^{Gln}$ has significant determinants in the acceptor stem, including the discriminator base (position 73) (Jahn *et al.*, 1991). Examples of tRNAs with significant identity in the anticodon, but with a contribution that falls short of that described for the valine and methionine systems, include *E. coli* $tRNA^{Thr}$ (Schulman and Pelka, 1990), yeast $tRNA^{Asp}$ (Putz *et al.*, 1991), yeast $tRNA^{Phe}$ (Sampson *et al.*, 1989), human $tRNA^{Phe}$ (Nazarenko *et al.*, 1992), and *E. coli* $tRNA^{Arg}$ (Schulman and Pelka, 1989). For these tRNAs, important secondary identity elements exist in other parts of the molecule: the discriminator base (nucleotide 73) and the D-stem in yeast $tRNA^{Asp}$ (Putz *et al.*, 1991), the discriminator base and G20 in the D-loop in yeast and human $tRNAs^{Phe}$ (Sampson *et al.*, 1989; Nazarenko *et al.*, 1992), and A20 in the D-loop of *E. coli* $tRNA^{Arg}$ (McClain *et al.*, 1990).

b. tRNAs with Identity Predominantly in the Amino Acid Acceptor Stem

In *E. coli* $tRNA^{Ala}$, the major identity determinant is located in a single base pair (position 3:70) in the amino acid acceptor stem (Hou and Schimmel, 1988; McClain and Foss, 1988). These conclusions have resulted from *in vivo* suppression studies and *in vitro* studies with synthetic RNAs, including truncated RNAs ("mini-" and "micro-helices"). Identity determinants have been studied by assaying the effects of their removal by substitution from $tRNA^{Ala}$, and by their transplantation into another tRNA. The G3:U70 basepair is the major determinant (McClain *et al.*, 1988; Hou and Schimmel, 1988), perhaps by virtue of the resultant helix irregularity (McClain *et al.*, 1988). Truncated $tRNA^{Ala}$ molecules comprising the amino acid acceptor stem and T stem (minihelix; Francklyn and Schimmel, 1989) were excellent substrates for alanylation *in vitro*, suggesting the absence of critical identity determinants in the D-stem and anticodon stem. Even a microhelix comprising the amino acid acceptor stem could be charged with alanine relatively efficiently, with a k_{cat}/K_M 60-fold lower than that of $tRNA^{Ala}$ (Francklyn and Schimmel, 1989). For these short substrates, the G3:U70 basepair also acts as the major identity determinant (Shi *et al.*, 1990). Using chemically synthesized microhelix $tRNA^{Ala}$ derivatives, Musier-Forsyth *et al.* (1991) have demonstrated that the un-basepaired 2-amino group of G3, which projects into the minor groove of the RNA helix, is a critical recognition element.

In *E. coli* $tRNA^{Ala}$, other nucleotides play a minor role in modifying identity; there include the discriminator base (Shi *et al.*, 1990; McClain *et al.*, 1991), other basepairs in the acceptor stem (G2:C71 and G1:C72), G20 in the D-loop (McClain and Foss, 1988; McClain *et al.*, 1991), and possibly C60 in the T-loop (McClain and Foss, 1988).

All the eukaryotic $tRNAs^{Ala}$ sequenced to date contain the G3:U70 basepair (Sprinzl *et al.*, 1991). Human and insect (*Bombyx mori*) alanine suppressor tRNA genes bearing the G3:U70 basepair and their variants bearing A3:U70 or G3:C70 were synthesized and cloned in *E. coli*. *In vitro* alanylation of the $tRNAs^{Ala}$ purified from *E. coli* with the homologous purified insect or rat liver AlaRSs revealed that single nucleotide changes in the G3:U70 basepair eliminated the alanylation (Hou and Schimmel, 1989). These results imply that the major determinant of the $tRNA^{Ala}$ identity is conserved in evolution.

The identity of *E. coli* $tRNA^{His}$ is also concentrated in the amino acid acceptor stem, although apparently not to the degree it is in $tRNA^{Ala}$. A $tRNA^{His}$ minihelix (T-stem and acceptor stem) could be histidylated with a k_{cat}/K_M 140-fold lower than native, fully modified $tRNA^{His}$ (Francklyn and Schimmel, 1990). A microhelix could be charged by *E. coli* HisRS with a k_{cat}/K_M 500-fold lower than $tRNA^{His}$. The extra G:C basepair present at the 5′/3′ end of the acceptor helix that involves the discriminator base of *E. coli* $tRNA^{His}$ was shown to be a crucial determinant for histidine charging (Himeno *et al.*, 1989).

c. Other Recognition Profiles

In general, tRNA modifications do not play a role in tRNA identity. However, two cases have been reported in which the tRNA modifications do play a crucial role not only in aaRS recognition, but also in codon recognition. *E. coli* $tRNA^{Ile}$, which decodes the codon AUA, contains a hypermodified base called lysidine at the wobble position of the anticodon. Prior to modification, the tRNA contains a CAU methionine anticodon and is efficiently aminoacylated *in vitro* by *E. coli* MetRS, but not by IleRS (Muramatsu *et al.*, 1988). Conversely, the lysidine-modified $tRNA^{Ile}$ is a poor substrate for MetRS, but a good substrate for IleRS. Therefore, the lysidine base in the anticodon is important for IleRS recognition, and also changes the coding role of the tRNA to recognize AUA isoleucine codons and not AUG methionine codons.

The second case concerns yeast $tRNA^{Asp}$, for which it was found in *in vitro* studies that $tRNA^{Asp}$ transcripts containing no modified bases were aminoacylated with arginine by yeast ArgRS with a specificity constant V_{max}/K_M only 20-fold lower than unmodified $tRNA^{Arg}$ transcripts and 550-fold higher than fully modified native $tRNA^{Asp}$ (Perret *et al.*, 1990). The unmodified $tRNA^{Asp}$ transcripts could be charged with aspartate by AspRS as efficiently as native, fully modified $tRNA^{Asp}$, and thus had dual specificity. It was concluded that the base modifications acted as antideterminants towards ArgRS, preventing the charging of the modified $tRNA^{Asp}$ with arginine (Perret *et al.*, 1990).

CHAPTER II

Specific valylation of turnip yellow mosaic virus RNA by wheat germ valyl-tRNA synthetase is determined by three anticodon loop nucleotides

Abstract

The valylation by wheat germ valyl-tRNA synthetase of anticodon loop mutants of turnip yellow mosaic virus RNA has been studied. RNA substrates 264 nucleotides long were made by T7 RNA polymerase from cDNA encompassing the 3′ tRNA-like region of genomic RNA. Substitution singly, or in combination, of three nucleotides in the anticodon loop resulted in very poor valylation (V_{max}/K_M less than 10^{-3} relative to wild type). These nucleotides thus represent the major valine identity determinants recognized by wheat germ valyl-tRNA synthetase; their relative contribution to valine identity, in descending order, was: the middle nucleotide of the anticodon (A56 in TYMV RNA), the 3′ anticodon nucleotide (C55), and the 3′-most anticodon loop nucleotide (C53). Substitutions in the wobble position (C57) had no significant effect on valylation kinetics, while substitutions of the discriminator base (A4) resulted in small decreases in V_{max}/K_M. Mutations in the major identity nucleotides resulted in large increases in K_M, suggesting that wheat germ valyl-tRNA synthetase has a lowered affinity for variant substrates with low valine identity. Comparison with other studies using valyl-tRNA synthetases from *E. coli* and yeast indicates that the anticodon has been phylogenetically conserved as the dominant valine identity region, while the identity contribution of the discriminator base has been less conserved. The mechanism by which anticodon mutations are discriminated also appears to vary, being affinity-based for the wheat germ enzyme, and kinetically-based for the yeast enzyme [Florentz *et al.*, (1991) Eur. J. Biochem. 195,229-234].

Introduction

Turnip yellow mosaic virus (TYMV) has a 6.3 kb (+)-sense RNA genome whose 3′ domain shares several characteristics with tRNA (Hall, 1979; Haenni *et al.*, 1982). The viral RNA can be efficiently and specifically valylated by valyl-tRNA synthetases (ValRS) from sources as diverse as *Escherichia coli* (Pinck *et al.*, 1970), yeast (Giegé *et al.*, 1978) and wheat germ (Dreher *et al.*, 1988). Further, TYMV RNA is valylated in plant cells during the replication cycle (Joshi *et al.*, 1982a), indicating successful competition for ValRS in the presence of high levels of tRNA. We are interested in TYMV RNA as an alternative substrate for ValRS, from whose study new characteristics of aminoacylation specificity may be learnt. By example, the efficient valylation of TYMV RNA, whose only known modified bases are in the 5′ cap, was the first demonstration that the presence of hypermodified bases is not necessary for aminoacylation (Briand *et al.*, 1977; Silberklang *et al.*, 1977). Our studies on the tRNA mimicry of TYMV RNA are also motivated by our desire to understand the relationship between valylation and replication in this virus (Chapter III in this thesis). In this chapter we present an analysis of the contribution that key nucleotides make to the valine identity of TYMV RNA as perceived by a homologous higher plant enzyme, wheat germ ValRS. This work parallels and extends our studies with TYMV RNA and yeast ValRS (Florentz *et al.*, 1991). To date, several studies have revealed the identity elements of specific tRNAs (reviewed in Normanly and Abelson, 1989; Schulman, 1991), including *E. coli* $tRNA^{Val}$ (Schulman and Pelka, 1988; Tamura *et al.*, 1991), but only two have so far addressed identity in higher eukaryotic systems ($tRNA^{Ala}$, Hou and Schimmel, 1989; $tRNA^{Phe}$, Nazarenko *et al.*, 1992).

There is evidence from structure-probing experiments using nucleases and chemical reagents that the 3′ 82 nucleotides of TYMV RNA can fold into a structure that closely resembles the L-conformation of tRNAs (Fig. II-1; Rietveld *et al.*, 1983; Dumas *et al.*, 1987). In this proposed structure, the similarities to canonical tRNAs include the 3′-CCA_{OH} terminus, a 12-base pair amino acid acceptor arm, and 7-membered loops analogous to the pseudouridine and anticodon loops. A valine anticodon CAC is present in the latter loop, whose sequence 59-CCCACAC-53 is similar to the CUIACAC (anticodons underlined; I = inosine) of lupine $tRNA^{Val}$ (Barciszewska and Jones, 1987) and CTAACAC of an *Arabidopsis thaliana* $tRNA^{Val}$ gene (Gokhman and Zamir, 1990), to date the only higher plant $tRNA^{Val}$ sequences available (Sprinzl *et al.*, 1991). The sequence within the pseudouridine loop in the viral RNA (38-UGCA-35) deviates somewhat from the conserved sequence found in tRNAs (TFCPu; F = pseudouridine, Pu = purine). The remainder of the tRNA-like structure differs widely in sequence from eukaryotic $tRNA^{Val}$'s. An important feature specific to the amino acid acceptor arm of the viral RNA is the presence of a pseudoknot near the 3′ terminus (Pleij *et al.*, 1985) (Fig. II-1).

In characterizing the valine identity of TYMV RNA, we have focused for a number of reasons on the nucleotides of the anticodon loop. This region has been shown to interact unambiguously with

yeast ValRS (Florentz and Giegé, 1986) and clearly contains a major determinant recognized by that enzyme (Florentz *et al.*, 1991). In *E. coli* $tRNA^{Val}$, the anticodon also contains major identity determinants (Schulman and Pelka, 1988; Tamura *et al.*, 1991), suggesting that valine identity elements have, like alanine determinants (Hou and Schimmel, 1989), been evolutionarily conserved. Indeed, the anticodon loop is the site of greatest sequence similarity among valylatable viral and transfer RNAs: all eukaryotic $tRNA^{Val}$ species (Sprinzl *et al.*, 1991) and tymoviral tRNA-like structures (van Belkum *et al.*, 1987b) share the sequence 5'-NACAC-3' (anticodon nucleotides underlined). Finally, identity is less likely to reside in those parts of the TYMV tRNA-like structure whose conformations deviate significantly from that of $tRNA^{Val}$, notably the acceptor stem containing the pseudoknot.

Our experimental design has been to deduce valine identity determinants by a subtractive approach. The goal has been to determine the minimal nucleotide substitutions (not involving universally conserved nucleotides) needed to reduce valylation to very low or undetectable levels. Our analysis permits a quantitation of the contribution provided by three nucleotides in the anticodon loop that are key members of the valine identity set. As expected from the fact that TYMV RNA can be valylated with *E. coli*, yeast and wheat germ ValRS, similar identity elements are perceived in the anticodon by the eukaryotic and prokaryotic enzymes.

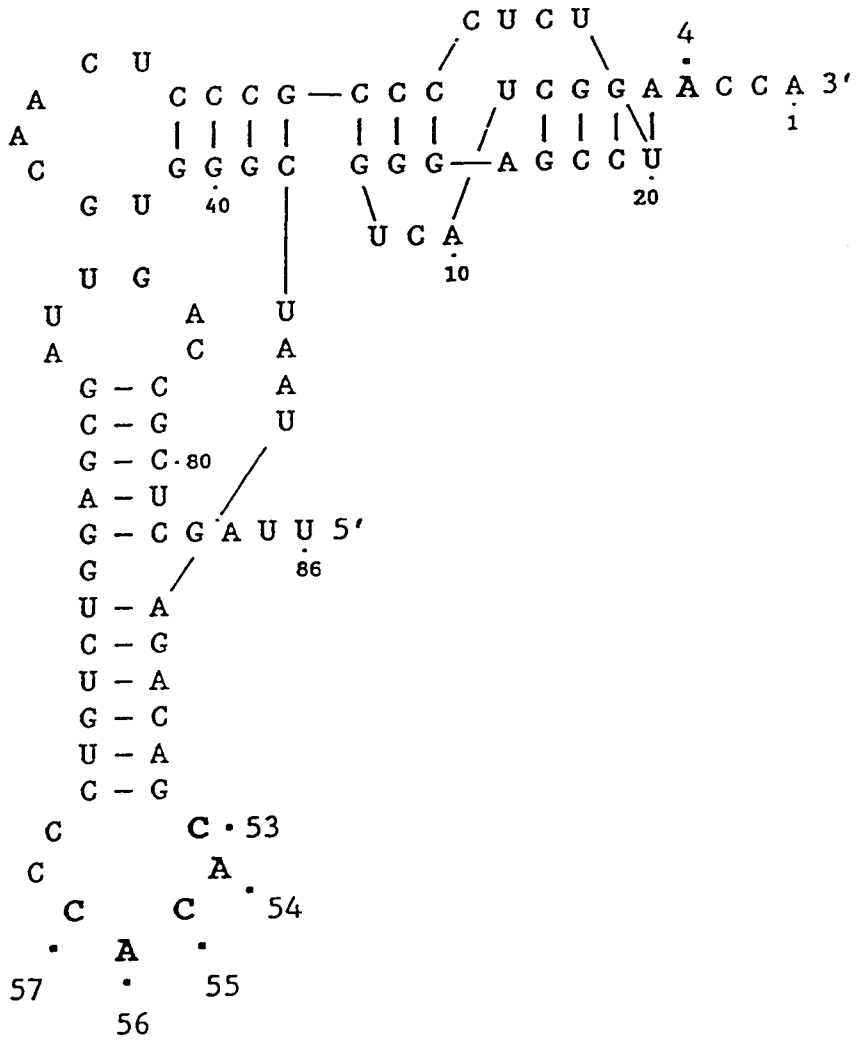

Figure II-1. The proposed L-conformation of the tRNA-like structure of TYMV RNA. The nucleotides substituted in the present studies are shown in bold and include the anticodon 57-CAC-55 and the discriminator base adjacent to the 3′-CCA. Note that nucleotides are numbered from the 3′ end, and only the 86 3′ nucleotides of the 264 nucleotide-long RNAs studied are shown. The 3′ 42 nucleotides are proposed to form the amino acid acceptor stem, which includes a pseudoknot formed by the 3′ 27 nucleotides. Nucleotides $^{5'}$82-47$^{3'}$ form the anticodon stem.

Materials and Methods

Materials. *BstN*I restriction enzyme and T4 RNA ligase were obtained from New England Biolabs, T7 RNA polymerase and T7 DNA polymerase (Sequenase) from U.S. Biochemicals, and Taq DNA polymerase from Promega. Deoxyoligonucleotides were synthesized by automated phosphoramidite chemistry, and purified where necessary on 20% polyacrylamide/7 M urea gels. All enzymes were used as recommended by the manufacturer. [^{3}H]L-valine, [α-^{32}P]UTP, [α-^{32}P]dATP and [5′-^{32}P]cytidine 3′,5′-bisphosphate were obtained from New England Nuclear.

A partially purified cytoplasmic extract from wheat germ, enriched by ammonium sulfate precipitation and DEAE-cellulose chromatography (Steinmetz and Weil, 1986), was used as the source of the ValRS activity. One unit was defined as the amount of enzyme that catalyzes the addition of 1 pmole of [^{3}H]valine to TYMV RNA per minute at 30°C (0.6 μM wild-type transcript RNA, experimental conditions as listed below).

Wild-type and variant TYMV RNAs. Most of the RNAs studied were transcripts arising from cloned DNAs related to mpT7YSma, an M13 clone derived from pT7YSma (Dreher *et al.*, 1988). Replicative form DNA was purified on CsCl gradients and treated with ribonuclease followed by proteinase K to ensure the absence of bacterial tRNA. The DNA was linearized to completion with *BstN*I restriction endonuclease prior to transcription (essentially as described by Dreher *et al.*, 1988) with T7 RNA polymerase (15 units/μg DNA) in the presence of 100 μg/ml DNA, 2 mM each nucleoside triphosphate and 20 Ci/mol [α-^{32}P]UTP. The 264 nucleotide-long RNA transcripts were purified by electrophoresis on 5% polyacrylamide gels run in Tris-borate buffer, followed by electroelution, dialysis against water, and ethanol precipitation in the presence of sodium acetate. The RNAs were
redissolved in water and their concentrations were calculated after determining the incorporated [^{32}P]UMP by liquid scintillation counting.

Mutant variants of mpT7YSma were generated by standard deoxyoligonucleotide-directed mutagenesis using dUMP-containing single-stranded DNA templates (Kunkel *et al.*, 1987). The entire inserts of all mutant clones were sequenced using T7 DNA polymerase.

In a few instances, substrate RNAs were transcribed with T7 RNA polymerase directly from DNA templates made in a polymerase chain reaction, using the opposing deoxyoligonucleotides d(TAATACGACTCACTATAGGGAGAGGGTCAAAGATTCG) and d(TGGTTCCGATGACCCTCG), and Taq DNA polymerase (Appendix I in this thesis). The former oligomer corresponds to the T7 promoter adjacent to TYMV RNA sequences, while the latter oligomer is complementary to the 3′ end of TYMV RNA. The amplified DNA corresponds exactly to the TYMV sequences present in the mpT7YSma-related clones, and ends precisely at the 3′-CCA.

Analysis of 3′ termini of RNA transcripts. RNAs were labelled at the 3′ end by the addition of [5′-^{32}P]cytidine 3′,5′-bisphosphate with T4 RNA ligase (Dreher *et al.*, 1984). After purification by gel electrophoresis to remove degraded molecules, the labelled RNA was analyzed in two ways. The identity of 3′ bases was determined by complete digestion with a mixture of ribonucleases T1, A and T2, followed by two dimensional thin layer chromatography on cellulose plates [first dimension, isobutyric acid-0.5 M NH_4OH, 5:3 (v/v); second dimension, isopropanol-conc. HCl-water, 70:15:14, (v/v/v)] and counting with a ß-emission scanner (Ambis Systems, San Diego). Complete digestion with ribonuclease T1, followed by separation on 20% polyacrylamide/7 M urea gels and densitometry of autoradiographs determined the proportion of transcripts yielding the hexamer expected from 3′-labelled wild-type RNA. Results from the two techniques were combined to determine the proportion of RNAs with 3′-CCA termini as 75 ± 5% for transcripts made from *BstN*I-linearized DNA and 63 ± 5% for transcripts made from DNA templates generated by the polymerase chain reaction.

Valylation assays. Valylation assays were performed in 25 mM Tris-HCl (pH 8.0), 2 mM $MgCl_2$, 1 mM ATP, 0.1 mM spermine and 10 μM [^{3}H]valine (12 Ci/mmol) at 30°C. Kinetic parameters were determined by estimating initial valylation rates over RNA concentrations between 10 and 5000 nM, as appropriate, and analyzing data using double-reciprocal Lineweaver-Burk plots. For the less active mutants, valylations were carried out at twice the above specific activity of [^{3}H]valine, with increased levels of enzyme, and over longer time periods, in order to reliably measure initial valylation rates. The valylation rate was shown to be directly proportional to enzyme concentration over the range of enzyme levels used. Valylation was determined in TCA precipitation assays using Whatman 3MM filters counted in a liquid scintillation spectrometer set to detect both [^{3}H]valine and [^{32}P]RNA.

Results

The synthesis of tRNA-like substrates for ValRS. RNA comprising the 3′ region of TYMV genomic RNA can be transcribed *in vitro* from *BstN*I-linearized mpT7YSma DNA with T7 RNA polymerase. The majority of these 264 nucleotide-long transcripts have 3′-CCA termini, and are as efficiently valylated as natural viral RNA (Dreher *et al.*, 1988). Via mutagenesis of the mpT7YSma DNA, a family of mutant RNAs with substitutions at five nucleotides in the anticodon loop (nucleotides 57-CACAC-53, Fig. II-1) was generated (Table II-1). These nucleotides include the anticodon (57-CAC-55) and nucleotides conserved among eukaryotic $tRNA^{Val}$ (Sprinzl *et al.*, 1991) and valylatable tymoviral RNA species (van Belkum *et al.*, 1987b). Substitutions of the discriminator base adjacent to the 3′-CCA were also studied.

Transcripts used in analyses of valylation kinetics were purified by gel electrophoresis. Because of the length of these RNAs (264 nt), it was not possible to obtain single base resolution, but this purification served to remove degraded molecules and aborted transcription products. The purified RNAs were a small family of related transcripts, the most abundant being the 3′-CCA species. The 3′ termini of all transcript preparations were analyzed as described in **Materials and Methods**, permitting the proportion of the 3′-CCA species in the total population to be deduced; within narrow limits, this proportion was the same for wild-type and all mutants (75 ± 5%). The contaminating RNAs possessed one, or less frequently two, additional nucleotides at the 3′ end, and most commonly terminated in guanosine. All RNA concentrations given in this paper refer to the 3′-CCA species. As shown by the similar valylation characteristics of the wild-type synthetic transcripts and a 3′ fragment prepared directly from virion RNA (Dreher *et al.*, 1988), the minor RNA species do not interfere noticeably with the determination of accurate kinetic parameters.

In some cases (indicated in Tables II-1 and II-2), transcripts were made from DNA templates arising from a polymerase chain reaction (PCR) after amplification from pTYMC-derived DNA. A lower proportion of 3′-CCA termini was present in these transcripts (63 ± 5%), but after adjustment to equal concentrations of the 3′-CCA RNAs, transcripts from PCR-generated or *BstN*I-linearized DNA yielded essentially the same kinetic parameters characterizing their valylation by wheat germ ValRS. Wild-type transcripts could be completely valylated (Fig. II-2, Table II-1). Lineweaver-Burk analysis of initial reaction rates yielded a K_M of 31 nM for the wild-type transcripts (Table II-1), substantially lower than that previously determined in a different buffer (550 nM, determined in 0.1 M HEPES pH 7.6, 48 mM KCl, 5 mM $MgCl_2$, 0.64 mM ATP: Dreher *et al.*, 1988). These results are in line with the influence of different electrolyte environments on the kinetic parameters of tRNAs (K_M values are lower at low ionic strength; Bonnet and Ebel, 1972). We have compared the two aminoacylation conditions, finding similar valylation rates at RNA concentrations well above either K_M, and similar discrimination between mutants (not shown). The present conditions, based on "accurate"

aminoacylation conditions used by Bare and Uhlenbeck (1986), were used in order to permit the determination of K_M and V_{max} values for inactive mutants with greatly elevated K_M's.

Valylation of anticodon mutants. Mutants with substitutions in two anticodon positions, the middle position (wt = A56) and the 3′ position (wt = C55), had severely impaired valylation properties (Fig. II-2, Table II-1). Mutants TY-G56 and TY-U56 could only be valylated at measurable rates with ValRS concentrations 10-fold higher than those used in the valylation of wild-type RNAs. The K_M for both transcripts was about 100-fold higher than for the wild-type, while V_{max} values were about 50-fold lower than for wild-type transcripts. The specificity of valylation of these RNAs, reflected in their V_{max}/K_M relative to wild-type, was about 10^{-4}, indicating the clear importance of A56 as a valine identity element. Mutants with the 3′ anticodon nucleotide replaced by each of the alternative bases were studied. The valylation of each mutant was impaired, and none could be completely charged under normal conditions (Fig. II-2). As for the nucleotide 56 mutants, substitution of C55 resulted in greatly elevated K_M values, 50-75-fold higher than for wild-type RNA (Table II-1). The effect of the nucleotide 55 mutations on V_{max} values were much smaller, and varied depending on the sequence change: TY-U55 had a V_{max} similar to wild-type, but the transversion substitution mutants TY-A55 and TY-G55 had V_{max} values decreased by factors of 3 and 8, respectively, relative to wild-type. With relative V_{max}/K_M values ranging from $1.7\text{x}10^{-2}$ to $1.5\text{x}10^{-3}$ for these mutants, C55 is clearly an important valine identity element recognized by wheat germ ValRS.

With 4 codons in the genetic code specifying valine, ValRS must accept $tRNA^{Val}$ species with at least some variations in the wobble position; inosine and cytidine are common (Sprinzl *et al.*, 1991). We studied mutants with the TYMV wobble nucleotide C57 changed to each of the unmodified alternatives: TY-G57, TY-A57, TY-U57. Both K_M and V_{max} values for these mutants were similar to those of wild-type RNA (Table II-1), indicating that nucleotide 57 is not used by wheat germ ValRS in substrate discrimination.

Valylation of mutants with substitutions in the 3′ part of the anticodon loop. The partial valylatability of TY-U55 made it clear that significant valine identity resides outside the anticodon nucleotides of TYMV RNA. Because the nucleotides 54-AC-53 flanking the anticodon on the 3′ side are conserved among all higher eukaryotic valylatable RNAs, the contribution of these nucleotides to the valine identity of TYMV RNA was studied. Among eukaryotic elongator tRNAs, the analogous nucleotides, number 37 (adjacent to the anticodon) and 38, are only purines and never G, respectively (Grosjean *et al.*, 1982; Sprinzl *et al.*, 1991). We have studied all possible substitutions of unmodified bases replacing A54, and all
but G replacing C53 (Fig. II-1). Mutants TY-G54, TY-C54, TY-U54, TY-A53 and TY-U53 could all be completely valylated under normal conditions (Fig. II-2, Table II-1).

Substitution of A54 with a purine (TY-G54) yielded an RNA with kinetic parameters not significantly different from those of wild-type RNA (Table II-1). The mutants with pyrimidine

substitutions (TY-C54 and TY-U54) also were excellent substrates for ValRS, although their V_{max}/K_M values were slightly decreased relative to wild-type. A54 cannot be considered as a valine identity element used in the recognition of TYMV RNA by wheat germ ValRS, considering the exclusion of pyrimidines from eukaryotic tRNA molecules at this position.

Replacement of C53 with a pyrimidine (TY-U53) likewise resulted in an excellent substrate for ValRS. Although the K_M was 6-fold higher than for the wild-type RNA, the V_{max} was also increased, resulting in a relative V_{max}/K_M of 0.32 (Table II-1). In contrast, substitution with a purine (TY-A53), resulted in a V_{max}/K_M decreased relative to wild-type by a factor of 11. These results suggested that C53 contributes to the valine identity of TYMV RNA, but less strongly than nucleotides A56 and C55.

Effects of combined substitutions in identity elements. In order to further explore the role of C53 as an identity element, mutant TY-U55/A53, combining substitutions of C55 and C53, was prepared and studied. The valylation rates of this RNA could only be measured at elevated ValRS concentrations, and had a K_M 94-fold higher than that of wild-type RNA (Table II-2). Its V_{max} was decreased 20-fold relative to wild-type, resulting in a relative V_{max}/K_M of 4.2×10^{-4}. The combined substitutions thus resulted in an RNA retaining only a low residual valylation capacity, with a valine specificity almost as low as those of mutants TY-G56 and TY-U56. Other combinations of substitutions at C55 and C53 are likely to result in RNAs at least as inactive for valylation as TY-U55/A53, since the presence of a purine at nucleotide 55 resulted in low V_{max}/K_M values (Table II-1). These results demonstrate the importance of both C53 and C55 as valine identity elements.

The three valine identity nucleotides that we have found with the preceding experiments all appear to be directly recognized by ValRS in its binding of the TYMV RNA substrate, since substitution of these nucleotides resulted in large increases in K_M. To investigate whether identity at these three nucleotides is independently discriminated, we studied the effect on valylation of multiple changes in the anticodon loop. The effect of multiple mutations on aminoacylation can be predicted from the kinetic data obtained for single mutations. If the effects are additive, the relative specificity constant (rel. V_{max}/K_M) of a double mutant equals the product of the relative specificity constants of the single mutants (Carter *et al.*, 1984; Wells, 1990). In cases of cooperative or anticooperative effects, the calculated values of the relative specificity constants will deviate from the experimental determinations. Mutant TY-U55/A53, discussed above, had a relative V_{max}/K_M 3.8 times lower than expected if the individual mutations were additive (expected V_{max}/K_M: 0.017 x 0.093 = 0.0016, cf. experimentally determined V_{max}/K_M: 0.00042; Table II-2). Similarly, TY-U55/C54 and TY-U55/C54/A53 RNAs had relative V_{max}/K_M values 1.9 times and 2.6 times lower than expected, respectively, for independently detected, additive mutations (Table II-2). For these 3 mutants, there appears to be a mild cooperative effect (c.f. 14-fold deviation between expected and determined V_{max}/K_M for TY-U57/A55; see below) between the anticodon and flanking substitutions in degrading the valine identity as detected by wheat germ ValRS. The 3'-flanking substitutions A53 and C54 may well alter

the presentation of the anticodon, enhancing the detection of missing identity elements by ValRS. Mutant TY-ΔC58/U55/C54/A53, a fortuitously isolated mutant, is probably a more extreme case of such structural perturbation: the deletion of C58 contributes to the complete absence of valylation for this RNA (cf. TY-U55/C54/A53), even in assays using [^{3}H]valine at increased specific activity and high levels of ValRS. All other mutants studied retained a measurable valylation capacity. Apparently, the combination of anticodon substitutions and altered anticodon loop structure resulting from the deletion produced a molecule totally lacking valine identity. This emphasizes the localization of valine identity elements to the anticodon loop of TYMV RNA.

If combined mutations in the anticodon loop are able to potentiate the discrimination by the wheat germ ValRS of identity elements, the opposite effect would also seem possible. Indeed, the combination of substitutions at nucleotides 56 and 55 in mutants TY-U56/A55 and TY-G57/U56/G55 (Table II-2) resulted in V_{max}/K_M values not much lower than those of mutants with substitutions at nucleotide 56 alone (Table II-1). A surprising example was observed, however, with RNA TY-U57/A55 (Table II-2). This mutant was obtained after inoculation of Chinese cabbage plants with a TYMV genome carrying the A55 mutation. The A55 mutant did not give rise to systemic infections, but the spontaneously acquired second mutation C57→U permitted systemic spread and improved valine charging (Chapters III and IV in this thesis). TY-U57/A55 could be stoichiometrically valylated, and had a V_{max}/K_M only 13-fold reduced relative to wild-type. The addition of the C57→U substitution to TY-A55 increased the V_{max}/K_M by a factor of 16.3 (TY-U57/A55 vs. TY-A55), with improvements in both K_M and V_{max} (Table II-2); the experimentally determined V_{max}/K_M deviates from that expected if the mutations are additive by a factor of 14, representing a marked anticooperative effect. The compensating effects of the U57 and A55 mutations suggest that the anticodon loop is recognized as a structural unit, and that the phosphate backbone as well as functional groups on the purine or pyrimidine rings of identity nucleotides could be recognized in this system. We are aware of no similar example of such a marked effect of nucleotide context in decreasing the potency of an identity element. It will be interesting to determine whether this phenomenon is restricted to TYMV RNA, a molecule whose optimal charging requires conditions somewhat favoring mischarging. Certainly, a similar situation with tRNAs could result in decreased translational fidelity.

Valylation of mutants with substitutions adjacent to the 3′-CCA. The residual valine identity of mutants with substitutions at both nucleotides 56 and 55 suggested the possibility that weak valine identity elements exist outside the anticodon loop (although this suggestion is not supported by the fact that TY-ΔC58/U55/C54/A53 totally lacks valine identity). The discriminator base adjacent to the 3′-CCA is an identity element in several systems (Schulman, 1991), and substitutions at this nucleotide in TYMV RNA were found to decrease valylation by yeast ValRS (Florentz *et al.*, 1991) and in $tRNA^{Val}$ by *E. coli* ValRS (Tamura *et al.*, 1991). Mutants TY-C4 and TY-G4 were both excellent substrates for the wheat germ ValRS (Table II-1). Both RNAs could be valylated to completion under normal

conditions, and had V_{max} values similar to wild-type. The K_M for TY-C4 did not differ significantly from that of the wild-type RNA, while the K_M for TY-G4 was elevated 6-fold. In contrast to the *E. coli* (Tamura *et al.*, 1991) and yeast (Florentz *et al.*, 1991) ValRS enzymes, the wheat germ enzyme discriminates only slightly against discriminator base mutants. Nevertheless, A4 could be considered a weak valine identity element.

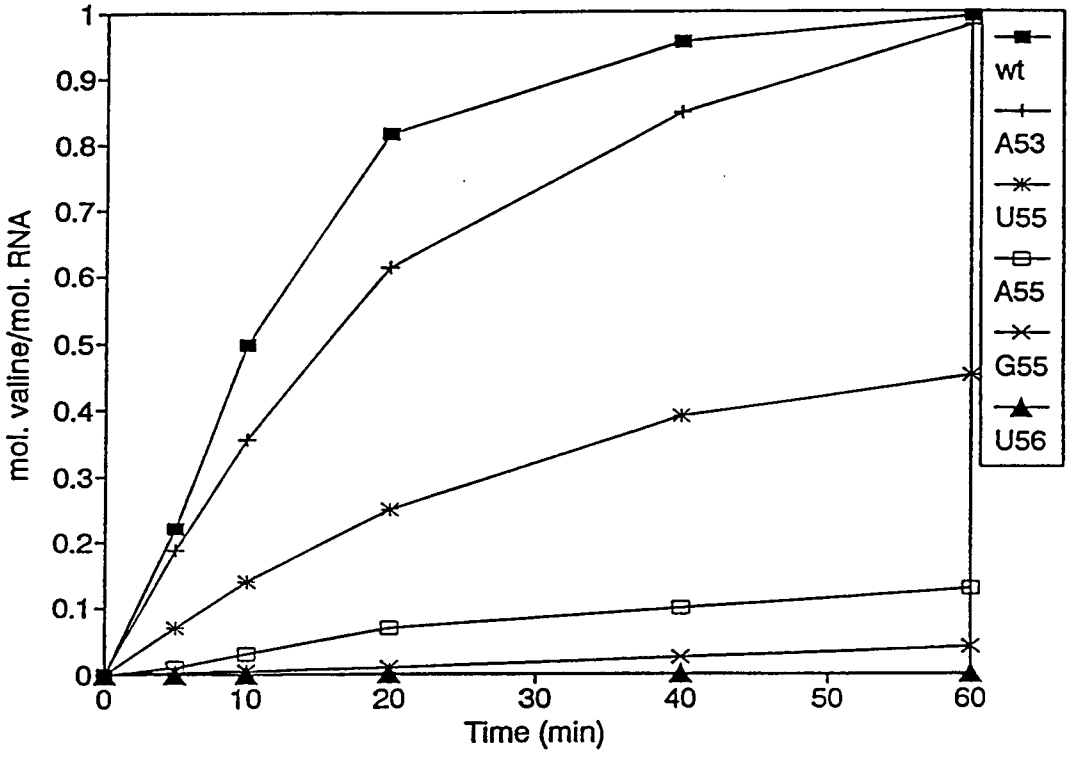

Figure II-2. Valylation curves for selected TYMV RNA transcripts (0.6 μM) charged with wheat germ ValRS. The transcripts represented are identified in the key: wt, wild type.

Table II-1: Valylation of anticodon loop and discriminator base mutants of TYMV RNA with wheat germ ValRS

Mutant	Anticodon loop sequence	mol val/mol RNA[a]	K_M (nM)[b]	Rel. V_{max}[c]	Rel. V_{max}/K_M	Loss of Specificity (x-fold)[d]
wild type	59-CCCACAC-53	1.01	31	1.00	1.00	
TY-G57	. . G . . .	0.98	38	0.95	0.78	1.3
-A57	. . A . . .	0.98	49	1.08	0.68	1.5
-U57[f]	. . U . . .	1.02	29	1.06	1.14	0.9
-G56	. . . G . .	<0.001	3200	0.024	0.00020[e]	5000
-U56	. . . U . .	<0.001	3300	0.016	0.00011[e]	9100
-U55	. . . . U .	0.45	1600	1.05	0.017[e]	59
-A55	. . . . A .	0.13	2300	0.39	0.0046[e]	220
-G55	. . . . G .	0.04	2200	0.12	0.0015[e]	670
-G54	. . . . . G .	0.99	38	0.99	0.81	1.2
-C54	. . . . . C .	1.05	105	0.76	0.22	4.5
-U54[f]	. . . . . U .	0.97	68	1.48	0.67	1.5
-A53	. . . . . A	0.92	157	0.47	0.093	11
-U53	. . . . . U	1.06	183	1.88	0.32	3.1
-C4		0.97	38	0.64	0.52	1.9
-G4		1.01	190	1.16	0.19	5.3

a. Extent of valylation after 60 min at 0.6 μM RNA and 20 units of ValRS.

b. Apparent K_M. Concentrations refer to the population of RNAs with 3'-CCA termini. Standard error, approx. 20%.

c. Standard error, approx. 20%.

d. Loss of valine charging specificity = the reciprocal of relative V_{max}/K_M.

e. Estimate derived both by computation from the measured V_{max} and K_M values and directly by determining the slope of the linear section of the plot of [RNA] *vs* initial rate of valylation (after Schulman and Pelka, 1988).

f. Transcript made from a DNA template generated by polymerase chain reaction.

Table II-2: Effects of combined substitutions in the anticodon loop of TYMV RNA

Mutant	Anticodon loop sequence	mol val/mol RNA[a]	K_M (nM)[b]	Rel. V_{max}[c]	Rel. V_{max}/K_M	Loss of Specificity (x-fold)[d]
wild type	59-CCCACAC-53	1.01	31	1.00	1.00	
-U56/A55	. . . UA . .	<0.001	2800	0.0071	0.000055[e]	18000
-C56/A55	. . . CA . .	<0.001	ND[f]	ND[f]	$<10^{-3}$	>1000
-G57/U56/G55	. . GUG . .	<0.001	1300	0.0074	0.00013[e]	7700
-U55	. . . . U . .	0.45	1600	1.05	0.017[e]	59
-A53	. . . . . A	0.92	157	0.47	0.093	11
-U55/A53	. . . . U . A	<0.001	2900	0.051	0.00042[e]	2400
-C54	. . . . . C .	1.05	105	0.76	0.22	4.5
-U55/C54	. . . . UC .	0.04	1590	0.12	0.0020[e]	500
-U55/C54/A53	. . . . UCA	<0.001	4100	0.021	0.00013[e]	7700
-ΔC58/U55/C54/A53	. . . UCA	0.00	-	0.00	0.00	∞
-U57[g]	. . U	1.02	29	1.06	1.14	0.9
-A55	. . . . A . .	0.13	2300	0.39	0.0046[e]	2200
-U57/A55[g]	. . U . A . .	1.03	520	1.28	0.075	13

a. Extent of valylation after 60 min at 0.6 μM RNA and 20 units of ValRS.

b. Apparent K_M. Concentrations refer to the population of RNAs with 3'-CCA termini. Standard error, approx. 20%.

c. Standard error, approx. 20%.

d. Loss of valine charging specificity = the reciprocal of relative V_{max}/K_M.

e. Estimate derived both by computation from the measured V_{max} and K_M values and directly by determining the slope of the linear section of the plot of [RNA] *vs* initial rate of valylation (after Schulman and Pelka, 1988).

f. Not determined.

g. Transcript made from a DNA template generated by polymerase chain reaction.

Discussion

Principal residence of valine identity of TYMV RNA in three residues of the anticodon loop. We have studied the effects of substitutions in the anticodon loop of TYMV RNA in diminishing the viral RNA's ability to be valylated by wheat germ ValRS. A systematic approach involving single and multiple substitutions has yielded a quantitative picture of the contribution towards valine identity made by the three major identity determinants recognized by wheat germ ValRS in TYMV RNA: A56, C55 and C53. Changes involving only these three nucleotides are able to reduce the V_{max}/K_M for valylation at least 10^3-fold relative to wild-type RNA (Tables II-1 and II-2).

The most important nucleotide conferring valine identity is A56. Single substitutions (TY-G56, TY-U56) resulted in RNA molecules with V_{max}/K_M about 10^{-4} relative to wild-type. Nucleotide C55 is the second important element of valine identity, with substitutions decreasing V_{max}/K_M values by 60- to 700-fold. Mutants with a purine nucleotide at this site were discriminated against more than the uridine mutant. The least potent of the three major identity nucleotides is C53. Substitution with adenosine decreased V_{max}/K_M 11-fold, although the uridine substitution had only a 3-fold effect. The importance of C53 as an identity determinant is better demonstrated by the low valylation of TY-U55/A53 relative to TY-U55 (Table II-2). The involvement of nucleotides in the anticodon as well as the 3′ of the anticodon loop in identity determination has also been seen in the *E. coli* glutamine system (Rould *et al.*, 1991; Jahn *et al.*, 1991).

The magnitudes of the effects on V_{max}/K_M of substitutions in A56 and C55 are similar to those observed in tRNAs whose aminoacylation identities reside mostly in localized, rather than distributed, sites on the molecule. Thus, for *E. coli* $tRNA^{Val}$ and $tRNA^{Met}$, substitution of two nucleotides within the anticodon decreased V_{max}/K_M for the cognate synthetase by about 10^4-fold (Schulman and Pelka, 1988), and the alteration of a G·U base pair in *E. coli* $tRNA^{Ala}$ decreased V_{max}/K_M by a similar amount (Shi *et al.*, 1990). By contrast, the identity elements of yeast $tRNA^{Asp}$ and $tRNA^{Phe}$ that are recognized by their cognate synthetases are scattered among three far-flung sites on the RNA, the anticodon, the D-arm and nucleotide 73, and substitutions at these sites independently result in decreases of V_{max}/K_M of only 10-15-fold in the phenylalanine system (Bruce and Uhlenbeck, 1982b; Sampson *et al.*, 1989) and 10-530-fold in the aspartic acid system (Pütz *et al.*, 1991).

All the mutants studied retained residual valylatability, except TY-ΔC58/U55/C54/A53, which was totally unable to accept valine. It is thus possible that features outside the anticodon loop contribute to valine identity in a minor way, perhaps in maintaining a conformation compatible with ValRS recognition. Nucleotide A4, whose substitution slightly decreased valylation by wheat germ ValRS (Table II-1), might affect the conformation of the pseudoknot and 3′ region of the amino acid acceptor arm (Florentz *et al.*, 1991). We consider nucleotide 54 also to serve such a structural purpose, although in conferring generic aminoacylation rather than specific valylation. Either of the

purines adenosine or guanosine is acceptable at this position (wild-type, TY-G54), but a pyrimidine mutant (TY-C54) had a 5-fold decreased V_{max}/K_M (Table II-1). This is probably the result of poorer base stacking of nucleotides 57 through 53, influencing the disposition of the anticodon. It is noteworthy that the analogous position in tRNAs (nucleotide 37) is always occupied by a purine (Sprinzl *et al.*, 1991).

Involvement of both K_M and V_{max} discrimination in selection of cognate RNA by wheat germ ValRS. All mutants with impaired valine identity had elevated K_M values, suggesting that significant discrimination by wheat germ ValRS occurs on the basis of substrate recognition and binding. The primary identity elements we have described in this paper (A56, C55, C53) are thus almost certainly nucleotides directly contacted by wheat germ ValRS. This is probably also true for the *E. coli* methionyl-tRNA synthetase/$tRNA^{Met}$ system, where substitution of the wobble base results in very high K_M values that can be suppressed by compensating amino acid substitutions in the synthetase (Ghosh *et al.*, 1990). In the two systems studied in most detail to date, the X-ray structures of both *E. coli* $tRNA^{Gln}$ (Rould *et al.*, 1991) and yeast $tRNA^{Asp}$ (Ruff *et al.*, 1991) bound to their cognate synthetases has revealed direct contacts between the synthetase and functional groups of anticodon bases of the tRNA.

Our observation that mutant TY-U57/A55 exhibited an unexpectedly high level of valine identity (Table II-2) suggests that the wheat germ ValRS may recognize the anticodon nucleotides in a different fashion, perhaps detecting a specific configuration of the phosphate backbone in combination with functional groups of bases at identity positions. Certain substitutions adjacent to the most significant identity element in TYMV RNA (A56) may modulate the efficiency of recognition of this nucleotide by the ValRS by altering the conformation of the anticodon loop in a subtle way. It will be interesting to see if this is more generally true for tRNA substrates of ValRS and other synthetases. Clearly, the significant valine identity of TY-U57/A55 raises the possibility that $tRNA^{Leu}$ with the same UAA anticodon might be valylated *in vivo*. The presence of one or more antideterminant elements (e.g. the long variable loop) in this tRNA would be necessary to preclude valylation.

Most mutants with diminished valine identity had decreased V_{max} values in addition to elevated K_M's. This was especially so for mutants with substitutions of A56. Nevertheless, the great importance of K_M discrimination for the wheat germ ValRS suggests a somewhat different substrate discrimination mechanism from that employed by the yeast enzyme (Florentz *et al.*, 1991). Competition studies and enzyme/RNA binding studies with TY-U56 and TY-G56 demonstrated only minor differences in ValRS interaction with wild-type relative to mutant RNAs (Florentz *et al.*, 1991), indicating that mutants were discriminated predominantly by a kinetic mechanism. We have performed similar competition experiments between the above mutants and wild-type viral RNA using wheat germ ValRS, and found no influence on the valylation rate of wild-type TYMV RNA in the presence of mutant RNAs (not shown). This is consistent with the mutants having elevated K_M's and with

differential substrate binding being a significant discrimination mechanism for wheat germ ValRS. In preliminary experiments (not shown), the mutants studied in this chapter using wheat germ ValRS yielded similarly ranked valylation activities with the yeast enzyme, indicating that the two enzymes detect similar identity determinants in the TYMV RNA. One significant difference between the two synthetases is the recognition of mutations at A4. TY-C4 and TY-G4 were excellent substrates for wheat germ ValRS (Table II-1), but could only be partially charged by yeast ValRS (Florentz *et al.*, 1991). Kinetic studies of the full set of mutants with yeast ValRS should elucidate the apparent mechanistic differences the two synthetases use in discriminating similar identity determinants. An understanding of ValRS structure, and a comparison of the sequences of the synthetases may also shed light on this problem.

Anticodon nucleotides are the dominant valine identity determinants across the phyla. In mapping the valine identity determinants recognized by wheat germ ValRS to the anticodon, our studies show that ValRS from bacterial (*E. coli*), lower eukaryotic (yeast) and higher eukaryotic (wheat germ) sources detect valine identity determinants in or near the anticodon of their substrates. In the *E. coli* system, there are 10^4-fold differences in V_{max}/K_M between $tRNA^{Val}$ with UAC (wild-type) and CAU anticodons (Schulman and Pelka, 1988) and between $tRNA^{Val}$ with UAC and UGC anticodons (Tamura *et al.*, 1991). Yeast ValRS, which recognizes TYMV RNA as an efficient substrate, discriminates the substitution of the middle position of the anticodon (mutants TY-G56, TY-U56) with a 20000-fold decrease in V_{max}/K_M (Florentz *et al.*, 1991). These same mutants were valylated by wheat germ ValRS with a 5000-9000-fold decrease in V_{max}/K_M (Table II-1). Thus, the anticodon is an important identity element recognized by ValRS from diverse sources, but the precise spectrum of identity determinants recognized by eukaryotic ValRS may differ from those recognized by the *E. coli* enzyme. In particular, the results of Schulman and Pelka (1988) suggest that the 3' nucleotide of the anticodon is a stronger determinant in *E. coli*. Knowledge of the roles of other anticodon loop nucleotides in determining the identity of *E. coli* $tRNA^{Val}$ awaits further analysis of that system.

Analysis of the charging of discriminator base mutants of TYMV RNA (TY-C4, TY-G4; Table II-1) indicated only a weak role for this nucleotide in the specificity of TYMV RNA valylation by wheat germ ValRS. In contrast, ValRS enzymes from *E. coli* and yeast appear to utilize the discriminator base as a significant identity element: while the A→G substitution at nucleotide 4 of TYMV RNA resulted in only a 5-fold decrease in V_{max}/K_M using the wheat germ enzyme (Table II-1), the same substitution resulted in a 300-fold decrease using yeast ValRS (Florentz *et al.*, 1991), and the A73→G substitution in *E. coli* $tRNA^{Val}$ resulted in a 55-fold difference using *E. coli* ValRS (Tamura *et al.*, 1991). Thus, while the anticodon has been conserved across the phyla as the primary identity element, the importance of the discriminator base varies. Comparison of the phenylalanine identity sets recognized in *E. coli*, yeast and human systems (Nazarenko *et al.*, 1992) likewise reveals a general conservation of identity elements, but with significant deviations especially between prokaryotes and

eukaryotes. A stronger conservation of identity determinants, focussed on a G·U base pair in the acceptor arm, appears to exist in the alanine system, as deduced from studies with $tRNAs^{Ala}$ and alanyl-tRNA synthetases from bacterial, insect and mammalian sources (Hou and Schimmel, 1989).

CHAPTER III

Turnip Yellow Mosaic Virus RNAs with Anticodon Loop Substitutions that Result in Decreased Valylation Fail to Replicate Efficiently

Abstract

Single and multiple nucleotide substitutions have been introduced into the anticodon loop of the tRNA-like structure of turnip yellow mosaic virus (TYMV) genomic RNA. We studied the effects of these mutations on *in vitro* valylation and on replication in Chinese cabbage protoplasts and plants. Only those mutants capable of efficient and complete valylation showed efficient replication in protoplasts and gave rise to systemic symptoms in whole plants. Mutants that accepted valine inefficiently (in some cases, V_{max}/K_M values were $< 10^{-3}$ relative to wild type) replicated to levels 200 to 500-fold below wild type in protoplasts (estimated on the basis of levels coat protein and genomic RNA). These mutants could not support systemic spread in plants. In one plant inoculated with TYMC-A55 RNA, which replicates poorly in protoplasts, systemic symptoms developed after a delay. The reversion in replication was accompanied by improved valine acceptance and the appearance of a U57 second site mutation. Our results indicate a correlation between valine acceptance activity and viral yield. Possible roles for valylation are discussed, and the present results are compared to similar studies with brome mosaic virus which suggested that tyrosylation is not crucial for brome mosaic virus replication [Dreher *et al.*, (1989), J. Mol. Biol. 206:425-438).

Introduction

Turnip yellow mosaic virus (TYMV) has a (+)-sense single-stranded RNA genome 6.3 kb long. In common with a number of other plant viruses, the 3′ region of TYMV RNA has distinctive characteristics similar to those of free transfer RNAs. The virion RNA, which terminates in 3′-CC_{OH}, can be adenylated by (CTP,ATP):TRNA nucleotidyltransferase (Joshi *et al.*, 1982). The resulting -CCA_{OH} terminus can be specifically and efficiently valylated by valyl-tRNA synthetase (ValRS) from wheat germ (Dreher *et al.*, 1988) or yeast cells (Giegé *et al.*, 1978). The valylated viral RNA can in turn form a ternary complex with GTP and elongation factors EF-Tu from *Escherichia coli* (Joshi *et al.*, 1984) or EF-1α from wheat germ (Joshi *et al.*, 1986). These properties are associated with a distinct domain encompassing the 3′ 82 nucleotides of the viral RNA, which can be folded into a tRNA-like structure whose probable three-dimensional conformation is similar to the L conformation of cytoplasmic tRNAs (Fig. III-1; Rietveld *et al.*, 1983; Dumas *et al.*, 1987). Despite the functional mimicry, sequence similarities to higher eukaryotic $tRNA^{Val}$ are limited to the 3′-ACCA end, a valine anticodon with 3′ flanking bases (57-CACAC-53; anticodon is underlined) and a degenerate version (38-UGCA-35) of the conserved TψCPu of tRNAS (ψ = pseudouridine, Pu = purine; Sprinzl *et al.*, 1991). These features are shown in Fig. III-1; note that nucleotides are numbered from the 3′ end of the adenylated RNA.

The role that the tRNA mimicry plays in the replication cycle of the virus remains incompletely understood. It is known that TYMV RNAs become valylated during replication in Chinese cabbage (Joshi *et al.*, 1982). Thus, TYMV RNA is an active substrate *in vivo* for host ValRS, and most likely also for host (CTP,ATP):tRNA nucleotidyltransferase, since the virion RNA inoculum lacks the 3′ adenosine residue necessary for aminoacylation. A leading question is whether the *in vivo* valylation is merely coincidental, or whether it is a necessary element of the replication machinery or its control. We have previously addressed this question with brome mosaic virus (BMV), another (+)-sense RNA virus. In BMV, the tyrosine-charging tRNA-like structure has been shown to function as the promoter for (-) strand synthesis (Miller *et al.*, 1986), suggesting a close relationship between tRNA mimicry and RNA replication. However, tyrosylation may not be a key part of that interdependence, since mutants that were expected on the basis of *in vitro* characterization to be tyrosylated inefficiently *in vivo*, replicated fairly well in barley protoplasts (Dreher *et al.*, 1989). Rather than tyrosylation, substrate activity for tRNA nucleotidyltransferase may be a more crucial function: the BMV tRNA-like structure acts as the 3′ telomere of the (+) strand, and host tRNA nucleotidyltransferase most likely acts as a telomerase to maintain intact 3′ termini during replication (Rao *et al.*, 1989).

In order to further investigate the role of aminoacylation in viral replication, the TYMV system offers advantages over BMV. In particular, the discoveries that valine identity determinants of *E. coli* $tRNA^{Val}$ are present in the anticodon, and that limited nucleotide changes can alter the aminoacylation

specificity of this tRNA (Schulman and Pelka, 1988), suggested that non-charging and mischarging TYMV RNAs might be constructed fairly readily. It was thought that such mutants would provide more convincing results than the partially charging BMV RNA mutants previously studied (Dreher *et al.*, 1989). We report here on mutant TYMV genomic RNAs carrying substitutions in the anticodon loop, some of which have very low valine accepting activities *in vitro*. The results show that valine acceptance of viral RNAs is an important criterion for the amplification of TYMV RNA.

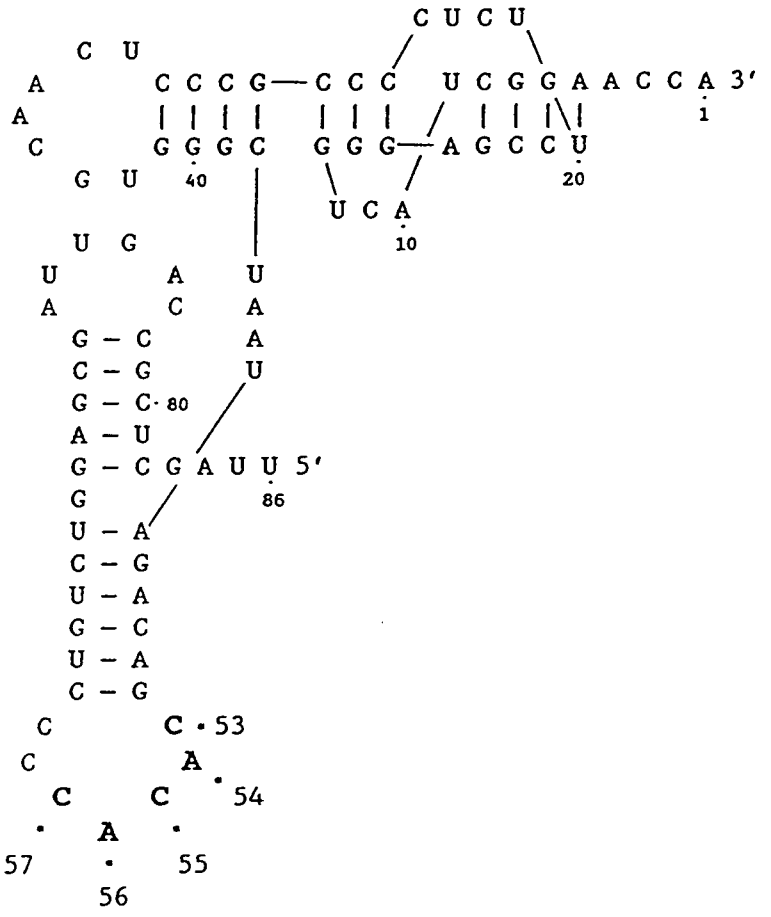

Figure III-1. Proposed L conformation of the tRNA-like structure of TYMV RNA showing the nucleotides at which substitutions have been made (shown in bold). They comprise the valine anticodon (57-CAC-55) and two further anticodon loop nucleotides conserved among valylatable viral and transfer RNAs. Note that nucleotides are numbered in ascending order from the 3′-CCA end, since the 5′ end of the fragment shown is connected to a further 6.2 kb of genomic sequence.

Materials and Methods

Materials. Chinese cabbage (*Brassica pekinensis* cv. Wong Bok) plants were grown in a growth chamber under 16 hr day-length at 21°C. T7 RNA polymerase was purchased from BRL, m^7GpppG cap analogue from New England Biolabs, InhibitAce ribonuclease inhibitor from 5 prime-3 prime, Inc. (West Chester, Pennsylvania), T7 DNA polymerase (Sequenase) and reverse transcriptase from United States Biochemical, *Thermus aquaticus* DNA polymerase from Promega, and restriction enzymes from Gibco-BRL, Boehringer-Mannheim, and New England Biolabs. Macerase and Cellulysin were purchased from Calbiochem. Synthetic deoxyoligonucleotides were made by automated phosphoramidite synthesis and purified on 20% polyacrylamide/7M urea gels.

Cloning, *in vitro* site-directed mutagenesis and transcription. In preparation for mutagenesis, a 258 bp *Sma*I-*Hind*III fragment from the 3′ end of the TYMV genomic cDNA clone pTYMC (Weiland and Dreher, 1989) was transferred to an M13 mp18 vector. Single stranded deoxyuridine-containing template DNA was generated in *E. coli* strain CJ236 and used for *in vitro* mutagenesis, directed by the appropriate 5′-phosphorylated synthetic deoxyoligonucleotides (Dreher and Hall, 1988b; Kunkel *et al.*, 1987). Mutant clones were screened either by direct sequencing or by plaque hybridization, and the sequence of the entire TYMV insert was verified prior to subcloning back to the genomic pTYMC clone as *Sma*I-*Hind*III fragments.

Plasmid DNAs were prepared from large cultures and the mutant sequences were confirmed by double-stranded DNA sequencing (Chen and Seeburg, 1985). Transcripts labelled with [α-^{32}P]UTP (0.1 Ci/mmol) were prepared from DNA templates linearized with *Hind*III and analyzed as described (Weiland and Dreher, 1989).

Protoplast and plant inoculations. Young healthy leaves (3-4 g) were taken from 6-week old Chinese cabbage plants that had been held in the dark for three days in order to deplete starch grains. Protoplasts were prepared and inoculated (5 μg of transcript RNA per $4x10^5$ cells) as described (Weiland and Dreher, 1989), except that protoplasts were released after incubation of leaf slices in the hydrolytic enzymes overnight at 23°C. Inoculated protoplasts were incubated under constant light at 25°C for 22 or 48 hr prior to harvest.

Three week-old Chinese cabbage plants with two true leaves were used for inoculations of whole plants. Each leaf was mechanically inoculated with 10 μl of RNA transcript (0.25 mg/ml) in 50 mM glycine, 30 mM K_2HPO_4 (pH 9.2), 1% bentonite and 1% celite. At times, plants were inoculated with a suspension of protoplasts harvested 48 hr post inoculation ($5x10^4$ cells/leaf). Plants were held as above and scored for symptom appearance and virus levels.

Analysis of viral products by Western and Northern blotting. The levels of coat protein in harvested protoplasts were analyzed in Western blots as described (Weiland and Dreher, 1989). Results were quantitated by scanning laser densitometry with reference to a dilution series of virus. In

most blots, the distribution of the horseradish peroxidase-labelled secondary antibody was detected using the chromogenic substrate 4-chloro-1-naphthol (detection limit of 2 ng of coat protein). Where necessary, about 10-fold higher sensitivity was achieved by using chemiluminescent development (ECL, Amersham International).

RNA was extracted from protoplasts, glyoxalated, electrophoresed and transferred to nylon membranes as described (Weiland and Dreher, 1989). The hybridization probe was a ^{32}P-labelled RNA transcript complementary to 0.9 kb at the 3′ end of TYMV RNA. Both full-length genomic and subgenomic RNAs could be detected (Weiland and Dreher, 1989). RNA levels were quantitated by scanning laser densitometry or with a ß-emission radioisotope scanner (Ambis Systems, San Diego).

Ribonuclease protection assays of RNAs labelled *in vivo*. Radiolabelled RNAs were extracted from protoplasts which had been cultured in medium containing carrier-free [^{32}P]orthophosphate (200 μCi/ml; Loesch-Fries and Hall, 1980). In order to preclude the detection of input (inoculated) RNA, both the inoculum and the analytical probe were nonradioactive. The deproteinized RNA extracts were mixed with the 0.9 kb RNA probe (see Fig. III-4) and denatured at 85°C for 5 minutes in the presence of 80% formamide, 40 mM Pipes (pH 6.7), 0.4 M NaCl and 1 mM EDTA (in a 30 μl reaction). After hybridization overnight at 55°C, 300 μl of ribonuclease solution containing 0.3 M NaCl, 10 mM Tris-HCl (pH 7.5), 5 mM EDTA, ribonuclease A (40 μg/ml) and ribonuclease T1 (2 μg/ml) were added to the samples and incubated at 30°C for 1 hr. Ribonucleases were removed by treatment with 50 μg/ml proteinase K in 0.5% SDS at 37°C for 30 minutes. After phenol/chloroform extraction, the samples were ethanol precipitated with carrier RNA, and then analyzed by electrophoresis on 1% agarose gels and autoradiography.

Virion RNA extraction and characterization. Virus was isolated from infected plants according to Lane (1986) and quantitated spectrophotometrically. Virion RNA was prepared from virus by two phenol/chloroform extractions. In order to assess the stability of mutated sequences during replication in plants, the region encompassing the tRNA-like structure was sequenced by dideoxy chain termination. This was done either directly with reverse transcriptase and a primer hybridizing to the 3′ end, or after further DNA amplification of the 3′ region of the genome via the polymerase chain reaction (Winship, 1989). The valine acceptances of the virion RNAs were studied by determining the amount of [^{3}H]valine bound in reactions catalyzed by valyl-tRNA synthetase present in an extract from wheat germ (Dreher *et al.*, 1988).

Valylation of genome-length transcripts. In order to make full-length genomic RNA transcripts capable of aminoacylation, the restriction overhangs were removed from *Hind*III-linearized pTYMC and selected mutant derivatives by treatment with mung bean nuclease (Dreher *et al.*, 1988). The treated DNAs were extracted with phenol/chloroform and ethanol-precipitated, and then used as templates for the synthesis of genomic transcripts (as described, except that cap analogue was omitted). The resultant transcripts were valylated as above. The 3′-termini were analyzed by 3′-labelling with

[5′-^{32}P]cytidine-3′,5′-bisphosphate, complete digestion with a mixture of ribonucleases and two-dimensional thin layer chromatography (Dreher *et al.*, 1989).

Results

Generation of TYMC RNA mutants with substitutions in the anticodon loop. For two reasons, our strategy for obtaining mutants with altered valylation properties has focused on substitutions of the nucleotides 56-ACAC-53 in the anticodon loop of TYMV RNA. Firstly, these nucleotides are present in all known valylatable eukaryotic RNAs, including valine-specific tRNAs (Sprinzl *et al.*, 1991) and tymoviral RNAs (van Belkum *et al.*, 1987). Protection experiments comparing the interaction of yeast ValRS with TYMV RNA and $tRNA^{Val}$ have suggested that these conserved nucleotides in the viral RNA are functionally analogous to the tRNA anticodon loop (Florentz and Giegé, 1986). Secondly, studies with *E. coli* $tRNA^{Val}$ have shown that the anticodon is a major site recognized by ValRS in discriminating its cognate tRNA from others (Schulman and Pelka, 1988).

Oligonucleotide-directed mutagenesis was used to introduce single and multiple substitutions involving each position in the anticodon loop from C53 through C57 (Fig. III-1, Table III-1). Nucleotide C57 corresponds to the wobble base of tRNA, which varies among different $tRNA^{Val}$ sequences (Sprinzl *et al.*, 1991). Nucleotides A56 and C55 complete the anticodon. The residues corresponding to the 3′ flanking nucleotides A54 and C53 are invariant in eukaryotic $tRNA^{Val}$; among all known eukaryotic tRNAs, the former base is always a purine and the latter is never a guanine (Grosjean *et al.*, 1982; Sprinzl *et al.*, 1991). These observations were considered in designing the mutants discussed below.

Mutations were made in an M13 clone containing the 3′ 258 bp of TYMV cDNA, and were subcloned into pTYMC after sequencing of the complete insert (Materials and Methods). This eliminated the possibility of introducing unwanted mutations outside the mutagenic target region. Clone pTYMC contains the entire genomic cDNA of TYMV adjacent to a T7 promoter at the 5′ end and with a unique *Hind*III site at the 3′ end. Infectious TYMC RNA can be made with T7 RNA polymerase from *Hind*III-linearized pTYMC in the presence of m^7GpppG cap analogue (Weiland and Dreher, 1989). Such transcripts made from pTYMC and its mutant derivatives (referred to as e.g. TYMC-U55) were used in the replication studies described below. These transcripts had four extra non-viral nucleotides (AGCU, directed by the *Hind*III restriction overhang) at the 3′ end, and were thus not valylatable. Studies with a number of viruses have shown that such short 3′ extensions do not alter the infectivity of transcripts (Ahlquist *et al.*, 1987). In barley, the 3′ ends of BMV RNAs undergo rapid turnover, with repair to a 3′-CCA terminus probably being a function of host tRNA nucleotidyltransferase (Rao *et al.*, 1989). Presumably, the 3′ ends of inoculated TYMC transcripts are processed *in vivo* in a similar way to produce a valylatable terminus.

***In vitro* valylation characteristics of mutant TYMV RNAs.** Mutations introduced into pTYMC as described above were also introduced into the vector mpT7YSma, from which short (264-

nucleotide long) RNAs spanning the tRNA-like structure can be transcribed with T7 RNA polymerase (Dreher *et al.*, 1988). These transcripts end in 3'-CCA and, unlike the genomic transcripts, are appropriate substrates for ValRS. To distinguish them from the genomic transcripts mentioned above, these short RNAs are referred to as e.g. TY-U55. In studies reported elsewhere, the valylation properties of anticodon loop mutants have been described in detail (Chapter II in this thesis). Table III-1 contains a summary of those data: valylation stoichiometries and V_{max}/K_M values. The latter parameter can be taken as an indication of the valylation efficiency of the mutant.

In order to verify that the valylation studies using short 3' RNAs (Table III-1) were generally valid for genome-length RNAs, the valylation of the genomic transcripts of a selection of mutants was studied. Full-length RNAs with 3'-CCA termini were transcribed from *Hind*III-linearized DNA templates after treatment with mung bean nuclease to remove the restriction overhang (Materials and Methods). The valylation of the genomic mutants parallelled that of the respective short transcripts (compare Fig. III-2a with Table III-1), indicating that the accessibility or conformation of the tRNA-like structure is not significantly perturbed by the presence of 6 kb of upstream RNA. The valylation data of Table III-1 is thus readily applicable to the genomic transcripts used in this study.

One of the goals of our mutational study was to obtain mischarging mutants. Preliminary studies have failed to detect mischarging of the mutant RNAs of Table III-1. Further work is needed to obtain such mutants.

Only those mutants capable of efficient valylation are able to replicate systemically in plants. Chinese cabbage plants were inoculated with capped full-length wild-type and mutant transcripts and the appearance of symptoms was checked over the two week period post inoculation. Systemic symptoms (indicated by symptoms in non-inoculated upper leaves) appeared 7 days post inoculation only in plants inoculated with RNAs capable of efficient valylation: wild-type, wobble base mutants (TYMC-G57, -U57, -A57), nucleotide 54 mutants (TYMC-G54, -C54, -U54), and one nucleotide 53 mutant (TYMC-U53; Table III-1A). The yields of the mutant viruses from symptomatic upper leaves were comparable to the yield of wild-type TYMC. Interestingly, TYMC-U57 replicated to significantly higher levels than TYMC. The appearance of symptoms was similar for all infected plants.

Sequencing of the tRNA-like structures of progeny RNAs showed that the mutant sequences were preserved (not shown). The mutant virion RNAs could also be valylated to the same extent as wild-type RNA in reactions catalyzed by wheat germ ValRS (Fig. III-2b). The valylation properties of these progeny virion RNAs are consistent with those of the short transcripts listed in Table III-1.

Replication of TYMC mutants in protoplasts. On the basis of the above whole-plant infectivity studies, we divided the mutants into two groups, those capable and those incapable of systemic infection. In order to investigate further the differences between the two groups, the mutants were inoculated onto Chinese cabbage protoplasts, and the levels of viral products were then analyzed

after 48 hr, or in some cases 22 hr, incubations. At harvest, a fraction of the cells was used to detect coat protein in Western blots (Fig. III-3a), while another fraction was used to detect genomic and subgenomic RNA in Northern blots (Fig. III-3b).

As in the whole plant studies, the mutants could be divided into two groups (A and B) on the basis of the replication behavior in protoplasts, whose characteristics are listed in Table III-1A and III-1B, respectively. The members of the first group replicated well, producing yields of coat protein and viral RNAs that were at least 10% of wild-type (Table III-1A). This group included all those able to produce systemic symptoms in plants (TYMC-G57, -A57, -U57, -G54, -C54, -U54 and -U53), but in addition mutant TYMC-A53. The latter mutant has the poorest valylation properties of this group (compare V_{max}/K_M values, Table III-1), although it can be completely valylated (Table III-1A). For members of this group, there was a direct correlation between the four parameters investigated: valylation efficiency, coat protein accumulation in protoplasts, viral RNA accumulation (genomic and subgenomic) in protoplasts, and yield of virus in systemically infected leaves. For mutant TYMC-A53, the replication rate in single cells may be too low to overcome the plant's defenses, resulting in limitation to inoculation foci and no systemic spread. The inability to spread systemically was confirmed by the absence of coat protein in Western blots of upper leaves; low levels of coat protein were detected in the inoculated leaves.

Group B (Table III-1B) included all other mutants studied. They replicated poorly in protoplasts (Fig. III-3), and corresponded to those mutants unable to replicate systemically in plants. These mutants had substitutions within the anticodon, at nucleotides 55, 56 and combinations including those nucleotides. Most group B mutants replicated to such low levels in protoplasts that viral products were difficult to detect; coat protein was detectable 48 hr, but not 22-24 hr after inoculation. Mutant TYMC-A55 replicated to the highest levels (about 50 fold lower than wild-type), while the other anticodon mutants yielded at most 200 times less than wild-type (Table III-1B). The detection and quantitation of viral products for these mutants was most accurate in Western blots analyzing for coat protein, chemiluminescent development providing c. 0.2 ng sensitivity. Northern blots were not useful due to the detection of small amounts of inoculum genomic RNA, and due to elevated background interfering with subgenomic RNA detection.

None of the group B RNAs could be efficiently valylated with wheat germ ValRS, having V_{max}/K_M values at best 59 times lower than wild-type RNA (for TY-U55), and in the other cases far lower. These RNAs could not be completely valylated in standard long (60 min) reactions (Table III-1). For these mutants, inefficient valylation correlates to basal levels of replication, and the ranking in replication generally follows the ranking in valylation efficiency.

There was a atypical member of group B, mutant TYMC-U55. It replicated poorly, yet could be completely valylated (only in the presence of excess ValRS). Clearly, the ability to valylate efficiently is not the sole criterion for efficient replication.

Evidence that all mutants are able to replicate to some degree. The detection of low but significant levels of coat protein in protoplasts inoculated with RNAs of group B mutants indicates that replication of input RNA had occurred. Coat protein is not translated from genomic RNA, being translated instead from the 0.7 kb subgenomic RNA that is colinear with the 3′ region of the genomic RNA. In brome mosaic virus, subgenomic RNA arises in a transcriptional event that uses (-) strand as its template (Miller *et al.*, 1985). Presumably, the same mechanism is used by TYMV, and thus the appearance of coat protein implies the generation of subgenomic RNA via (-) strand from the mutant input RNAs. Nevertheless, the possibility that coat protein may arise by translation of unreplicated 3′ RNAs generated by fragmentation of the RNA inoculum was considered. We therefore studied the *in vivo* synthesis of viral RNAs to obtain stronger evidence that group B mutants are capable of slow replication.

Unlabelled RNA transcripts were inoculated into protoplasts, which were then incubated in phosphate-free medium supplemented with carrier-free [^{32}P]orthophosphate. Protoplasts were harvested and the RNAs were extracted, denatured, annealed to an excess of non-radioactive 0.9 kb (-) sense RNA probe, and then treated with ribonuclease under conditions that protect double-stranded RNA. Digestion products were analyzed by gel electrophoresis and autoradiography. This assay detected radiolabelled double-stranded genomic RNA, (+) genomic strands (0.9 kb protected band) and subgenomic RNA (0.7 kb protected band; Fig. III-4). Note that this assay does not permit quantitation of amounts of RNAs synthesized during the labelling period, since the specific activities of [^{32}P]nucleotides vary with time until intracellular pools become saturated. Consistent with the results of Western detection, all group B mutants tested showed evidence of replication by this assay, in the form of double-stranded genomic RNAs and the radiolabelled 0.9 kb protected band that is indicative of (+) genomic RNA. Unfortunately, signals were not strong enough to permit detection of the 0.7 kb RNA indicative of radiolabelled subgenomic RNA for group B mutants. This band was evident in extracts of protoplasts inoculated with TYMC or TYMC-U57 RNAs (Fig. III-4).

Three negative control inoculations produced no evidence for radiolabel in similar products after incubation in protoplasts: mock inoculation (Fig. III-4); inoculation with uncapped genomic RNA transcripts, which are known to be unstable in cells (Ahlquist *et al.*, 1987); and inoculation with a deleted genomic RNA missing part of the non-structural gene necessary for replication, TYMC-ΔKpn^{2366}-Kpn^{3248} (not shown). The detection of radiolabelled double-stranded RNAs and coat protein in protoplasts makes it clear that replication, albeit at a low level, has occurred after inoculation with group B mutants. This conclusion is based on the use of techniques that are not confounded by the detection of input inoculum.

Coincident phenotypic reversion of replication and valylation. In one instance, systemic symptoms appeared in a plant inoculated with mutant TYMC-A55, which otherwise consistently failed to replicate well enough to support systemic spread. The plant had been inoculated with lysed

protoplasts harvested 48 hr after inoculation with TYMC-A55, and systemic symptoms appeared after a delay of 2-3 weeks, rather than the normal 7 days. On reinoculation onto plants, the newly acquired phenotype was stable and similar to wild-type, in terms of symptom appearance and virus yield (0.5 mg/g fresh weight, c.f. 1.1 mg/g for wild-type TYMC). The valylation of the progeny RNA was greatly improved over that of the parent (1.03 c.f. 0.13 mol. valine/mol. RNA; Chapter II; Fig. III-2b).

The 3′ region from the genomes recovered from the systemically infected plant was cloned, and three separate clones were sequenced. In no case was the phenotypic reversion due to a simple reversion at position 55, but in each case a C57 to U57 transition was present in addition to the original A55 mutation. This defines the progeny as second site suppressor mutants (SSSM).

(a)

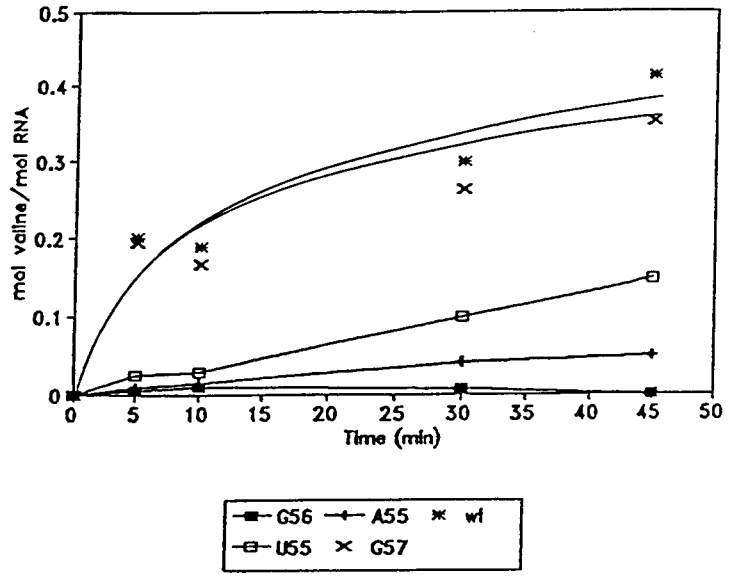

(b)

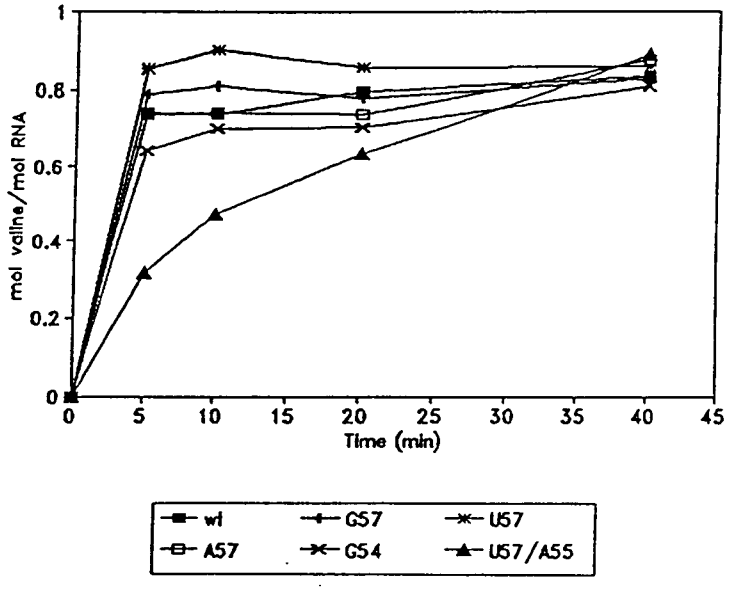

Figure III-2. Valylation *in vitro* of selected mutant genomic RNAs with wheat germ ValRS. (a) Valylation of transcripts (0.6 μM) made from pTYMC templates linearized with *Hind* III and treated with mung bean nuclease to remove restriction overhangs (Materials and Methods). These templates are designed to generate transcripts that have 3'-CCA termini capable of accepting valine. (b) Valylation of progeny virion RNAs (0.6 μM) extracted from systemically infected leaves of plants. wt, wild type; mutants are identified in Table III-1.

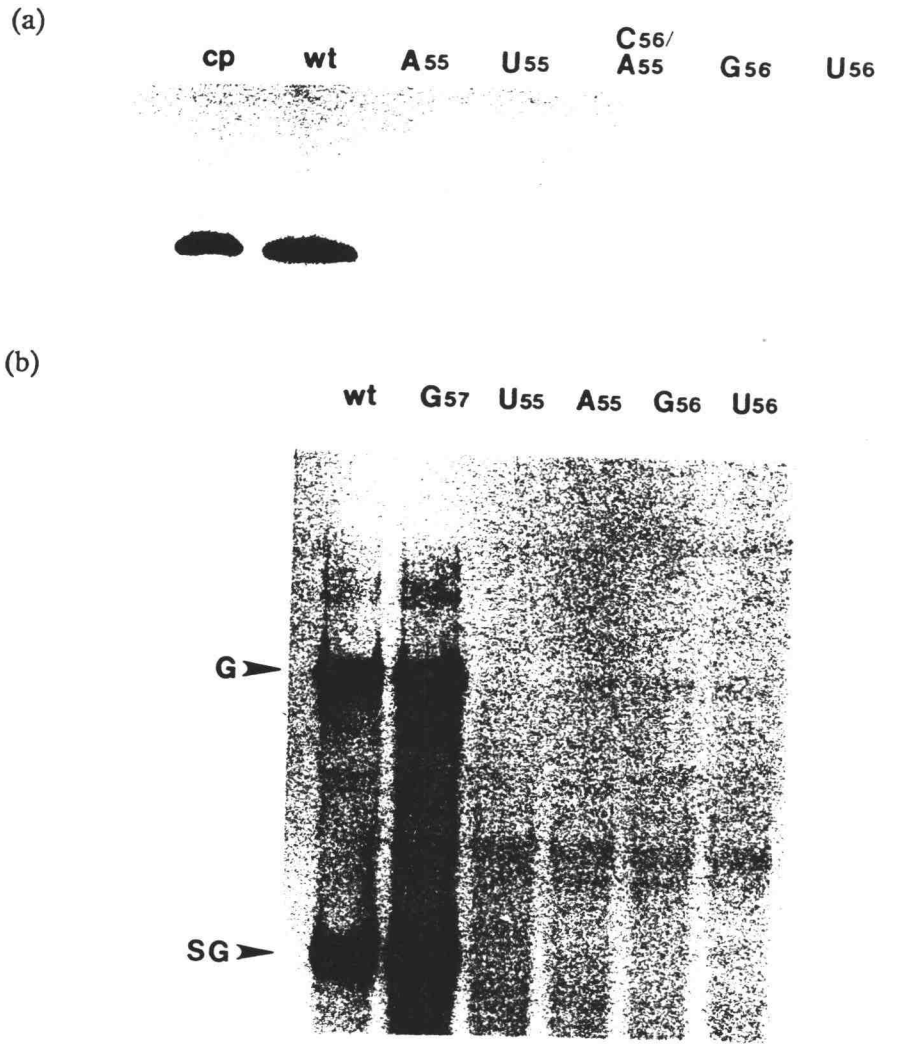

Figure III-3. Replication of TYMV mutants in Chinese cabbage protoplasts. Representative experiments that have contributed to the quantitative data in Table III-1 are shown. Protoplasts ($4x10^5$ cells) were inoculated with 5 μg of TYMC (wt) or mutant genomic transcripts, as indicated. (a) Detection of coat protein (20 kd) in Western blots made after separation of proteins on 14% polyacrylamide-SDS gels. Extracts were made from $2x10^5$ protoplasts harvested 48 hr after inoculation, and blots were developed using horseradish peroxidase-linked second antibodies and 5-chloro-1-naphthol color reagent. CP, coat protein (50 ng of TYMV virions). (b) Detection of viral genomic (G, 6.3 kb) and subgenomic (SG, 0.7 kb) RNAs in Northern blots. RNAs were extracted from $2x10^5$ protoplasts harvested 22 hr after inoculation. The hybridization probe was a ^{32}P-labelled RNA transcript complementary to 0.9 kb at the 3′ end of genomic RNA.

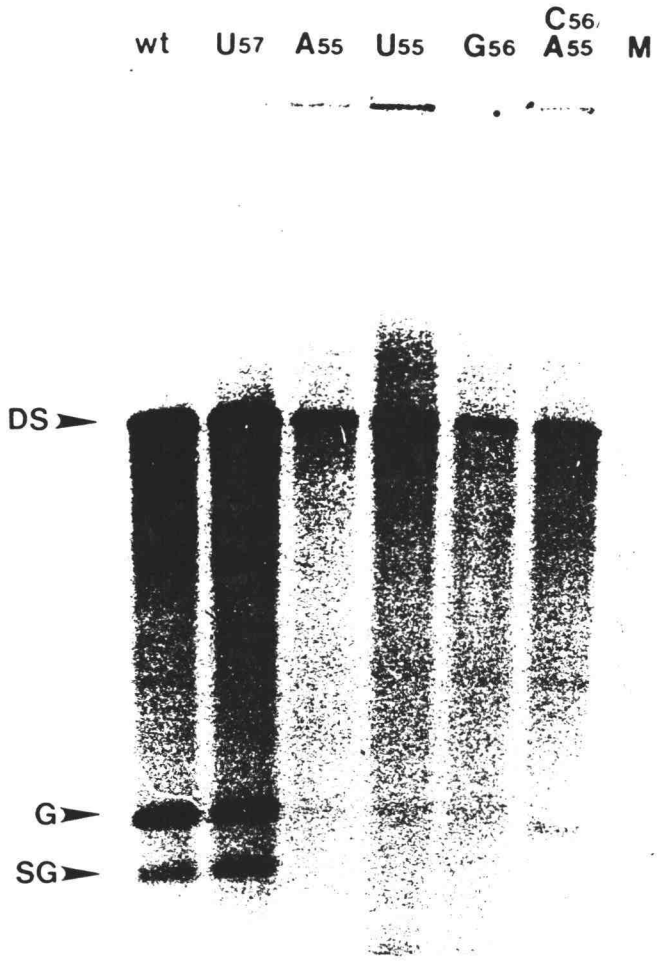

Figure III-4. Inoculated protoplasts were incubated for 24 hr in medium containing [^{32}P]orthophosphate. The *in vivo* labelled RNAs were extracted and analyzed in a ribonuclease protection assay explained in the text. Three forms of viral RNA, separated here by electrophoresis on 1% agarose gels, were protected: genomic double-stranded RNA (DS), the 0.9 kb protected fragment of (+) genomic RNA (G); and the protected subgenomic RNA (SG, 0.7 kb). The lane markings indicate the various inocula used: M, no RNA. The protected genomic band recovered from mutant TYMC-C56/A55 migrates slightly fast due to ribonuclease cleavage of the probe opposite the double mutation.

Table III-1. Properties of TYMV mutants with altered anticodon loops

	Mutant	Anticodon loop sequence	*In vitro* valylation properties[a] (264 nt-long 3'-RNAs)		Replication in Chinese cabbage, relative to wt (Genomic transcripts as inocula)				
					Protoplasts, 48 h.p.i.			Plants	
			mol val/ mol RNA[b]	Rel. V_{max}/K_M	CP[c]	Genomic RNA[d]	Sub-genomic RNA[d]	Virion[e]	Score[f]
A	wt	59-CCCACAC-53	1.01	1.00	1.0	1.0	1.0	1.0	9/9
	G57	. . G . . .	0.98	0.78	0.7	0.6	0.6	1.1	5/5
	A57	. . A . . .	0.98	0.68	1.6	1.1	1.3	0.7	3/3
	U57	. . U . . .	1.02	1.14	1.5	0.9	0.8	1.8	5/5
	G54	. . . . G .	0.99	0.81	0.8	1.0	0.8	0.8	3/3
	U54	. . . . U .	0.97	0.67	1.17	1.25	1.26	-	1/1
	C54	. . . . C .	1.05	0.22	0.24	0.3	0.2	0.5	1/1
	U53	. . . . . U	1.06	0.32	1.11	0.96	0.84	-	2/2
	A53	. . . . . A	0.92	0.093	0.12	-	-	NSS	0/7
B	U55	. . . U . .	0.45	0.017	0.002-0.005	D	ND	NSS	0/3
	A55	. . . A . .	0.13	0.0046	0.015-0.025	D	ND	NSS(r)	1(r)/3
	G55	. . . G . .	0.04	0.0015	≤0.002	D	ND	-	-
	U55/C54	. . . UC .	0.04	0.0020	0.002-0.005	-	-	-	-
	U55/A53	. . . U . A	$<10^{-3}$	0.00042	ND	-	-	-	-
	U55/C54/A53	. . . UCA	$<10^{-3}$	0.00013	ND	D	ND	-	-
	G56	. . G . . .	$<10^{-3}$	0.00020	0.002	D	ND	NSS	0/2
	U56	. . U . . .	$<10^{-3}$	0.00011	≤0.002	D	ND	NSS	0/2
	U56/A55	. . UA . .	$<10^{-3}$	0.000055	ND	D	ND	NSS	0/2
	C56/A55	. . CA . .	$<10^{-3}$	$<10^{-3}$	≤0.002	D	ND	NSS	0/2
	G57/U56/G55	. . GUG . .	$<10^{-3}$	0.00013	ND	D	ND	-	-

Table III-1. Properties of TYMV mutants with altered anticodon loops. All data represents averages of 3 or more experiments unless otherwise indicated. **wt**, wild type; **ND**, results were either undetectable or too low for a reliable estimate; **NSS**, no systemic symptoms observed and no coat protein detected in upper leaves; "-", no experiments performed; **D**, double-stranded genomic RNAs were detected by *in vivo* labelling (Fig. III-4), verifying a low level of RNA synthesis; **r**, reversion of phenotype observed after 2 weeks, resulting from second site suppressor mutations (see text).

a. Valylation catalyzed by wheat germ valyl-tRNA synthetase; standard errors for K_M, V_{max} are 20-25%.

b. Extent of valylation after 60 min at 0.6 μM RNA.

c. Coat protein levels determined in Western blots (see Fig. III-3a); st. error = 20-40%.

d. TYMV RNA levels determined in Northern blots (see Fig. III-3b); st. error = 20-40%.

e. TYMV levels determined after virion purification from systemically infected leaves; wild type yield was 1.1 mg/g fresh weight.

f. Number of plants with systemic symptoms/number of plants inoculated.

Discussion

Interdependence of valylation and replication. The study of a number of mutants with a range of valine identities has shown clearly that valine acceptance activity and the amplification of TYMV RNA are correlated. Only those mutants capable of complete valylation *in vitro* replicated systemically in plants (Table III-1A). Further, when a second mutation arose fortuitously from TYMC-A55 RNA inoculum, resulting in the acquisition of the ability to spread systemically in plants, there was a concomitant improvement in valylation efficiency. One exception to the correlation has been observed, but this concern a mutant that replicates poorly yet valylate well (TYMC-U55), rather than the reverse. Thus, valine acceptance is an important, but not the sole, criterion for replication. Anticodon loop mutant RNAs that valylate but fail to replicate well may, for instance, be promoter mutants, may be subject to mischarging or to base modification by tRNA-specific enzymes, or may have decreased stability or half lives resulting from the introduction of fragmentation sites or endoribonuclease recognition elements (Arraiano *et al.*, 1988). Valylation is also not obligatory for replication *per se*, since all mutants supported low levels of RNA synthesis (Fig. III-4). Rather, valylation is able to enhance those low replication rates to the rates observed in wild-type infections.

The mechanism by which the ability of TYMV RNA to be valylated influences the yield of virion RNA has not been established. RNA synthesis may be directly influenced by the presence or absence of bound valine. Based on the finding that the tRNA-like structure of brome mosaic virus RNA functions as the (-) strand promoter (Miller *et al.*, 1986), it has been hypothesized that aminoacylation may play a role in modulating (-) strand initiation rates (Dreher and Hall, 1988a). Our results are consistent with such a suggestion, and invite speculation that host elongation factor might, as with Qß replicase (Blumenthal and Carmichael, 1979), be part of the replication complex (Dreher and Hall, 1988a; Hall, 1979). As with tRNA, elongation factor binds preferentially to aminoacylated viral RNA (Joshi *et al.*, 1986). An alternative role for valylation may be in regulating the function of a particular RNA as a template for (-) strand synthesis versus translation (Florentz *et al.*, 1984). Perturbation of the normal partitioning of (+)-sense RNAs between these functions could be detrimental to RNA amplification. A third mechanism by which valylation might be necessary for efficient amplification of viral RNA is by stabilizing the 3′ end against the action of exonucleases. However, because viral RNAs are such efficient substrates for host (CTP,ATP):tRNA nucleotidyltransferase, which maintains intact 3′ termini of tRNAs, this enzyme is thought to be responsible for stabilizing viral 3′ ends (Rao *et al.*, 1989). Decreased stability by the endonucleotyic mechanism mentioned above could not be generally applicable to all mutants because of the expected sequence specificity of such an event. Finally, valylation is clearly not involved in packaging, since the virion RNAs lack the 3'-terminal A residue that is necessary for aminoacylation (Briand *et al.*, 1977).

It should be noted that, at present, the correlation discussed above relates valylation determined

in vitro to replication *in vivo*. It is unfortunately not easy to quantify the valylation status of viral RNAs *in vivo*, especially for poorly replicating mutants. Surprisingly, there are very few studies relating *in vitro* and *in vivo* aminoacylation of tRNAs. In one relevant study, yeast elongator $tRNA^{Met}$ was shown to be mischarged with phenylalanine by yeast phenylalanyl-tRNA synthetase with a k_{cat}/K_M only 200-fold lower than that of the cognate $tRNA^{Phe}$ (Feldmann and Zachau, 1977), yet there is adequate discrimination *in vivo*. The very poor valylation we have observed for several TYMV RNA mutants *in vitro* makes it unlikely that these become significantly valylated *in vivo*. It is also unlikely that the mutants capable of systemic spread do not become readily valylated *in vivo*. We are thus confident that the valylation data presented in Table III-1 for these mutants reasonably predict their valylation potential in cells; nevertheless, the *in vivo* valylation status of mutant RNAs will need to be determined experimentally.

Comparison with brome mosaic virus. Experiments conducted with BMV have previously led to the conclusion that efficient tyrosylation is not crucial for replication (Dreher *et al.*, 1989). For example, two BMV mutant RNA3's (Δ5′ and 5′AGA) had initial *in vitro* tyrosylation rates 5% and 3% of wild-type, respectively, and could not be completely aminoacylated. Yet these mutants replicated to levels greater than 50% of wild-type. Comparable TYMV mutants are TYMC-A55 and -U55/C54, with initial valylation rates (at 150 nM) 4% of wild-type, and final valylation levels 13% and 4% of wild-type, respectively. These mutants yielded at best 2.5% of wild-type. The differences between the two viral systems remain to be clarified. Although the experimental strategies of the two studies were similar, the BMV study involved the replication in *trans* of the mutant, while the present study used 3′ mutations *cis* to the non-structural protein-encoding sequences (a *trans* replication system could not be established). The BMV studies have since been extended to include the positioning of 3′ mutations on RNA2, a genomic RNA encoding a protein essential for replication. Negative mutations are rather more detrimental in that context (Rao and Hall, 1990), but do not change previous conclusions (Dreher *et al.*, 1989).

The differences between the conclusions derived from the BMV and TYMV studies may have other explanations. In neither case has the *in vivo* aminoacylation status of the mutant viral RNAs been established. This deficiency is more serious in interpreting the BMV results, since no mutants comparable to the range of very poorly valylating mutants described in this paper were obtained. On the other hand, a detailed characterization of promoter elements in the TYMV RNA will assist in interpreting the results in this paper. Finally, it is possible that the role and relevance of aminoacylation is not the same among the various plant RNA viruses that exhibit tRNA mimicry. More research is needed to elucidate this phenomenon genetically and biochemically.

CHAPTER IV

Second Site Suppressor Mutations Assist in Studying the Function of the 3′ Noncoding Region of TYMV RNA

Abstract

The 3′ noncoding region of turnip yellow mosaic virus RNA includes an 82-nucleotide-long tRNA-like structure domain and a short upstream region that includes a potential pseudoknot overlapping the coat protein termination codon. Genomic RNAs with point mutations in the 3′ noncoding region that result in poor replication in protoplasts and no systemic symptoms *in planta* were inoculated onto Chinese cabbage plants in an effort to obtain second site suppressor mutations. Putative second site suppressor mutations were identified by ribonuclease protection and sequencing, and were then introduced into genomic cDNA clones to permit their characterization. A C-57→U mutation in the tRNA-like structure was a strong suppressor of the C-55→A mutation which prevented both systemic infection and *in vitro* valylation of the viral RNA. Both these phenotypes were rescued in the double mutant. An A-107→C mutation was a strong second site suppressor of the U-96→G mutation, permitting the double mutant to establish systemic infection. The C-107 and G-96 mutations are located on opposite strands of one helix of a potential pseudoknot, and the results support a functional role for the pseudoknot structure. A mutation near the 5′ end of the genome (G+92→A), at position -3 relative to the initiation codon of the essential ORF-206, was found to be a general potentiator of viral replication, probably due to enhanced expression of ORF-206. The A+92 mutation enhanced the replication of TYMC-G96 in protoplasts, but was not a sufficiently potent suppressor to permit systemic spread of the A+92/G-96 double mutant in plants.

Introduction

Turnip yellow mosaic virus (TYMV) has a positive-sense single-stranded RNA genome 6.3 kb long. The entire sequences of the genome of a European isolate (Morch *et al.*, 1988) and an Australian isolate (Keese *et al.*, 1989) determined. We have reported the sequence of TYMC, the Corvallis strain of TYMV, which is clonally propagated in cDNA form in plasmid pTYMC (Dreher and Bransom, 1992). In common with several other plant viruses, including brome mosaic virus (BMV) and tobacco mosaic virus (TMV), the 3′-terminal region of TYMV RNA comprises a tRNA-like structure (recently reviewed by Mans *et al.*, 1991). In TYMV RNA, this structure is 82 nucleotides long (Fig. IV-1) and can be specifically recognized by several tRNA-associating proteins such as valyl-tRNA synthetase and (CTP,ATP):tRNA nucleotidyltransferase from wheat germ (Dreher *et al.*, 1988), yeast (Joshi *et al.*, 1982b) or *Escherichia coli* (Joshi *et al.*, 1982a) and by elongation factor EF-Tu from *E. coli* (Joshi *et al.*, 1984) or EF-1α from wheat germ (Joshi *et al.*, 1986). The tRNA-like structures are thought to play a role in viral RNA replication (Dreher and Hall, 1988a) and for TYMV there is a strong correlation between the valine acceptance and replication *in vivo* of RNAs with mutations in the tRNA-like structure (Chapter III in this thesis). The mechanism by which the ability to be valylated contributes to successful replication remains unclear, however.

A second readily recognizable feature of the 3′ noncoding region of BMV and TMV RNAs is the presence of one or more pseudoknots upstream of the tRNA-like structure. Three consecutive pseudoknots are present at this location in TMV RNA (van Belkum *et al.*, 1985), and mutations that delete or disrupt secondary structural elements of the downstream pseudoknot result in a loss of replication in tobacco plants or cells (Takamatsu *et al.*, 1990). In the 3′ noncoding region of BMV RNA3, there are four consecutive pseudoknots (Pleij *et al.*, 1987), and deletion studies have indicated the importance of this region for successful viral replication in barley protoplasts (F. Lahser and T. C. Hall, personal communication). In TYMV RNA, a potential pseudoknot overlaps the termination codon of the coat protein gene (Rietveld, 1984; Fig. IV-1), but no experiments have investigated the role of this part of the TYMV genome in virus viability. Pseudoknots have recently become recognized as structural elements involved in the regulation of gene expression, such as translational readthrough (Wills *et al.*, 1991) and frameshifting (Brierley *et al.*, 1989; Chamorro *et al.*, 1992; Dinman *et al.*, 1991). It is possible that the recognition and binding of proteins to pseudoknots is involved in regulatory events (Pleij, 1990; Schimmel, 1989; Tang and Draper, 1989), and the interaction of one or more proteins with the pseudoknots present in the 3′ noncoding regions upstream of the tRNA-like structures of TMV and BMV RNAs may participate in events controlling viral RNA replication.

Our previous studies have characterized the decreased replication that results from certain substitutions in the 3′ tRNA-like structure of TYMV RNA (Chapter III in this thesis). During those

studies, it was noticed that in rare cases systemic symptoms appeared (with considerable delay) when mutants normally incapable of supporting systemic infection were inoculated onto Chinese cabbage plants. The symptoms were considered to derive from the replication of a novel mutant virus that had arisen from the inoculum by acquiring one or more mutations as a result of polymerase error during the limited replication the mutants were capable of supporting. The RNA-dependent polymerases of viruses are known to be relatively error-prone (Domingo and Holland, 1988). In the studies reported here, our aim was to explore the ability of such plant inoculation experiments to yield novel mutants with second site suppressor mutations that might open up new avenues for studying the role of the 3′ noncoding region (including the potential pseudoknot) and tRNA-like structure of TYMV RNA. We show that second site suppressor mutations can be readily isolated, and present results based on such a mutation that support a role for a pseudoknot immediately upstream of the tRNA-like structure.

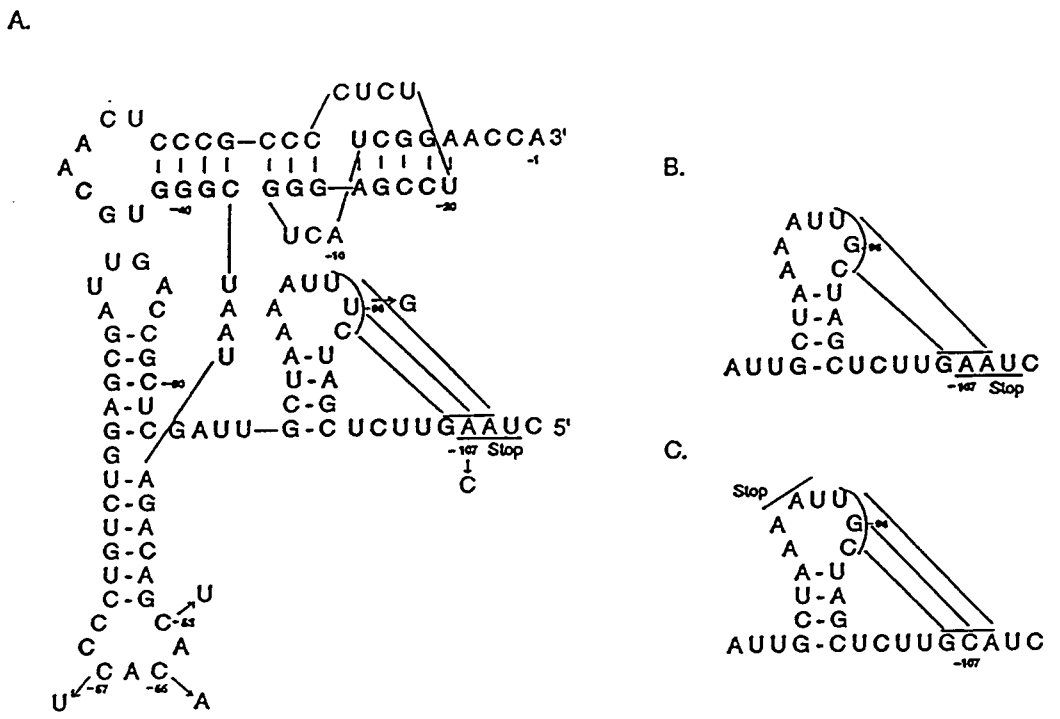

Figure IV-1. Secondary structure model of the 3′ noncoding region of TYMV RNA. A. The L-conformation of the tRNA-like structure of wild type TYMC RNA is shown, with a pseudoknot present in the amino acid acceptor stem near the 3′ end. The basepairs contributing to a potential pseudoknot upstream of the tRNA-like structure is also shown, together with the coat protein termination codon (stop), which it overlaps. The various mutations in the 3′ noncoding region studied in this paper are indicated. B. The potential pseudoknot is disrupted in mutant TYMC-G96 RNA. C. The potential pseudoknot of mutant TYMC-C107/G96 RNA, similar to that of TYMC RNA. The C-107 mutation causes an extension of the coat protein ORF, to terminate as indicated. Nucleotides are numbered from the 3′ end and carry a "-" symbol to differentiate from nucleotides near the 5′ end (Fig. IV-2).

Materials and Methods

Materials. Chinese cabbage (*Brassica pekinensis* cv. Wong Bok or Spring A-1) plants were grown in a growth chamber under 16 hr day-length at 21°C. The hybrid cultivar Spring A-1 was used in most experiments and was preferred over Wong Bok due to greater genetic uniformity. Plasmid pTYMC (Weiland and Dreher, 1989), from which infectious genomic RNA (TYMV-Corvallis strain, referred to as TYMC) can be transcribed with T7 RNA polymerase, is shown in Fig. IV-2. T7 RNA polymerase and reverse transcriptase were purchased from Life Sciences, m^7GpppG cap analogue from New England Biolabs, InhibitAce ribonuclease inhibitor from 5 prime-3 prime, Inc., T7 DNA polymerase (Sequenase) from United States Biochemical, *Thermus aquaticus* DNA polymerase from Promega, and restriction enzymes from Gibco-BRL, Boehringer-Mannheim, and New England Biolabs. Macerase and Cellulysin were purchased from Calbiochem. Synthetic deoxyoligonucleotides were made by automated phosphoramidite synthesis and purified on 20% polyacrylamide/7M urea gels.

Protoplast and plant inoculations. Young healthy leaves (3-4 g) were taken from 6-week-old Chinese cabbage plants that had been held in the dark for three days in order to deplete starch grains. Protoplasts were prepared and inoculated (5 μg of transcript RNA per $4x10^5$ cells) as described (Weiland and Dreher, 1989), except that protoplasts were released after incubation of leaf slices in the hydrolytic enzymes overnight at 25°C. Inoculated protoplasts were incubated under constant light at 25°C for 48 hr prior to harvest.

Three-week-old Chinese cabbage plants with two true leaves were used for inoculations of whole plants. Each leaf was mechanically inoculated with 10 μl of RNA transcript (0.25 mg/ml) in 50 mM glycine, 30 mM K_2HPO_4 (pH 9.2), 1% bentonite and 1% celite. At times, plants were inoculated with a suspension of lysed protoplasts harvested 48 hr post inoculation ($5x10^4$ cells/leaf).

Virion RNA extraction and characterization. Virus was isolated from infected plants by polyethylene glycol precipitation according to Lane (1986) and quantitated spectrophotometrically. Virion RNA was prepared from virus by double phenol/chloroform extraction and one chloroform/isoamyl alcohol extraction, followed by ethanol precipitation. In order to assess the stability of mutated sequences during replication in plants, the regions encompassing the relevant mutations were reverse-transcribed and amplified by polymerase chain reaction (PCR) using the oligomers described below. The presence of mutations was determined either directly by sequencing the PCR products (Winship, 1989) or by digesting with diagnostic restriction enzymes that cleaved the wild-type but not mutant sequence.

Cloning and transcription. In the preparation of several mutants, PCR was used to generate small mutated fragments for substitution into pTYMC. Each fragment was completely sequenced prior to subcloning, in order to verify the presence of only the desired mutations. Sequences with mutations in the 3′ noncoding region were PCR-amplified as 260 bp fragments using the 5′ oligomer

d(GGGTCAAAGATTCGATTC) and the 3′ oligomer d(TTCGAGCTCAAGCTTGGTTCCGATG), which includes a *Hind*III site positioned at the 3′ end of the genomic sequence. Mutant pTYMC-U53 was made in this way from cDNA clone mpTY-U53, which was used for *in vitro* valylation studies (Chapter IV in this thesis). Mutants pTYMC-U57/A55 and pTYMC-C107/G96 were generated from mutant virion RNA or total RNA isolated from infected tissue, respectively, by PCR amplification after reverse transcription primed by the above 3′ oligomer (Kawasaki, 1990). The amplified mutant fragments were treated with *E. coli* Klenow polymerase to remove non-base-paired termini, digested with *Hind*III restriction endonuclease, and subcloned into the *Sma*I^{6062} and *Hind*III$^{3'}$ sites of pTYMC (Fig. IV-2).

Mutant pTYMC-G96 was generated via 3′ PCR amplification as above. After amplification of 260 bp fragments from wild-type pTYMC and from the fortuitously isolated mutant clone pTYMC-U53/G96, each was digested with *Alu*I (which cleaves 82 nucleotides from the 3′ end of the genomic sequence). The purified 5′ fragment from pTYMC-U53/G96 and 3′ fragment from pTYMC were then religated and subcloned into the *Sma*I^{6062} and *Hind*III$^{3'}$ sites of pTYMC.

Mutant pTYMC+A92 was also created via reverse transcription and PCR from mutant virion RNA. PCR to create pTYMC+A92 used a 5′ 59-mer oligomer corresponding to a 5′ *Eco*RI site and the T7 promoter fused to TYMC nucleotides 1-35 and the 3′ oligomer d(ATGGTAATACATCAGG) to produce a 564 bp fragment. The mutant fragment was substituted into the *Eco*RI$^{5'}$ and *Nco*I^{210} sites of pTYMC. To make pTYMC+A1460, full-length cDNA was made from mutant virion RNA using the 3′ genomic oligomer and second strand DNA was made by priming with the 5′ 59mer. The mutant fragment was substituted into pTYMC by subcloning between the *Pst*I^{1309} and *BamH*I^{1755} sites. [PCR analysis for the A+1460 mutation used the 5′ oligomer d(CCTGAGGCAACATTGG) to prime at nucleotide 1240 and the 3′ oligomer d(AGCATGGACTTCTGTTCG) to prime opposite nucleotide 1573].

The combinatorial mutants pTYMC-G96+A92, pTYMC-G96+A1460, pTYMC-G96/U53+A92 and pTYMC-G96/U53+A1460 were made by subcloning fragments using restriction sites shown in Fig. IV-2.

Plasmid DNAs were prepared from 50 ml bacterial cultures and the mutant sequences were confirmed by double-stranded DNA sequencing (Chen and Seeburg, 1985). Capped genomic transcripts labelled with [α-^{32}P]UTP (0.1 Ci/mmol) were prepared with T7 RNA polymerase from DNA templates linearized with *Hind*III and analyzed as described prior to inoculation (Weiland and Dreher, 1989).

Analysis of viral products by Western and Northern blotting. The levels of coat protein in harvested protoplasts were analyzed in Western blots using horseradish peroxidase-labelled secondary antibody and the chromogenic substrate 4-chloro-1-naphthol (detection limit of 2 ng of coat protein) as

described (Weiland and Dreher, 1989). Results were quantitated by scanning laser densitometry with reference to a dilution series of virus (Chapter III in this thesis).

RNA was extracted from protoplasts, glyoxalated, electrophoresed through 1% agarose and transferred to nylon membranes as described (Weiland and Dreher, 1989). The hybridization probe was a ^{32}P-labelled RNA transcript complementary to 0.9 kb at the 3′ end of TYMV RNA (*Pst*I-*Hind*III fragment, Fig. IV-2), permitting the detection of both genomic and subgenomic RNAs (Chapter III in this thesis). RNA levels were quantitated by scanning laser densitometry or with a ß-emission radioisotope scanner (Ambis Systems, San Diego).

Ribonuclease protection assays. Antisense RNA probes (minus strand) were prepared by transcription with T7 or T3 RNA polymerase after subcloning appropriate fragments from pTYMC into the vector pT7/T3α-18, which contains the T3 and T7 promoters (Gibco-BRL). Probes representing TYMC sequences between the following restriction sites were used: full-length (*Hind*III$^{3'}$-*Eco*RI$^{5'}$), *Hind*III$^{3'}$-*Nco*I^{210}, *Hind*III$^{3'}$-*BamH*I^{1755}, *Hind*III$^{3'}$-*Sst*I^{3286}, *BamH*I^{1755}-*Nco*I^{210}, and *BamH*I^{1755}-*Eco*RI$^{5'}$. Virion RNAs (2 μg) were mixed with antisense RNA probes (1 μg), and denatured at 85°C for 5 min in the presence of 40 mM piperazine-N,N′-bis[2-ethanesulfonic acid] (PIPES, pH 6.7), 0.4 M NaCl, 1 mM EDTA and 80% formamide (in a 30 μl reaction). After hybridization overnight at 55°C, 300 μl of ribonuclease solution containing 10 mM Tris-HCl (pH 7.5), 0.3 M NaCl, 5 mM EDTA, ribonuclease A (32 μg/ml) and ribonuclease T1 (1.6 μg/ml) were added to the samples and incubated at 30°C for 1 hr (Myers *et al.*, 1985; Lopez-Galindez,1988; Grange *et al.*, 1990). Ribonucleases were removed by treatment with 50 μg/ml proteinase K in the presence of 0.5% SDS at 37°C for 30 min. After phenol/chloroform extraction, the samples were ethanol precipitated, and then analyzed by electrophoresis on agarose or polyacrylamide gels.

In vitro valylation of transcripts. 264-nucleotide-long fragments corresponding to the 3′ region of TYMC and derivative mutant RNAs were synthesized by transcription from *Bst*NI-linearized cDNA clones and used in studies on valylation kinetics as described (chapter IV in this thesis). Valylation was determined by the incorporation of [^{3}H]valine by a valyl-tRNA synthetase activity present in an extract from wheat germ (Chapter IV in this thesis).

In order to permit the synthesis of full-length genomic RNA transcripts capable of aminoacylation, the restriction overhangs generated by *Hind*III linearization of pTYMC and selected mutant derivatives were removed by treatment with mung bean nuclease (Dreher *et al.*, 1988). The treated DNAs were extracted with phenol/chloroform and ethanol precipitated, and then used as templates for the synthesis of genomic transcripts by T7 RNA polymerase (as described above, except that cap analogue was omitted). The resultant transcripts were valylated to determine the moles of valine bound per mole of mutant RNA relative to wild-type RNA.

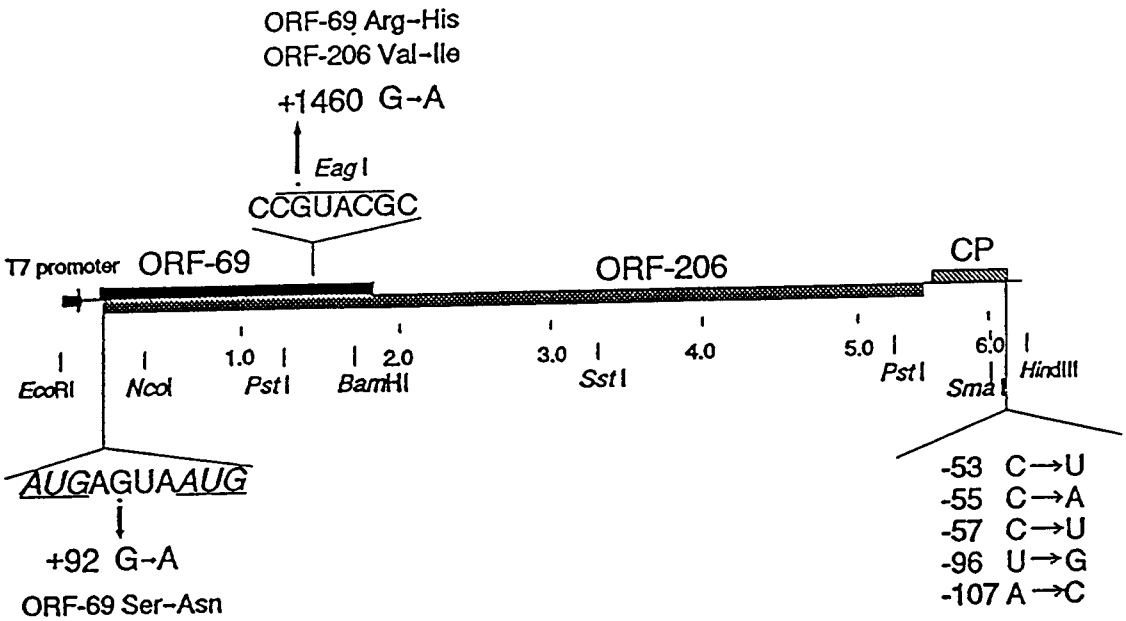

Figure IV-2. Diagram of pTYMC, the genomic cDNA clone from which infectious transcripts can be generated with T7 RNA polymerase. The mutations from the 5' region of the genome that were studied in this paper are indicated, together with the effect each substitution has on open reading frames. The mutations in the 3' noncoding region are summarized (refer Fig. IV-1 for more detail). The three ORFs of TYMC RNA are indicated: ORF-69, ORF-206 and the coat protein ORF (CP) and restriction sites used for cloning are shown. Nucleotides toward the 5' end are numbered conventionally and marked "+", while those near the 3' end are numbered from the 3' end and marked "-".

Results

Recovery of variants capable of systemic infection after inoculation with replication-deficient TYMC mutants. Our previous studies on the replication of TYMC RNAs with mutations in the tRNA-like structure yielded two instances of phenotypic reversion after the inoculation of Chinese cabbage plants with protoplasts infected with poorly replicating TYMC mutants (Chapter III in this thesis). TYMC-A55 replicated poorly in protoplasts and usually produced no systemic infection in plants, but delayed systemic symptoms appeared in one of three plants inoculated. In the second instance, delayed systemic symptoms were reported in one of five plants inoculated via protoplasts with RNA containing G-96/U-53 mutations. Since the viruses responsible for both of these phenotypic reversions appeared to harbor second site suppressor mutations, we have characterized the above mutants and further explored the potential for obtaining second site mutations capable of suppressing deleterious mutations in the 3′ noncoding region of TYMV RNA.

The plant with symptoms originating from a TYMC-A55 RNA inoculum developed systemic symptoms after 3-4 weeks, whereas symptoms appeared 7 days after inoculation with wild-type TYMC. Virion RNA was prepared and reverse transcribed using a primer hybridizing to the 3′ end. The 3′ region was amplified by PCR to yield a 260 bp fragment, whose sequence revealed a C-57→U mutation in the wobble position of the anticodon in addition to the original A-55 mutation (Fig. IV-1). The U-57 mutation thus appeared to suppress the poor replication phenotype resulting from the A-55 mutation.

Systemic symptoms were derived from a TYMC-G96/U53 RNA inoculum, which in most cases does not give rise to systemic infection (Table IV-1). The sequence of the 3′ region of the virion RNA, obtained after PCR amplification as above, revealed the presence of only the U-53 mutation. Ribonuclease protection experiments using antisense RNA probes indicated the presence of a novel mutation in this virion RNA (Fig. IV-3) that was shown by sequencing of the appropriate PCR-amplified fragment to be a G+1460→A substitution. As shown in Table IV-1, TYMC-U53 replicates like wild-type TYMC in both Chinese cabbage protoplasts and plants. It thus appeared possible that the A+1460 mutation was able to partially suppress the G-96 mutation, although the latter had reverted to wild-type prior to full symptom development.

Two further mutations with potential second site suppressor activity were isolated after inoculation of plants with protoplasts infected with TYMC-G96 RNA. Fourteen of 21 plants developed systemic symptoms 14-21 days after inoculation, while no symptoms developed in the remaining 7 plants (Table IV-1). Total RNAs were extracted from the symptomatic tissue of the 14 plants, reverse transcribed with the TYMC-specific 3′ primer, and the 3′ 260 bp fragments were PCR-amplified as above. Digestion of the amplified fragments with the restriction enzyme *Dra*I, which cleaves the wild-type $^{-96}$TTTAAA^{-91} but not the mutant $^{-96}$GTTAAA^{-91} sequence, followed by sequencing of *Dra*I-resistant fragments, showed that the G-96 mutation was retained in 2 of the plants, but had reverted in the

remaining 12. The virion RNA from one of the plants that retained the G-96 mutation contained an A-107→C mutation. Virion RNAs from the other plant were subjected to ribonuclease protection analysis followed by PCR amplification and sequencing, resulting in the detection of a G+92→A mutation (the wild-type G+92 sequence was present also in a mixed population). The novel mutations from these two plants appeared to be suppressors of the G-96 mutation.

The U-57 mutation suppresses the defective valylation and replication caused by the C-55→A mutation. The U-57/A-55 double mutation was transferred into plasmid pTYMC as described to yield pTYMC-U57/A55. The replication of TYMC-U57/A55 in Chinese cabbage protoplasts and plants was studied by inoculation with capped transcripts made from *Hind*III-linearized plasmid DNA with T7 RNA polymerase, and compared with that of wild-type TYMC and of the mutants TYMC-U57 and TYMC-A55 (Table IV-2). Protoplasts inoculated with TYMC-U57/A55 RNA accumulated coat protein (detected on Western blots) to a level 85% that of protoplasts inoculated with wild-type TYMC RNA; accumulations of genomic and subgenomic RNAs, determined from Northern blots, were 65% and 45% relative to wild-type, respectively (Table IV-2). Inoculation of plants resulted in systemic symptoms indistinguishable from wild-type, and virions could be isolated from infected tissue in a yield similar to that from wild-type infections (Table IV-2). Comparison of these results with those describing the replication of TYMC-A55 RNA (Table IV-2) clearly shows that the U-57 is a potent suppressor of the deleterious effect of the A-55 mutation with regard to replication.

Table IV-2 also summarizes our studies reported elsewhere (Chapter II in this thesis) on the valylation properties of a 3′ fragment of TYMV RNA that carries the UAA anticodon (U-57/A-55 double mutation). TY-U57/A55 RNA could be valylated to completion by wheat germ valyl-tRNA synthetase and had a V_{max}/K_M (a measure of the efficiency of valylation) of 0.075 relative to wild-type RNA. By contrast, TY-A55 RNA could only be 13% valylated and had a relative V_{max}/K_M of 0.0046 (Chapter IV in this thesis; Table IV-2). With regard to valylation, the U-57 mutation also strongly suppresses the effect of the A-55 mutation.

Replication of TYMC-G96 and TYMC-G96/U53 in protoplasts. In order to characterize the replication properties of these two mutants that gave rise to the suspected second site suppressor mutations described above, capped genomic transcripts were prepared from pTYMC-G96 and pTYMC-G96/U53 and inoculated onto Chinese cabbage protoplasts. These clones were verified to contain only the indicated mutations by sequencing the mutant *Sma*I^{6062}-*Hind*III$^{3'}$ fragments (Fig. IV-2) that had been introduced into pTYMC (Materials and Methods). Chinese cabbage protoplasts inoculated with TYMC-G96 RNA accumulated highly variable amounts of coat protein, ranging between 0.02 and 0.3 relative to wild-type (Fig. IV-4; Table IV-1). In the course of these studies, 10 separate batches of protoplasts (principally cv. Spring A-1) were inoculated with TYMC-G96 RNA; in some cases triplicate inoculations were made using the same preparation of transcript RNA. The results appeared to vary depending on the batch of protoplasts rather than other variables such as the transcript

preparation or the particular inoculation. In previous experiments (Weiland and Dreher, 1989; Chapter III in this thesis), we have never observed such variability.

Since virus amplified in isolated protoplasts is not able to spread and infect other cells (spread in plants being via the plasmodesmatal connections between cells), it is unlikely that a spontaneous mutant capable of efficient replication could give rise to the higher levels of replication observed with some TYMC-G96 inoculations. Such mutations are relatively rare events, and would need to occur independently in many cells, since the Western-blot signals in protoplast inoculation experiments are the result of viral replication in at least 80% of the cells. Nevertheless, we PCR-amplified and sequenced the 3′ region of RNAs extracted from protoplast batches that supported relatively high levels of coat protein synthesis, and found the G-96 mutation (and no wild-type sequence) to be present in all cases. The frequent reversion to U-96 on inoculation of the infected protoplasts to plants (Table IV-1) is consistent with the absence of second site suppressor mutations in the RNAs replicated in the protoplasts. Taken together, we can thus conclude that the replication levels determined from Western blots refer to the replication of TYMC-G96 and not of some altered genotype. With regard to the variable levels of replication in protoplasts, we suggest that the deleterious effect of the G-96 mutation is sensitive to variations in the status of the host cells that we currently do not understand.

Protoplasts inoculated with TYMC-G96/U53 RNA accumulated coat protein to levels 0.02 of wild-type (Fig. IV-4; Table IV-1). Unlike the situation with TYMC-G96 inoculations, the yields of coat protein were consistent between experiments. Table IV-1 and Fig. IV-4 also show the replication properties of TYMC-U53, which has a phenotype in plants similar to wild-type.

The C-107 mutation is a potent second site suppressor of the G-96 mutation. The C-107/G-96 double mutation was introduced into pTYMC to yield pTYMC-C107/G96. The absence of other mutations in the 3′ noncoding region was verified by sequencing. The ability of genomic transcripts from this clone to support replication in protoplasts and systemic infection of plants was then studied and compared with wild-type TYMC and mutant TYMC-G96 transcripts. Protoplasts inoculated with TYMC-C107/G96 RNA consistently accumulated coat protein to levels 45% those of TYMC-inoculated protoplasts (Fig. IV-4; Table IV-1). When protoplasts infected with TYMC-C107/G96 were inoculated to plants, normal systemic symptoms developed with no delay relative to wild-type. The double mutation sequence has been stably maintained after two serial passages through Chinese cabbage cv. Spring A-1 plants. By contrast, systemic TYMC-G96 infection was never observed, and TYMC-G96 replication in protoplasts was variable but never as efficient as that of TYMC-C107/G96. The C-107 mutation is thus an efficient suppressor of the G-96 mutation.

The U-96→G mutation is positioned to disrupt basepairing that is part of a potential pseudoknot overlapping the UAA codon that terminates the coat protein ORF (Figs. IV-1, IV-2). The spontaneously recovered A-107→C mutation restores the ability for the pseudoknot to form in TYMC-G96 RNA, by replacing the $^{-108}$AAG^{-106}/$^{-97}$CUU^{-95} stem of the wild-type RNA with $^{-108}$ACG^{-106}/$^{-97}$CGU^{-95}

in the TYMC-C107/G96 double mutant (Fig. IV-1). In addition to its positioning within the potential pseudoknot, the C-107 mutation falls within the natural coat protein termination codon $^{-105}$UAA^{-107}. The substitution of UAA with UAC is expected to result in the addition of a 5-amino acid extension (Tyr-Val-Leu-Asp-Arg) to the 140-residue wild-type coat protein, with termination occurring at the $^{-94}$UAA^{-92} codon (Fig. IV-1). Preliminary results suggest that the C-terminal extension results in less stable virions (C.-H. Tsai, unpublished observations).

The rescued replication of the double mutant relative to TYMC-G96 suggests a function for the pseudoknot. We have previously reported that sequences between nucleotides -82 and -159 are involved in obtaining optimal valylation rates (Dreher *et al.*, 1988), although this result has been disputed (Mans *et al.*, 1990). In order to determine whether altered valylatability, which is crucial for replication (Chapter III in this thesis), might explain the replication properties of mutants with substitutions affecting the potential pseudoknot, the valylation of these mutant RNAs was studied. The kinetics of valylation by wheat germ valyl-tRNA synthetase was studied in detail on mutant RNAs containing the 3′-258 nucleotides of viral RNA as described (Chapter IV in this thesis). The results presented in Table IV-3 show that the G-96 mutation (mutants TY-G96 and TY-G96/U53) had very little effect on valylation kinetics, less than the U-53 mutation (mutant TY-U53) which had no detectable effect on the viral phenotype *in vivo* (Table IV-3).

Uncapped genomic RNAs with 3′-CCA termini compatible with valylation were prepared for the above mutants in order to determine whether the mutations in the potential pseudoknot could affect valylation in the context of the 6.3 kb genomic RNA. A possible role for the pseudoknots upstream of the tRNA-like structures in TYMV, TMV and BMV RNAs might be as a spacer arm to ensure the spacial separation of the 3′-tRNA-like domain from the remaining genomic RNA, ensuring accessibility to the relevant aminoacyl-tRNA synthetase and other proteins needed for replication. Only minor differences in the *in vitro* valylation by wheat germ valyl-tRNA synthetase were observed between wild-type TYMC, TYMC-G96, TYMC-C107/G96 and TYMC-G96/U53 (Fig. IV-5). Thus, altered valylation does not explain the replication behavior of mutants containing the C-107 and G-96 mutations.

Mutation A+92 as a potential second site suppressor of mutation G-96. Mutants TYMC+A92, TYMC-G96+A92 and TYMC-G96/U53+A92 were constructed and sequencing verified the presence of only the indicated mutations. Protoplasts inoculated with TYMC+A92 RNA accumulated coat protein to levels 1.6 times that present in wild-type infections (Fig. IV-4; Table IV-1), and inoculation of plants resulted in systemic infections indistinguishable from wild-type but with higher virion yields (1.8 relative to wild-type). The mutant sequence was stable in plants. The G+92→A mutation lies between the tandem initiation codons at the 5′ end of the TYMV RNA (Fig. IV-1; Dreher and Bransom, 1992), and results in a Ser→Asn substitution of the second codon of ORF-69, which encodes a protein that is necessary for cell-to-cell movement in plants but not for replication

in protoplasts (Bozarth *et al.*, 1992). The A+92 mutation also places a more optimal nucleotide in the -3 position relative to the AUG codon that initiates ORF-206 (Kozak, 1987; Cavener and Ray, 1991). The improved replication of TYMC+A92 relative to wild-type might thus be due to more efficient translation of ORF-206, which encodes proteins essential for replication (Weiland and Dreher, 1989), although no clear enhancement of translation was observed *in vitro* using a reticulocyte lysate (not shown).

Protoplasts inoculated with TYMC-G96+A92 and TYMC-G96/U53+A92 RNAs accumulated coat protein to levels 0.21 and 0.02 relative to wild-type, respectively (Fig. IV-4; Table IV-1). The variable replication characteristic of TYMC-G96 was not observed. Both mutations were shown by sequence analysis after PCR amplification to be retained in the protoplasts inoculated with TYMC-G96+A92 (not shown). When protoplasts infected with TYMC-G96+A92 were inoculated onto plants, systemic symptoms appeared after 7 days in 8 plants and after 11 days in the remaining plant inoculated (Table IV-1). RNA from the systemically infected tissues was assayed for the retention of the G-96 mutation by PCR-mediated amplification of 3′ sequences followed by *Dra*I digestion of the amplified fragment. In all but the plant with delayed symptoms, there was a reversion of G-96 to the wild-type U-96 sequence (Table IV-1), while in each of 5 plants tested, the A+92 mutation was retained. Even in the plant with delayed symptoms, G-96 was present only in early systemic infection, being replaced by the U-96 revertant by the time symptoms had fully developed. The replication of RNA with the G-96 mutation in early symptomatic leaves remote from the inoculated leaf suggests that the defect resulting from this mutation affects some aspect of viral infection other than movement in the plant.

The above results indicate that the A+92 mutation can act as a potentiator of viral replication, both in the wild-type and the TYMC-G96 mutant, perhaps by virtue of increased translational expression of ORF-206. The A+92-mediated suppression of the poor replication phenotype that results from the G-96 mutation is not sufficient, however, to support systemic spread in plants, which occurred only after reversion of the G-96 mutation. Reversion did nevertheless occur more frequently and more rapidly in the presence of the A+92 mutation (compare TYMC-G96 and TYMC-G96+A92, Table IV-1).

Mutation A+1460 as a potential second site suppressor of mutation G-96. Mutants TYMC+A1460, TYMC-G96+A1460 and TYMC-G96/U53+A1460 were constructed and verified to contain only the indicated mutations. Protoplasts inoculated with TYMC+A1460 RNA accumulated coat protein to levels 0.9 relative to wild-type, and TYMC+A1460 inoculum supported normal systemic symptom formation *in planta* (Table IV-1). The G+1460→A mutation, which results in an Arg→His substitution in ORF-69 and a Val→Ile substitution in ORF-206, thus had no noticeable phenotype.

Protoplasts inoculated with TYMC-G96+A1460 and TYMC-G96/U53+A1460 RNA

accumulated coat protein to levels of 0.02-0.3 and 0.02 relative to wild-type, respectively (Table IV-1). The variability of viral replication after inoculation with TYMC-G96+A1460 was like that following inoculation with TYMC-G96 RNA. Plants inoculated with lysates of protoplasts infected with TYMC-G96+A1460 developed systemic symptoms in 10 out of the 12 plants inoculated, with symptoms appearing 14-21 days after inoculation. *Dra*I digestion of the 3' 260 bp fragments amplified from total RNA extracted from the symptomatic leaves after reverse transcription and PCR showed that the G-96 mutation had reverted to the wild-type U-96 in all 10 plants. The presence of the A+1460 mutation was studied in the systemic tissue by reverse transcription and PCR amplification, followed by digestion with the *Eag*I restriction enzyme, which cleaves the wild-type ^{1459}CGTACG^{1464}, but not the mutant ^{1459}CATACG^{1464} sequence. In all 5 progeny RNAs tested, the PCR products were *Eag*I-resistant, indicating the retention of the A+1460 mutation. Because the replication behavior of TYMC-G96 and TYMC-G96+A1460 are similar — and similarly variable — it is clear that the A+1460 mutation has no detectable activity in modifying the phenotype of the G-96 mutation, and is not a useful second site suppressor.

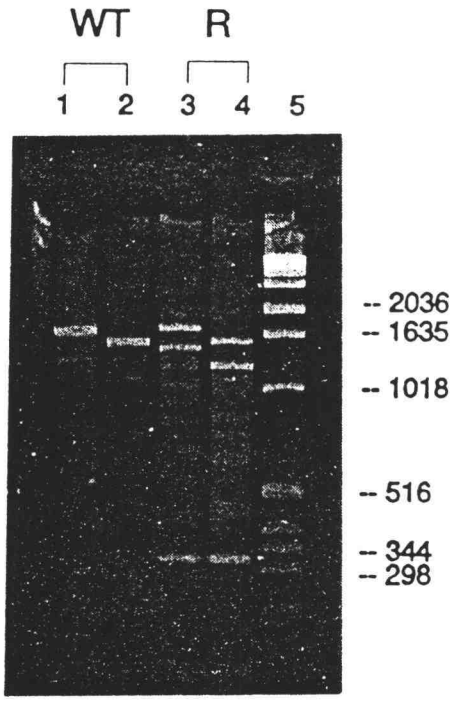

Figure IV-3. Localization of the A+1460 mutation by ribonuclease protection analysis. Virion RNAs from plants infected with TYMC (wt) or a genetic variant arising from TYMC-G96/U53 inoculum (R) were annealed to the indicated antisense RNA probes and digested with a mixture of ribonucleases. The products were electrophoresed on a 1% agarose gel and stained with ethidium bromide. Lane 1, wt RNA probed with *EcoRI*$^{5'}$-*BamHI*^{1755} probe (1.75 kb); lane 2, wt RNA probed with *NcoI*^{210}-*BamHI*^{1755} probe (1.55 kb); lane 3, R RNA probed with *EcoRI*$^{5'}$-*BamHI*^{1755} probe; lane 4, R RNA probed with *NcoI*^{210}-*BamHI*^{1755} probe; lane 5, DNA markers (1 kb, Gibco-BRL) with sizes indicated in bp. The cleavage pattern of the R RNA indicates a mutation c. 310 nucleotides upstream of the 3′ end of the probe, i.e. at about nt. 1445; sequence analysis revealed the A+1460 mutation.

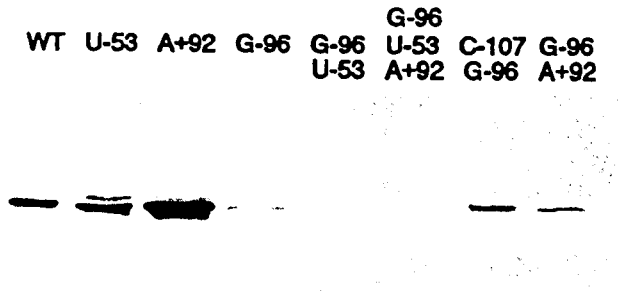

Figure IV-4. Coat protein accumulations in Chinese cabbage protoplasts inoculated with wild type and mutant TYMC transcripts. Representative experiments that have contributed to the data of Table 2 are shown. Protoplasts were harvested 48 hr after inoculation with the indicated derivatives of TYMC RNA. Extracts were separated on a 14% polyacrylamide-SDS gel, blotted and probed with anti-TYMV antiserum. The blot was developed using horseradish peroxidase-linked second antibodies and 5-chloro-1-naphthol color reagent.

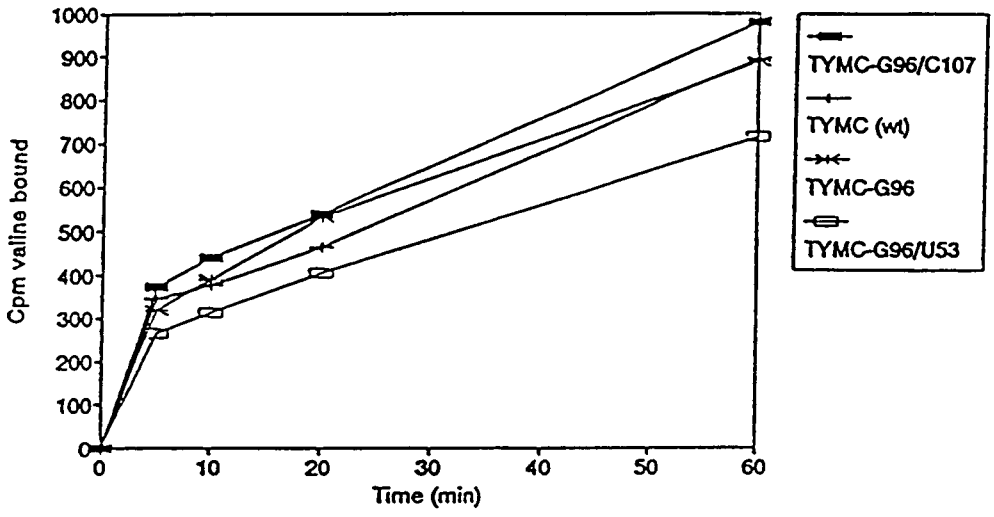

Figure IV-5. Comparative *in vitro* valylation of wild type and mutant genomic RNAs. The full-length genomic RNAs indicated (0.2 μM) were valylated (shown as cpm of [^{3}H]valine bound per aliquot) with wheat germ valyl-tRNA synthetase.

Table IV-1: Second site suppression of the G-96 mutation[a]

Mutant	Relative coat protein[b]	Appearance of systemic symptoms (dpi)[c]	Score[d]	Sequence of progeny[e]
TYMC (wt)	1.0	7	5/5	wt
TYMC-U53	1.1	7	2/2	U-53
TYMC-G96	0.02-0.3	14-21	14/21	(r)[f];U-96
TYMC-G96/U53	0.02	21	1/5	(r)[g]
TYMC-C107/G96	0.45	7	5/5	C-107/G-96
TYMC+A92	1.6	7	3/3	A+92
TYMC-G96+A92	0.21	7 (11)[h]	9/9	A+92/U-96
TYMC-G96/U53+A92	0.02	ND	ND	ND
TYMC+A1460	0.9	7	1/1	A+1460
TYMC-G96+A1460	0.02-0.3	14-21	10/12	A+1460/U-96
TYMC-G96/U53+A1460	0.02	ND	ND	ND

a. All data represent averages of at least three experiments.

b. Coat protein levels determined in Western blot analyses of extracts from Chinese cabbage protoplasts harvested 48 hpi; error $\approx 20\%$.

c. Time of appearance (days post-inoculation) of recognizable symptoms in the upper leaves of inoculated Chinese cabbage plants.

d. Number of Chinese cabbage plants with systemic symptoms/number of plants inoculated.

e. Sequences at the mutant loci of viral RNA in fully symptomatic systemically infected leaves.

f. (r) refers to the delayed appearance of systemic infection in two plants (genotypes found to be A+92/G-96 and C-107/G-96, described in the text). The remaining 12 symptomatic plants were infected with the revertant U-96 genotype.

g. (r) refers to the delayed appearance of systemic infection in one plant (genotype found to be A+1460/U-53, described in the text).

h. Symptoms were observed in 8 plants after 7 days and in one plant after 11 days (see text).

ND, not determined.

Table IV-2: U-57 suppression of the A-55 phenotype[a]

Mutant	In vitro valylation properties (264 nt-long 3′ RNAs)[b]		Replication in Chinese cabbage relative to wt (genomic RNA as inocula)				
			Protoplasts harvested 48 hpi			Plants	
	mol of val/ mol of RNA[c]	Relative V_{max}/K_M	Coat Protein[d]	Genomic RNA[e]	Subgenomic RNA[e]	Relative virion yield[f]	Systemic symptoms score[g]
wt	1.0	1.0	1.0	1.0	1.0	1.0	9/9
A-55	0.13	0.0046	0.02[h]	D[h]	-	-	1(r)/3[h]
U-57	1.0	1.1	1.5[h]	0.9[h]	0.8[h]	1.8[h]	5/5[h]
U-57/A-55	1.0	0.075	0.85	0.65	0.45	1.0	3/3

a. All data represent averages of three or more experiments. nt, nucleotide; wt, wild type; D, double-strandedgenomic RNA detected by *in vivo* labelling (Chapter III in this thesis) in place of quantitation of single-stranded genomic RNA, the very low level of which for this mutant resulted in interference by inoculum RNA; -, none detected; (r), reversion of phenotype resulting from acquisition of second site suppressor mutation.

b. Valylation by wheat germ valyl-tRNA synthetase, summarized from Chapter II; error for V_{max}/K_M determination is ≈20%.

c. Extent of valylation after 60 min at 0.6 μM RNA (3′-CCA species).

d. Coat protein levels determined in Western blots; error ≈20%.

e. TYMC RNA levels determined in Northern blots; error ≈20%.

f. Virion yields determined after purification from systemically infected leaves.

g. Number of plants with systemic symptoms/number of plants inoculated.

h. Data from Chapter III in this thesis.

Table IV-3: *In vitro* valylation properties of 3′ genomic fragments[a]				
Mutant	**mol of val/ mol of RNA[b]**	**Apparent K_M (nM)**	**Relative V_{max}**	**Relative V_{max}/K_M**
TY (wt)	1.0	31	1.0	1.0
TY-G96	0.98	72	1.3	0.54
TY-U53[c]	1.1	183	1.9	0.32
TY-G96/U53	1.0	212	2.4	0.35

a. Valylation kinetics determined using wheat germ valyl-tRNA synthetase and 264-nucleotide-long transcripts that include the 3′ noncoding region of TYMV RNA. RNA concentrations refer to the proportion of 3′-CCA-terminating transcripts present (Chapter II). Errors for K_M, V_{max} are 20%. wt, wild-type.

b. Extent of valylation after 60 min at 0.6 μM RNA.

c. Data taken from Chapter II in this thesis.

Discussion

In an error-prone viral replication system, a mutant with a poor replication rate has the potential to give rise to fitter, more successfully replicating variants that will rapidly outgrow and replace the original mutant inoculum. The new variant genomes will occasionally harbor second site suppressor mutations that can help shed light on the defect of the original mutation, often in unexpected ways. We have explored this approach for studying the role of the 3′ noncoding region of TYMV RNA, using mutant RNAs TYMC-A55, TYMC-G96 and TYMC-G96/U53 as the original inocula. These RNAs replicate detectably in protoplasts, so that there is significant potential for the generation of mutations by polymerase error. They do not, however, support systemic infection in plants (Tables IV-1, IV-2), so that a more successful revertant or second site suppressor mutant that outgrows the inoculum to produce systemic symptoms is easily detected. We have investigated 4 novel mutations generated in this way. Two are potent second site suppressors that provide new insights, discussed below. The third mutation (A+92) is a weak second site suppressor of the G-96 mutation that probably functions non-specifically by enhancing the expression of the essential ORF-206. The fourth mutation (A+1460) does not detectably suppress the G-96 mutation (from which inoculum it was recovered) and appears to be a silent mutation under our experimental conditions. It was thus either recovered entirely by accident, or perhaps the mutation did act to weakly suppress the effects of the G-96 mutation in the particular conditions present in the inoculated plant (in a way we have not been able to reproduce). In any case, the inability of the A+1460 mutation to prevent the reversion of the coupled G-96 mutation shows that it is not a useful second site suppressor.

Anticodon recognition by valyl-tRNA synthetase and the TYMV replication system. The recovery of the U-57 mutation as a suppressor of the poor replication phenotype that results from the A-55 mutation has provided an important strengthening of our previously determined correlation between valylation and viral replication (Chapter III in this thesis). The two mutations were combined in the genomic mutant TYMC-U57/A55, which replicates systemically to generate virion yields similar to wild-type, and in a short transcript representing the 3′ 258 nucleotides of the viral RNA that can be conveniently used for *in vitro* valylation studies with wheat germ valyl-tRNA synthetase (Chapter II in this thesis). As discussed more fully in chapter II, the short TY-U57/A55 mutant, with a UAA anticodon, is unexpectedly well valylated based on the valylation activities of the single mutants TY-U57 and TY-A55. We have postulated from the anticooperativity that exists between the two mutations that valyl-tRNA synthetase is sensitive to the conformation of the phosphate backbone as well as functional groups on the bases of the anticodon (Chapter II in this thesis). This is quite unlike the recognition of the $tRNA^{Gln}$ anticodon by *E. coli* glutaminyl-tRNA synthetase, shown by X-ray crystallography to involve highly specific contacts to the base of each anticodon nucleotide (Rould *et*

al., 1991), in such a way that the anticooperativity between two mutations such as we have observed could not exist.

The unexpectedly efficient valylation observed for the U-57/A-55 double mutant has thus suggested a novel recognition of the RNA by the valyl-tRNA synthetase. More pertinent to our viral studies, however, is the correlation between the viral replication and valylation for TYMV RNA with the deleterious A-55 mutation and TYMV RNA with the rescued U-57/A-55 double mutation. This result strongly suggests that an interaction with valyl-tRNA synthetase — either as a catalyst that adds valine to the 3′ end and then plays no further role, or as a less transient ligand and subunit of the replication complex — is crucial for the replication of TYMV RNA. This is to be differentiated from the unlikely possibility that one of the viral proteins essential for replication has an RNA binding domain much like that of valyl-tRNA synthetase, a domain that might have been recruited from the host gene and used in minus strand promoter binding. In fact, no homologies to aminoacyl-tRNA synthetases are known in TYMV-encoded ORFs, and it seems inconceivable that a viral protein interacting with the tRNA-like structure in an essential function could duplicate the properties observed for the A-55 and U-57/A-55 mutations as well as the several anticodon mutations previously studied (Chapter III in this thesis).

Evidence for the existence of a pseudoknot upstream of the tRNA-like structure. The G-96 mutation is clearly detrimental to the successful replication of TYMV. The mutation disrupts one of the stems of a potential pseudoknot just upstream of the tRNA-like structure (Fig. IV-1). A stable, strong second site suppressor mutation that overcomes the effect of the G-96 mutation and permits the virus to infect plants systemically is the C-107 mutation. The C-107/G-96 double mutant RNA would be expected to contain a similar pseudoknot to that of the wild-type RNA, with a C:G base pair rather than U:A. Although further mutants will need to be analyzed in the future, it appears likely that the suggested pseudoknot exists in TYMC RNA and that it appears to be involved in some step that is important for the successful replication of the virus. It is unlikely that the extension of the coat protein ORF that results from the C-107 mutation accounts for the suppressor phenotype, since the larger coat protein appears to form virions that are unstable during normal virus isolation (C.-H. Tsai, unpublished observations). The extension to the coat protein ORF should thus be considered a detrimental mutation, and may be responsible for the modestly suboptimal levels of coat protein detected in protoplasts infected with TYMC-C107/G96.

Nuclease cleavage and chemical accessibility studies are consistent with the presence of the suggested pseudoknot, although they are also consistent with a different conformation (Florentz *et al.*, 1982; Rietveld, 1984). The short helical stems impart only a marginal stability, such that the pseudoknot may need to be stabilized by the binding of some factor *in vivo*. Analysis of the sequences of other tymoviral RNAs shows the potential for two pseudoknots upstream of the tRNA-like structure in ononis yellow mosaic virus RNA (Ding *et al.*, 1989), but no potential pseudoknots have been located

(C. W. A. Pleij, personal communication) in the RNAs of kennedya yellow mosaic virus (Ding *et al.*, 1990a) or eggplant mosaic virus (Osorio-Keese *et al.*, 1989). Clearly, the relevance of the putative pseudoknot in TYMV RNA requires further experimental support. In TMV RNA, the existence of 3 pseudoknots upstream of the tRNA-like structure is supported by nuclease mapping experiments (Garcia-Arenal, 1988), and an important function in some aspect of the replication cycle has been demonstrated (Takamatsu *et al.*, 1990).

Functional interaction between the G-96 and U-53 mutations. The U-53 mutation appears to be a neutral mutation with respect to replication in protoplasts and plants (Table IV-1). In combination with G-96, however, the U-53 mutation has an influence on the viral phenotype. Comparing TYMC-G96 with TYMC-G96/U53 and TYMC-G96+A1460 with TYMC-G96/U53+A1460, the presence of U-53 resulted in a loss of the highly variable replication in protoplasts, with replication occurring at the lower levels observed in the absence of U-53. This consistently lower level of replication (by virtue of the lower opportunity for polymerase errors) presumably explains the observation that TYMC-G96/U53 inoculum was more stable in plants, with a lower rate of reversion to U-96 than for TYMC-G96 inoculum (Table IV-1). Comparing TYMC-G96+A92 and TYMC-G96/U53+A92, the U-53 mutation reversed the suppressor effect of the A+92 mutation, since TYMC-G96/U53+A92 replicated to only 0.02 times the level of wild-type in protoplasts, as judged by coat protein accumulation.

No secondary structural interaction between G-96 and U-53 appears feasible (Fig. IV-1), but if such an interaction were to exist, it would presumably interfere with valylation of the viral RNA and decrease the efficiency of replication. The genetic interaction between these two mutant nucleotides is sufficiently strong to overcome the effect of the A+92 mutation in stabilizing the variable replication of TYMC-G96. The formulation of a molecular explanation for these effects will require further studies that may uncover unknown functional properties of the 3′ noncoding region of TYMV RNA. The emergence of this and the other questions discussed in this paper from a search for second site suppressor mutations illustrates the usefulness of this approach in studying the roles of the 3′ regions of viral RNAs.

CHAPTER V

Studies on the Mischarging of Turnip Yellow Mosaic Virus RNA by Wheat Germ Aminoacyl-tRNA Synthetases

Abstract

Experiments aimed at assessing whether aminoacylation specifically by valine is required for the replication of turnip yellow mosaic virus have been performed. A potential role for histidylation of TYMV RNA previously suggested by *in vitro* studies with yeast histidyl-tRNA synthetase [Rudinger *et al.* (1992) Nucleic Acids Res. 20:1865-1870], was not supported by studies with the wheat germ enzyme. No significant histidylation was found, and TYMV RNA appears to be specifically chargeable by valine in higher plant cells. Replacement of the ability of TYMV RNA to become charged with valine by the ability to become charged with methionine was studied with two mutant RNAs that were deficient in valylation but could be fully charged *in vitro* with methionine by wheat germ methionyl-tRNA synthetase. The combined C55→U and C53→A mutations produced a switch in the identity of the TYMV RNA from valine to methionine, and indicated that U55 and A53 are major determinants of methionine identity recognized by wheat germ methionyl-tRNA synthetase. TYMC RNAs carrying these double mutations were previously shown to replicate very poorly in Chinese cabbage protoplasts. These result suggests that the requirement for 3′ valylation of the viral RNA is specific, or at least cannot be satisfied by methionylation.

Introduction

Turnip yellow mosaic virus (TYMV) is a positive strand RNA virus with a monopartite genome 6.3 kb long. The viral RNA possesses a 5′ m^7GpppG cap structure and a tRNA-like structure at the 3′ end (Pinck *et al.*, 1970; Rietveld *et al.*, 1983) which can be efficiently and specifically valylated by valyl-tRNA synthetase (ValRS) from different sources, such as *Escherichia coli* (Pinck *et al.*, 1970), yeast (Giegé *et al.*, 1978), and wheat germ (Dreher *et al.*, 1988). It also can be valylated in plant cells in competition with the cellular $tRNA^{Val}$ during the replication cycle (Joshi *et al.*, 1982). In previous studies, we demonstrated that the valylation is crucial for efficient viral RNA replication in Chinese cabbage protoplasts and plants (Chapter III in this thesis).

As described in the previous chapters, the anticodon loop possesses a valine anticodon 57-CAC-55 and two nucleotides to the 3′ (54-CA-53) which are identical to the analogous nucleotides of all eukaryotic valylatable tRNAs (Sprinzl *et al.*, 1991) or tRNA-like structures (van Belkum *et al.*, 1987). We have identified three nucleotides in the anticodon loop as the major valine identity elements of the TYMV tRNA-like structure as recognized by wheat germ ValRS (Chapter II in this thesis). The middle nucleotide of the anticodon (A56) is the most important determinant, followed by the 3′ anticodon nucleotide C55, while the 3′-most anticodon loop nucleotide C53 is a significant but considerably less potent determinant.

Although we have already demonstrated that the valylation of TYMV RNA is correlated with its replication, the specific involvement of aminoacylation by valine to TYMV RNA replication is still a matter of conjecture. In order to answer whether the role of valine in TYMV RNA replication can be replaced by other amino acid, the mischarging capabilities of TYMV RNA and its mutant derivatives have been studied. Transcripts of the TYMV 3′ tRNA-like structure and its derivatives were recently shown to be mischarged with yeast histidyl-tRNA synthetase (HisRS) *in vitro* (Rudinger *et al.*, 1992). In the present studies, we have studied the mischarging abilities of wild-type and mutant TYMV RNAs, using the more homologous wheat germ HisRS. Based on expectations from research on *E. coli* $tRNA^{Met}$, for which identity appears to almost entirely reside in the anticodon (Schulman and Pelka, 1988; Schulman, 1991), we have also studied mischarging with methionine by wheat germ MetRS. If the wheat germ MetRS also detects anticodon identity determinants, TYMV RNAs with the methionine (CAU) anticodon might be active substrates for methionylation.

Materials and Methods

Materials. InhibitAce ribonuclease inhibitor was purchased from 5 prime-3 prime, Inc., T7 DNA polymerase (Sequenase) from United States Biochemical, *Thermus aquaticus* DNA polymerase from Promega, and restriction enzyme *BstN*I and T4 RNA ligase from New England Biolabs. Synthetic deoxyoligonucleotides were made by automated phosphoramidite synthesis and purified where necessary on 20% polyacrylamide/7M urea gels. [^{3}H]L-Valine, [^{3}H]L-Histidine, [^{35}S]L-Methionine, [α-^{32}P]UTP and [5′-^{32}P]cytidine 3′, 5′-bisphosphate were obtained from New England Nuclear. T7 RNA polymerase was prepared after overexpression in *E. coli* (Davanloo *et al.*, 1984) according to (Grodberg and Dunn, 1988; Zawadzki and Gross, 1991).

Purified yeast HisRS was a kind gift from Drs. C. Florentz and R. Giegé (Strasbourg, France). A partially purified cytoplasmic extract from wheat germ, enriched by ammonium sulfate precipitation and DEAE-cellulose chromatography (Steinmetz and Weil, 1986), was used as the source of the wheat germ ValRS, MetRS, and HisRS activities. Tobacco mosaic virus (TMV) U2 and U5 strains and satellite virus (STMV) were kind gifts from Dr. J. A. Dodds.

Cloning of tRNA genes. Pairs of long overlapping deoxyoligonucleotides corresponding to tRNA sequences coupled to the T7 RNA polymerase promoter were used to synthesize $tRNA^{Met}$ and $tRNA^{His}$ genes. The sequences correspond to the wheat germ and lupine $tRNA^{Met/CAU}$ and lupine $tRNA^{His/GUG}$ (Sprinzl *et al.*, 1991). The deoxyoligonucleotides used were: for the $tRNA^{Met}$ gene, the 5′-57mer 5′-d(TAATACGACTCACTATAGGGGTGGTGGCGCAGTTGGCTAGCGCGTAGGTCTCATAAT)-3′, and the 3′-46mer 3′-(AGAGTATTAGGACTCCAGCTCTCAAGCTCGGAGAGAGTGGGGTGGT)d-5′ (overlap regions underlined); for the $tRNA^{His}$ gene, the 5′-57mer 5′-d(TAATACGACTCACTATAGGTGGCTGTAGTTTAGTGGTTAGAACACAACGTTGTGGCC)-3′, and the 3′-45mer 3′-(CAACACCGGCAACTTTGGACCCAAGCTTAGGGTCGTCGGTGTGGT)d-5′. Thirty-five pmole of each pair of kinased oligomers were incubated at 85°C for 5 min, and annealed by transferring to 57°C for 10 min, followed by slow cooling to 35°C. The annealed oligomers were treated with 1 unit of Klenow polymerase in a final volume 30 μl in the presence of 67 nM of each dNTP. After a 30 min incubation at 37°C, the synthesized double-stranded DNA fragments were cloned into the *Sma*I of the M13 vector mp18. A $tRNA^{Val/AAC}$ gene corresponding to lupine $tRNA^{Val}$ (*Arabidopsis thaliana* $tRNA^{Val}$ differs by the insertion of a U16 in the D-loop, and by the substitutions G59→A and U60→C in the T-loop) was assembled using eight oligomers corresponding to both strands of the $tRNA^{Val}$ sequence coupled to the T7 RNA polymerase promoter. After assembling, the double-stranded DNA fragment containing *Eco*RI and *Kpn*I restriction sites at each end was cloned into the vector pUC118 (Chapter II in this thesis).

RNA preparations. Plasmid DNA of clones containing the tRNA gene was prepared either by LiCl/polyethylene glycol precipitation or using an ion-exchange column (QIAGEN, Inc.), and

subsequently linearized with *BstN*I endonuclease. Since the $tRNA^{His}$ gene contains an internal *BstN*I site that precluded the use of the 3'-*BstN*I site for linearization of transcriptional templates, the DNA template for transcription of the $tRNA^{His}$ gene was prepared by oligo-directed polymerase chain reaction (PCR) as described (Chapter IV and Appendix I in this thesis). The transcription of the tRNAs were carried out in 150 μl reactions at a DNA concentration of 100 μg/ml, in 80 mM Hepes-KOH pH 7.5, 12 mM $MgCl_2$, 2 mM spermidine, 10 mM DTT, 3 mM each nucleoside triphosphate, and 20 Ci/mol [α-^{32}P]UTP (Gurevich *et al.*, 1991). In cases requiring transcripts with 5' monophosphate termini, 20 mM guanosine monophosphate was added to the reactions (Tamura *et al.*, 1991). Although yeast $tRNA^{Phe}$ (Sampson and Uhlenbeck, 1988) and $tRNA^{Asp}$ (Perret *et al.*, 1990) with monophosphate and triphosphate 5'-termini are kinetically indistinguishable, it is possible for other tRNAs that 5'-triphosphates may interfere with aminoacylation properties.

Viral RNA and tRNA transcripts were purified by non-denaturing polyacrylamide gel electrophoresis as described (Chapter II in this thesis). The termini of these transcripts were analyzed according to Dreher *et al.* (1984; see also Chapter II in this thesis). Results showed the proportion of RNAs with 3'-CCA termini to be 62 $\pm$ 5% for transcripts made from *BstN*I-linearized DNA and 50% for $tRNA^{His}$ transcripts made from DNA templates generated by PCR. TMV RNAs were purified from virions using the same protocol as that used for TYMV RNA purifications (Lane, 1986). The yields of virion RNAs were about 150 μg per mg of TMV and 700 μg per mg of STMV.

Aminoacylation assays. Aminoacylation assays for mischarging were performed under three different reaction conditions. Condition H1 for histidylation was 100 mM Hepes-KOH pH 7.4, 4 mM $MgCl_2$, 3 mM ATP, 30 mM KCl, 1 mM DTT, and 10 μM [^{3}H]histidine (9 Ci/mmol) (based on conditions of Chen and Somberg, 1980). Condition M1 for methionylation varied from condition H1 in containing 100 mM Hepes-KOH pH 8.0 and 10 μM [^{35}S]Methionine (1.6 Ci/mmol) (Barciszewska *et al.*, 1979). Condition 2, used for both HisRS and MetRS, were the same low ionic strength conditions previously used for wheat germ ValRS: 25 mM Tris-HCl pH 8.0, 2 mM $MgCl_2$, 1 mM ATP, 0.1 mM spermine, and 10 μM [^{3}H]histidine (9 Ci/mmol) or [^{35}S]Methionine (1.6 Ci/mmol). Condition 3 corresponded to the best histidine mischarging of TYMV RNAs obtained with yeast HisRS (Mg^{2+}/ATP ratio 7.5/0.5; Rudinger *et al.* 1992).

All the reactions were carried out at 30°C in a final volume of 25 μl, in the presence of 0.1 μM RNAs. The reactions were stopped by spotting 4 μl aliquots onto 1.9 cm Whatman-3MM paper disks impregnated with 20% trichloroacetic acid. After three washes with 5% cold trichloroacetic acid, and single sequential washes (5 min) with 95% ethanol, 95% ethanol/ether (1/1), and ether, the disks were air-dried and counted in a toluene-0.3% 2,5-diphenyloxazole (PPO)-0.01% 1,4-bis-2-(4-methyl-5-phenyloxazolyl) benzene (POPOP) scintillation mixture. The levels of aminoacylation were determined from the incorporation of radioactive amino acids, and were corrected for the proportion of correctly terminated (3'-CCA) RNAs present.

Results and Discussion

Histidylation of tRNAs. *In vitro* histidylation with the wheat germ extract showed that the $tRNA^{His}$ transcript was fully charged with histidine in conditions 2 and 3 (Mg^{2+}/ATP ratios of 2/1 or 7.5/0.5, respectively), although a level of only 0.79 mol/mol was achieved in condition H1 (Mg^{2+}/ATP ratio of 4/3) (Table V-1). These results verify the presence of HisRS activity in the wheat germ extract. The $tRNA^{Val}$ and $tRNA^{Met}$ transcripts could only be mischarged with histidine to levels 0.02 to 0.05 mol/mol under all three conditions tested (60 min reactions). These results indicate only very low levels of mischarging of the non-cognate tRNAs ($tRNA^{Val}$ and $tRNA^{Met}$) by the wheat germ HisRS.

In contrast to the minimal mischarging of the non-cognate tRNA transcripts by wheat germ HisRS, the natural hypermodified yeast $tRNA^{Val}$ could be mischarged with histidine to a level of 0.3 mol/mol by yeast HisRS (Rudinger *et al.*, 1992, using condition 3). Although the specificity constant V_{max}/K_M of this mischarging was 250-fold lower than that for the histidylation of the yeast $tRNA^{His}$ transcript, it was not characteristic of the usual mischarging of noncognate tRNAs; V_{max}/K_M values for the valylation of yeast $tRNA^{Met}$ by yeast ValRS (Giegé *et al.*, 1987) and for the arginylation of yeast $tRNA^{Asp}$ by yeast ArgRS (Perret *et al.*, 1990) were 12,000- and 13,000-fold lower than the values for charging of the cognate tRNA, respectively. We used the same enzyme to study the histidylation of the unmodified higher plant $tRNA^{Met}$ and $tRNA^{Val}$ transcripts, and observed charging to levels of 0.19 and 0.05 mol/mol, respectively (condition 3). The lower mischarging of $tRNA^{Val}$ with yeast HisRS in our experiments compared with those of Rudinger *et al.* (1992) may be due to the use of different $tRNA^{Val}$ species (there are 17 nucleotide differences between the yeast $tRNA^{Val/IAC}$ and the lupine $tRNA^{Val/AAC}$ sequences), or due to the use of different levels of HisRS. Nevertheless, the significant mischarging of wheat germ $tRNA^{Met}$ by the yeast HisRS (Table V-1), together with the results of Rudinger *et al.* (1992), indicate that yeast HisRS is (at least under some conditions) an unusually promiscuous enzyme, clearly more so than the wheat germ HisRS. Note that condition 3 (Mg^{2+}/ATP ratio of 7.5/0.5) promotes mischarging (Giegé *et al.*, 1972).

Histidylation of TY-Sma and its Derivatives. *In vitro* histidylation experiments with wheat germ HisRS showed that the TY-Sma transcript (a 264-nucleotide-long TYMV RNA containing the tRNA-like structure) could not be detectably charged in condition H1, while low levels of histidine charging (0.06 mol/mol) were observed in conditions 2 and 3. The shorter transcript TY-Alu (88 nucleotides long) could be histidylated to a level 0.07 mol/mol, while the 42-nucleotide-long TY-AA transcripts comprising the 12-basepair acceptor stem (Fig. V-1) was histidylated to levels of 0.10 to 0.15 mol/mol (Table V-1). The histidine mischarging levels were similar for all 3 conditions used.

Replacement of the valine anticodon 57-CAC-55 with the histidine anticodon 57-GUG-55, as in TY-GUG RNA, did not result in significantly higher mischarging with histidine by wheat germ HisRS (Table V-1). Two additional RNAs, TY-C4 and TY-G4, with mutations in the amino acid acceptor

stem, also showed only minimal histidylation, to levels less than 0.08 mol/mol under all 3 conditions. The above experiments indicate that TYMV RNAs, and the derivatives tested, cannot be efficiently mischarged by the homologous HisRS. These results contrast with the observations made with yeast HisRS, both as reported by Rudinger *et al.* (1992) and from our own experiments (see below).

Parallel experiments studying the histidylation of the above TYMV-derived RNAs by yeast HisRS were conducted, but were restricted to condition 3 as used by Rudinger *et al.* (1992). TY-Sma, TY-Alu and TY-AA RNAs were histidylated to levels of 0.16, 0.75 and 0.20 mol/mol, respectively. TY-GUG was histidylated to a level 0.33 mol/mol, and TY-C4 and TY-G4 were histidylated to levels 0.47 and 0.13 mol/mol, respectively. In most cases, we observed substantially lower mischarging levels than Rudinger *et al.* (1992), despite the use of the same enzyme preparation. Presumably, different levels of enzyme activity were used in the different experiments. Nevertheless, both studies agree that significant mischarging of TYMV-derived RNAs can occur with yeast HisRS.

Possible histidine identity elements in TYMV RNA. The significant charging with histidine of the short transcript TY-AA by the wheat germ and yeast HisRS enzymes suggests that the TYMV RNA amino acid acceptor stem contains important determinants of histidine identity for both enzymes. This indication is in line with the conclusion that there are important determinants recognized by *E. coli* HisRS in the amino acid acceptor stem of *E. coli* $tRNA^{His}$. Short derivatives of $tRNA^{His}$, comprising only the acceptor- and T-stems ($minihelix^{His}$), or the acceptor stem ($microhelix^{His}$), were rather efficient substrates *in vitro* for *E. coli* HisRS (V_{max}/K_M values 150- and 500-fold lower, respectively, than that of native $tRNA^{His}$; Francklyn and Schimmel, 1990).

The histidylation of other TYMV RNA derivatives indicated major differences in the recognition of TYMV RNA between yeast HisRS and wheat germ HisRS. All of the longer RNAs were more poorly charged by the wheat germ HisRS, suggesting the presence of antideterminants in the upstream portion of the tRNA-like structure. With the yeast enzyme, however, TY-Alu, TY-GUG and TY-C4 were histidylated to higher levels than TY-AA (Table V-1). It seems possible that the valine anticodon acts as an antideterminant towards yeast HisRS: (i) mutation of the CAC anticodon to GUG improved histidylation (see also Rudinger *et al.*, 1992), and (ii) TY-Alu is known to exist in an alternative conformation in which the anticodon is not present (Mans *et al.*, 1990; see Fig. V-1).

Histidylation of TMV RNAs. TMV virion RNAs (U2 and U5 strains) were histidylated as controls in condition H1 with wheat germ HisRS and in condition 3 with yeast HisRS. Similar levels of histidylation (0.12 to 0.17 mol/mol) were observed for TMV virion RNAs incubated with either enzyme (Table V-1). In order to determine whether conditions that promote mischarging (Giegé *et al.*, 1972) would enhance the levels of histidylation by wheat germ HisRS, TMV U2 RNAs were histidylated *in vitro* in the presence of 10% DMSO or 5% ethanol. No enhanced charging was found in those conditions (data not shown). The histidylation levels we have observed are significantly lower than those reported in the literature (0.36-0.40 mol/mol using yeast HisRS; Carriquiry and Litvak,

1974; Beachy *et al.*, 1976). The reason for the discrepancy is uncertain, but may relate to different experimental conditions or to inaccurate estimates of 3′ ends in the older studies, which were done before the accurate length of TMV RNA was known. In any case, the studies all agree that TMV RNA can only be partially charged with histidine.

Methionylation of TY mutants and tRNA^{Met}. The major identity elements of tRNA^{Val} and tRNA^{Met} in *E. coli* were localized to the anticodons, and the charging specificities could be switched almost completely by exchanging the anticodon triplet (Schulman and Pelka, 1988). The major determinants of the valylation of TYMV RNA by wheat germ ValRS have also been localized to the anticodon loop (Chapter II in this thesis). Therefore, we suspected that changes made in the anticodon loop of TYMV RNA that matched the anticodon-loop nucleotides conserved in tRNA^{Met} might switch the charging ability from valine acceptance to methionine acceptance. Sequence compilation of all cytoplasmic elongator and initiator tRNA^{Met} molecules in eukaryotes shows that the sequences in the anticodon loop of these molecules are highly conserved: 32-C(C/U)CAUAA-38 (anticodon underlined, position 33 is in most cases C, with a U in a few initiator tRNAs; C34 is modified in some cases; A37 is modified in all cases; Sprinzl *et al.*, 1991).

We studied the methionylation with wheat germ MetRS of the wheat germ tRNA^{Met} transcript, as well as of TY-Sma and its derivatives, TY-U55 (59-CCCAUAC-53), TY-U55/A53 (59-CCCAUAA-53) and TY-U55/C54/A53 (59-CCCAUCA-53) (Fig. V-1). tRNA^{Met} could be charged to levels 0.91 and 0.95 mol/mol in conditions M1 and 3, respectively, demonstrating the presence of active MetRS in the wheat germ extract. In condition 2, however, a methionylation level of only 0.73 mol/mol was obtained (Table V-2). Condition 2 is a low ionic strength condition, and has been used for characterizing the valylation of TYMV RNAs (Chapter II in this thesis). These results indicate the importance of selecting appropriate conditions in order to obtain optimal charging, and that the optimum conditions may vary from enzyme to enzyme.

TY-Sma RNA could barely be mischarged with methionine by wheat germ MetRS, to levels between 0.02 and 0.03 mol/mol under the three conditions tested. The methionylation levels of TY-Sma derivatives increased in correspondence with the presence of substitutions that matched the anticodon loop sequence more closely to that of tRNA^{Met}, regardless of the conditions used (Table V-2). In all cases, charging was highest in condition 3: 0.15 mol/mol for TY-U55, 1.00 mol/mol for TY-U55/A53, and 0.99 mol/mol for TY-U55/C54/A53. High methionylation levels were also obtained in condition 2. In contrast to the results with tRNA^{Met}, condition 2 was more optimal for the methionylation of TY-Sma derivatives than condition M1. The above results suggest that the determinants for methionylation by wheat germ MetRS are localized in the anticodon loop, as are those recognized by the *E. coli* MetRS.

Relationship between valine and methionine identities. Although mutants TY-U55/A53 and TY-U55/C54/A53 could be fully methionylated (at least in condition 3), the initial rate of

methionylation was obviously slower than that of the $tRNA^{Met}$ transcript (Fig. V-2). Further experiments are required to characterize the kinetic parameters of these two mutants in order to fully understand their methionylation characteristics, but it appears that the TY-Sma variants do not possess the full level of methionine identity present in $tRNA^{Met}$. This may reflect the absence of further methionine determinants outside the anticodon loop, or the presence of antideterminants in the viral tRNA-like structure.

The methionine acceptance of the TY-Sma derivatives is inversely correlated with their valine acceptance (Table V-2). RNAs with mutations in the anticodon loop that change the valine identity determinants so as to correspond to nucleotides conserved in eukaryotic $tRNA^{Met}$ species had decreased levels of valylation and increased levels of methionylation, relative to TY-Sma. Two positions, 55 and 53, in the TYMV anticodon loop are crucial for switching the charging ability from valine to methionine. These two positions, previously identified as the major valine determinants in TYMV RNA (Chapter II in this thesis), also appear to play a role in determining the methionine identity. Although an additional C54 mutation enhanced the level of methionylation compared to that of TY-U55/A53 in conditions M1 and 2 (Table V-2), the analogous position in tRNAs has never been found to be a pyrimidine (Sprinzl *et al.*, 1991). Thus, the C54 mutation we have studied is not relevant to the identity of $tRNA^{Met}$, but this mutation does appear to contribute to the methionine identity in the TYMV RNA context. It remains to be determined whether the involvement of this nucleotide in methionine identity is direct, or indirect via a conformational change in the anticodon loop.

The three positions in the anticodon have been shown to be important identity determinants in the charging of *E. coli* $tRNA^{Met}$ by *E. coli* MetRS (Schulman and Pelka, 1984; Schulman, 1991). Our results indicate that the 3′ anticodon position is also a determinant for MetRS from wheat germ, but further experiments are needed to assess the methionine identity contribution of the other anticodon nucleotides. The contribution of the 3′ anticodon loop nucleotide to methionine identity has not been studied in the *E. coli* system.

Conclusions: Does TYMV Replication specifically require valylation?

In previous studies we showed that valylation is required for efficient TYMV replication in Chinese cabbage protoplasts and plants (Chapter III in this thesis). TYMV RNAs with mutations introduced into the anticodon loop of the tRNA-like structure could not be valylated, or possessed decreased *in vitro* valylation rates. The replication level of those mutants studied *in vivo* was correlated to their defective valylation specificity. The mutant TYMC-A55 had a valylation specificity constant (V_{max}/K_M) 200-fold less than wild-type, and a replication rate 50-fold less than that of wild-type RNA (Chapter IV in this thesis). A second-site suppressor mutation in the wobble position of the anticodon (C57 → U57) enhanced the valylation specificity constant 16-fold, while raising the replication rate 40-fold relative to TYMC-A55. Based on the assumption that the *in vitro* valylation rate reflects the valylation of viral RNAs *in vivo*, these results argue strongly that valylation is important for TYMV RNA replication. Consistent with this idea, no mutants with a high level of replication and poor valylatability have thus far been isolated.

Mutants TY-U55/A53 and TY-U55/C54/A53 have been demonstrated to possess very low valine acceptance, but quite efficient methionine acceptance *in vitro*. However, these two mutants did not replicate in Chinese cabbage protoplasts and plants, and indeed were among the worst replicating mutants studied (Chapter III in this thesis). If the methionylation of these two mutants observed *in vitro* reflects the methionylation *in vivo*, the implication can be two-fold: (i) valylation rather than aminoacylation in general is required, and is critical for TYMV RNA replication; or (ii) the nucleotides involved in switching the amino acid acceptance from valine to methionine (positions 55 and 53) also serve directly as elements of the promoter controlling TYMV (-)-strand RNA synthesis, i.e. nucleotides directly contacted by the replicational machinery. The ability of the C57→U57 mutation to suppress the negative effect of the C55→A55 mutation on the levels of replication suggests that C55 is not a primary sequence-specific promoter element. In addition, *in vitro* replication studies have indicated that TYMV RNA fragments as short as 38 nucleotides long (Gargouri-Bouzid *et al.*, 1991) and TY-AA (42-nucleotides long; P. Georgel, unpublished observations) could replicate *in vitro*, suggesting that the nucleotides in the anticodon loop might not be part of the promoter governing TYMV (-)-strand RNA synthesis. Rather, these nucleotides may influence RNA replication by influencing 3' valylation.

Further investigations are needed to test the valylation or methionylation of TYMV and its derivatives *in vivo*. These experiments will be demanding, due to the low concentrations of TYMV RNAs relative to tRNAs in the infected cell. In order to fully understand the relationship between the aminoacylation and replication of TYMV RNA, it will be helpful to define the promoter for (-)-strand RNA synthesis.

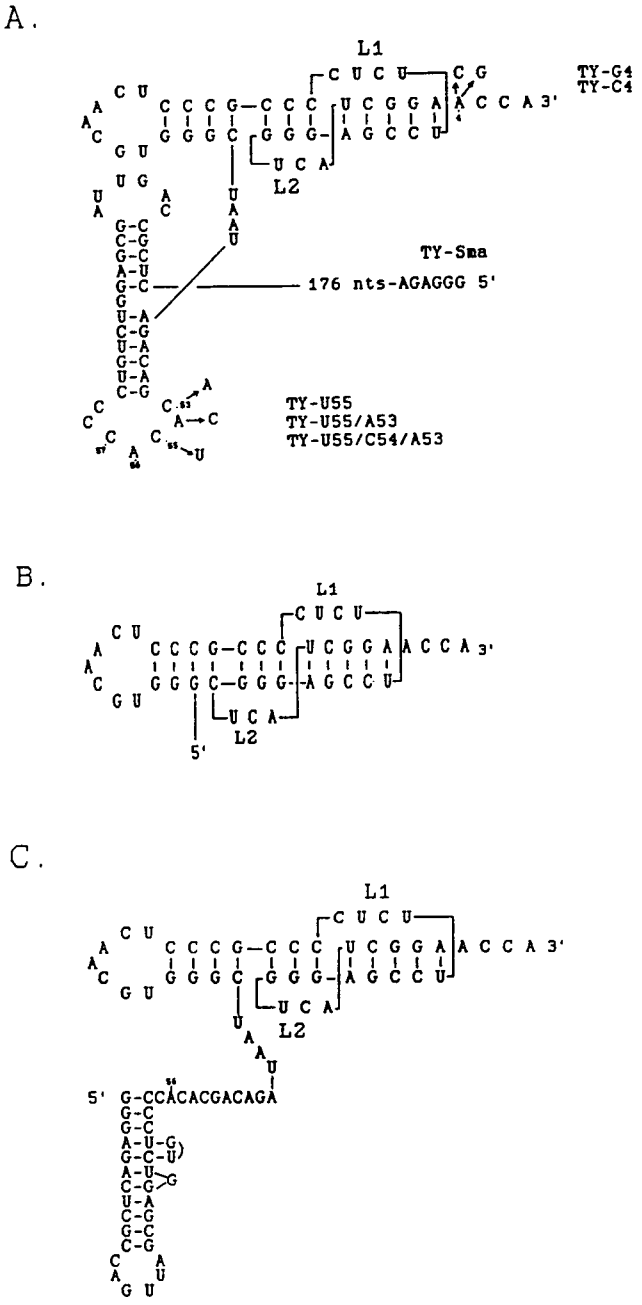

Figure V-1. Secondary structure model of the 3′ tRNA-like structure of TYMV RNA. (A) Transcript TY-Sma contains the L-shaped tRNA-like structure and upstream 176 nucleotides of TYMV RNA, as well as 6 nucleotides of 5′ nonviral sequence 5′-GGGAGA. Mutant transcripts derived from TY-Sma are also indicated. (B) Short transcript TY-AA mimicking the amino acid acceptor arm of TYMV RNA (Rudinger *et al.*, 1992). (C) Alternative folding of transcript TY-Alu, which contains 82 nucleotides of TYMV RNA and the nonviral 6 nucleotides 5′-GGGAGA- (after Mans *et al.*, 1990).

Table V-1. Levels of *in vitro* histidylation of tRNA transcripts, TYMV RNA transcripts and TMV virion RNAs by wheat germ or yeast histidyl-tRNA synthetases.

	Wheat germ HisRS			Yeast HisRS (condition 3)	
RNA	**condition H1[a]**	**condition 2**	**condition 3**	**Tsai[b]**	**Rudinger[c]**
$tRNA^{His}$	0.79[e]	0.97	1.13	0.94	
$tRNA^{Met}$	0.03	0.04	0.05	0.19	
$tRNA^{Val}$	0.04	0.02	0.04	0.05	0.30[f]
TY-Sma	0.00	0.06	0.06	0.16	0.25
TY-GUG	0.02	0.06	0.01	0.33	
TY-Alu	0.04	0.07	0.01	0.75	0.85
TY-AA	0.10	0.15	0.11	0.20	0.35
TY-C4	0.04	0.03	0.01	0.47	0.45
TY-G4	0.01	0.07	0.08	0.13	0.60
TMV-U2	0.15	-	-	0.17	
TMV-U5	0.12	-	-	0.14	

a. Condition H1: 100 mM Hepes-KOH pH 7.4, 4 mM $MgCl_2$, 3 mM ATP, 30 mM KCl, 1 mM DTT, and 10 μM [^{3}H]histidine (9 Ci/mmol).

Condition 2: 25 mM Tris-HCl pH 8.0, 2 mM $MgCl_2$, 1 mM ATP, 0.1 mM spermine, and 10 μM [^{3}H]histidine (9 Ci/mmol).

Condition 3: 25 mM Tris-HCl pH 8.5, 7.5 mM $MgCl_2$, 0.5 mM ATP, and 10 μM [^{3}H]histidine (9 Ci/mmol).

b. Data from the current experiments.

c. Data taken from Rudinger *et al.* (1992).

d. Transcripts correspond to wheat germ $tRNA^{Met/CAU}$, lupine $tRNA^{His/GUG}$, and lupine $tRNA^{Val/AAC}$.

e. Extent of histidylation (mol his/mol RNA) at plateau at 0.1 μM of 3'-CCA ends.

f. Purified, fully modified yeast $tRNA^{Val}$.

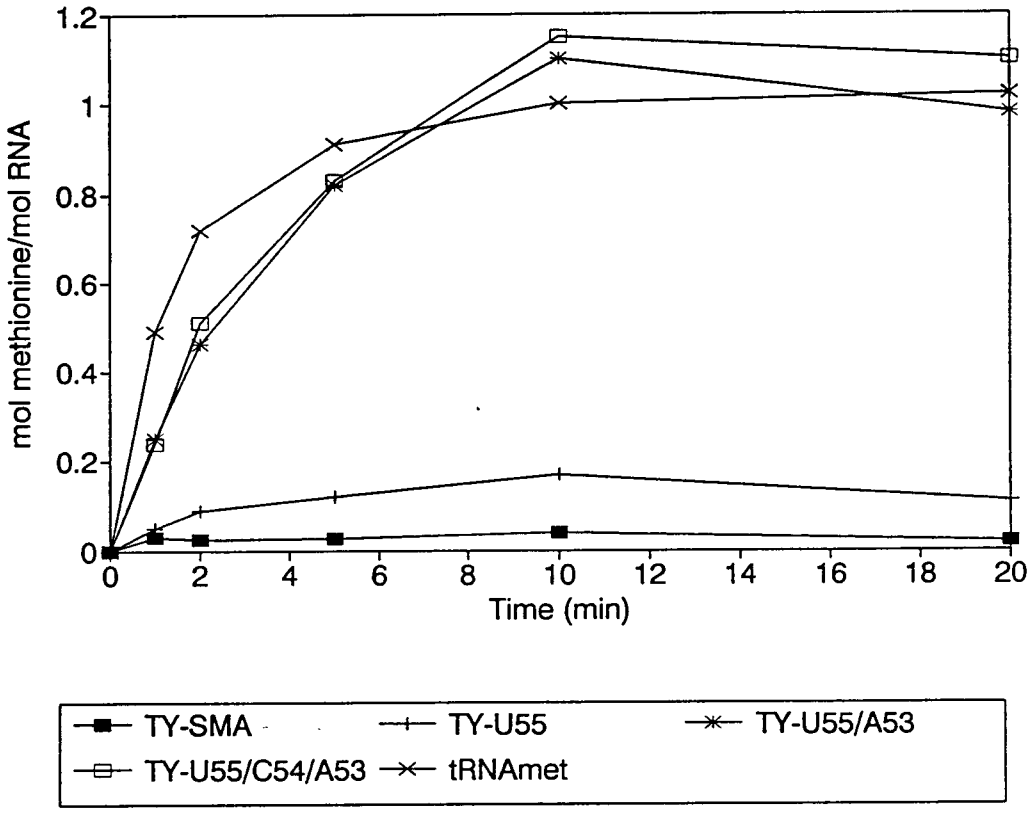

Figure V-2. Methionylation curves for wheat germ $tRNA^{Met}$ transcript and 3' transcripts of TYMV RNA charged with wheat germ MetRS. Aminoacylations were at 30°C in Condition 3, with RNAs present at 1μM of 3'-CCA termini.

Table V-2. Aminoacylation levels of tRNA and 3′ TYMV RNA transcripts by wheat germ methionyl- and valyl-tRNA synthetases.

	Methionylation			Valylation[a]
Mutant	**condition M1[b]**	**condition 2**	**condition 3**	**condition 2**
TY-Sma	0.02[c]	0.03	0.03	1.01
TY-U55	0.01	0.09	0.15	0.45
TY-U55A53	0.18	0.50	1.00	<0.001
TY-U55C54A53	0.30	0.86	0.99	<0.001
$tRNA^{Met}$	0.91	0.73	0.95	-

a. Valylation data were taken from Chapter II in this thesis.

b. Conditions are given in Table V-1, except that 10 μM [^{35}S]Methionine (1.6 Ci/mmol) was used for methionylation; condition M1 is condition H1 adjusted to pH 8.0.

c. Extent of methionylation (mol met/mol RNA) at plateau (after 40 min) at 0.1 μM of 3′-CCA ends.

CONCLUSIONS

The genomes of several positive strand RNA plant viruses contain an intriguing tRNA-like structure at their 3′ ends. Viruses with a range of morphologies and genome plans have this feature: TYMV and the tymoviruses have monopartite genomes and icosahedral particles; BMV and the bromoviruses, and CMV and the cucumoviruses have tripartite genomes and icosahedral particles; TMV and the tobamoviruses have monopartite genomes and rod-shaped particles; TRV and the tobraviruses have bipartite genomes and rigid rod-shaped particles; BSMV and the hordeiviruses have tripartite genomes and rigid rod-shaped particles. Among these viruses, TYMV has achieved the highest form of tRNA mimicry. The tertiary conformation of its tRNA-like structure is very similar to that of canonical tRNAs, TYMV RNA is an excellent substrate for ValRS and NTase, and valylated TYMV RNA can bind elongation factor. Further, the results presented in Chapter II demonstrate that the anticodon present in the tRNA-like structure plays a role in ValRS recognition and in valine identity determination that is equivalent to the role of anticodons in many tRNAs. Other viral tRNA-like structures exhibit lower forms of tRNA mimicry: TMV RNA is only partially chargeable with histidine, and TRV RNAs cannot be charged, although they are substrates for NTase.

The valylatable tRNA-like structure of TYMV RNA provides an opportunity to study the identity elements controlling the valylation of TYMV RNA. This has been studied using the homologous ValRS from wheat germ. Kinetic parameters obtained from *in vitro* valylation studies of anticodon loop mutants identified three nucleotides as the major determinants of valine acceptance of TYMV RNA. In descending order of contribution to valine identity, these are the middle nucleotide of the anticodon (A56), the 3′ anticodon nucleotide (C55), and the 3′-most anticodon loop nucleotide (C53). All mutants with impaired valine acceptance had elevated K_M values, suggesting that the three identity nucleotides might directly contact wheat germ ValRS. These studies have shown that the aminoacylation behavior of a viral tRNA-like structure is determined by a small set of identity elements, as it is with tRNAs. As with tRNAs, TYMV appears to be efficiently chargeable by only one amino acid when using higher plant aminoacyl-tRNA synthetases. Recent studies have suggested that TYMV RNA may be aminoacylated with other amino acids, especially histidine. Results in Chapter V indicate that wheat germ MetRS and HisRS are not able to appreciably aminoacylate TYMV RNA. The similar overall characteristics of TYMV RNA and canonical tRNAs as substrates for aminoacylation underline the extent of tRNA mimicry achieved by the viral RNA.

With tRNAs, it is possible to switch amino acid identities by changing a small number of nucleotides. It should likewise be possible to transplant another amino acid identity into TYMV RNA. *In vitro* methionylation of two mutants TY-U55/A53 and TY-U55/C54/A53 containing anticodon loop sequences conserved among eukaryotic $tRNA^{Met}$ molecules were investigated using wheat germ MetRS. These RNAs could be fully methionylated, although their initial rate of methionylation was slower than

that of a $tRNA^{Met}$ transcript. The results of these studies indicate that nucleotides U55 and A53 are the major determinants of methionine identity recognized by wheat germ MetRS, and that the pseudoknot in the amino acid acceptor stem does not interfere with MetRS interaction. Wheat germ MetRS and ValRS both utilize positions 55 and 53 as identity determinants, but these enzymes recognize different bases at these sites in a mutually exclusive manner. This has presumably evolved as a mechanism to help prevent the existence of tRNAs with dual charging specificities. Further experiments are needed to identify the contributions of the methionine identity of other nucleotides in the anticodon as was shown in *E. coli* $tRNA^{Met}$ recognized by *E. coli* MetRS. It will be interesting to switch the identity determinants of valylation to methionylation or *vice versa* in the higher plant $tRNA^{Val}$ and $tRNA^{Met}$.

The above studies on TYMV RNA variants with altered aminoacylation properties provided an opportunity to test the relevance of aminoacylation to the replication of TYMV *in vivo*. Chapter III demonstrates that there is a direct relationship between the *in vitro* aminoacylation and *in vivo* replication of TYMV RNA, and that valylation is crucial for efficient viral replication. TYMV RNAs with mutations in the anticodon loop of the tRNA-like structure could not be valylated, or possessed decreased *in vitro* valylation rates (Chapter II). The replication rate of these mutants studied *in vivo* was correlated to their defective valylatability (Chapter III). Dramatic decreases in valylatability and replication were observed in response to mutations of A56, in the middle of the anticodon, and/or C55, the 3′ anticodon nucleotide. Mutation in the 3′-most nucleotide of the anticodon loop (C53 → A53) had minor effects on both activities. The correlation between *in vitro* valylation and *in vivo* replication of TYMV RNA is strengthened by the second-site suppressor mutant TYMC-U57/A55. A mutation introduced into TYMC-A55 RNA at the wobble position (C57 → U57) of the anticodon, presumably by polymerase error during replication *in planta*, simultaneously enhanced the *in vitro* valylation rate and *in vivo* replication of the mutant RNA. These results strongly suggest that the valylation of viral RNA is an important event in the infection cycle. This conclusion relies on the assumption that the *in vitro* valylation properties are good predictors of valylation *in vivo*. Unfortunately, it is difficult to assay the *in vivo* valylation status of the viral RNAs, especially for non-replicating mutants. It is known that the virion RNAs lack the 3′-A residue and are not valylated, and the concentration of viral 3′ ends potentially available for valylation is relatively low.

The question of the specific importance of valine aminoacylation, and whether another amino acid might functionally replace valine, has not been extensively addressed in this thesis. However, studies with two mutants, TY-U55/A53 and TY-U55/C54/A53, suggest that methionine may not be able to replace valine. These two mutant RNAs could be charged to completion with methionine *in vitro*, but did not replicate in Chinese cabbage protoplasts and plants, and indeed were among the worst replicating mutants studied. Further studies will be needed to support this conclusion. A specific role for valylation in TYMV RNA replication would suggest: (1) host ValRS is involved in TYMV RNA replication as a component of the replicase and can not be replaced by another aminoacyl-tRNA

synthetase; or (2) the valine amino acid functions as an integral part of the recognition site on the (+)-strand template that is bound by the replication machinery responsible for (-) strand synthesis.

A different relationship appears to exist between aminoacylation and replication in the BMV system. Studies similar to those we have conducted with TYMV led to the conclusion that efficient tyrosylation is not crucial for the replication of BMV RNAs (Dreher *et al.*, 1989). In TMV RNA, which can not be completely aminoacylated *in vitro*, the relationship between aminoacylation and replication has not been studied in detail. However, the relatively inefficient histidine charging suggests a less than crucial role. Experiments demonstrating that TMV RNAs with heterologous 3'-ends comprising tRNA-like structures capable of accepting valine and tyrosine are able to replicate *in vivo* (Ishikawa *et al.*, 1988; 1991) suggest that the specificity of charging is also not critical in the TMV system. These observations lead to the conclusion that the role and relevance of aminoacylation is not the same among the various plant RNA viruses that exhibit tRNA mimicry.

In addition to the tRNA-like structure in the 3' non-coding region of these viral RNA genomes, higher order structures are often found in the region immediately upstream of the tRNA-like structure. Nucleotides between the termination codon of the coat protein ORF and the tRNA-like structure of TYMV RNA can form a pseudoknot. Results in Chapter IV suggest that this pseudoknot plays an important role in viral replication. A single nucleotide substitution that destabilizes the base-pairing needed for the formation of the pseudoknot resulted in poor replication and failure to infect plants systemically. A mutant with a reverted phenotype isolated from the plant which had been inoculated with the pseudoknot-defective mutant, was found to harbor a second-site suppressing mutation that restored the potential to form a pseudoknot. This pseudoknot could function as a recognition feature for the binding of a protein, perhaps part of the viral RNA replication machinery. One or more viral proteins might first bind to this pseudoknot whereas the downstream tRNA-like structure is bound by a host factor (e.g. ValRS). Whether this ValRS might be involved as a subunit of the replicase complex is not clear. If ValRS were part of the replicase complex, then this complex may form as a result of protein-protein interactions between the viral factors bound to the pseudoknot and ValRS bound to the tRNA-like structure. If ValRS is not part of the complex, then it should simply dissociate after valine is bound to the tRNA-like structure. The tRNA-like structure with a valine at the 3' end might then serve as a specific promoter for (-)-strand synthesis, and be bound by viral proteins, perhaps channelled to the 3' end via initial binding to the upstream pseudoknot. Certainly, other host factors (e.g. EF1α) may be involved in TYMV replication complexes. Biochemical characterization of the subunits of TYMV replicase would complement the genetic studies reported in this thesis.

BIBLIOGRAPHY

Adhin, M. R., Alblas, J. and van Duin, J. 1990. Secondary structure at the 3′ terminal region of RNA coliphages: comparison with tRNA. Biochim. Biophys. Acta 1050:110-118.

Adrian, M., Timmins, P. A. and Witz, J. 1992. *In vitro* decapsidation of turnip yellow mosaic virus investigated by cryo-electron microscopy: a model for the decapsidation of a small isometric virus. J. Gen. Virol. 73:2079-2083.

Agranovsky, A. A., Dolja, V. V., Gorbulev, V. G., Kozlov, Yu. V. and Atabekov, J. G. 1981. Aminoacylation of barley stripe mosaic virus RNA: polyadenylate-containing RNA has a 3′-terminal tryosine-accepting structure. Virology 113:174-187.

Alhquist, P., Dasgupta, R. and Kaesberg, P. 1981. Near identity of 3′ RNA secondary structure in bromoviruses and cucumber mosaic virus. Cell 23:183-189.

Ahlquist, P., French, R. and Bujarski, J. J. 1987. Molecular studies of brome mosaic virus using infectious transcripts from cloned cDNA. Adv. Virus Res. 32:215-242.

Algranati, I. D. and Goldenberg, S. H. 1977. Translation of natural mRNA in cell-free systems from a polyamine-requiring mutant of *Escherichia cloi*. Biochem. Biophys. Res. Commun. 75:1045-1051.

Anderson, E. J., Qiu, S. G. and Schoelz, J. E. 1991. Genetic analysis of determinants of disease severity and virus concentration in cauliflower mosaic virus. Virology 181:647-655.

Andino, R., Rieckhof, G. E. and Baltimore, D. 1990. A functional ribonucleoprotein complex forms around the 5′ end of poliovirus RNA. Cell 63:369-380.

Argos, P. 1988. A sequence motif in many polymerases. Nucl. Acids Res. 16:9909-9916.

Arraiano, C. M., Yancey, S. D. and Kushner, S. 1988. Stabilization of discrete mRNA breakdown products in *ams pnp rnb* multiple mutants of *Escherichia coli* K-12. J. Bacteriol. 170:4625-4633.

Balint, R. and Cohen, S. S. 1985a. The incorporation of radiolabeled polyamines and methionine into turnip yellow mosaic virus in protoplasts from infected plants. Virology 144:181-193.

Balint, R. and Cohen, S. S. 1985b. The effects of dicyclohexylamine on polyamine biosynthesis and incorporation into turnip yellow mosaic virus in Chinese cabbage protoplasts infected *in vitro*. 144:194-203.

Bare, L. and Uhlenbeck, O. C. 1985. Aminoacylation of anticodon loop substituted yeast tyrosine transfer RNA. Biochemistry 24:2354-2360.

Barciszewska, J., Joachimiak, A., Rafalski, A., Barciszewski, M., Twardowski, T. and Wiewiórowski, M. 1979. Conservation of the structures of plant tRNAs and amninoacyl-tRNA synthetases. FEBS Letters 102:194-197.

Barciszewska, M. and Jones, D. S. 1987. Nucleic Acids Res. 15:1333

Bastin, M. and Hall, T. C. 1976. Interaction of elongation factor 1 with aminoacylated brome mosaic virus and tRNAs. J. Virol. 20:117-122.

Beachy, R., Zaitlin, M., Bruening, G. and Israel, H. W. 1976. A genetic map for the cowpea strain of TMV. Virology 73:498-507.

Beer, S. V. and Kosuge, T. 1970. Spermidine and spermine-polyamine components of turnip yellow mosaic virus. Virology 40:930-938.

Blackburn, E. H. and Szostak, J. W. 1984. The molecular structure of centromeres and telomeres. Annu. Rev. Biochem. 53:163-194.

Blackburn, E. H. 1990. Telomeres: structure and synthesis. J. Biol. Chem. 265:5919-5921.

Blumenthal, T., Landers, T. A. and Weber, K. 1972. Bacteriophage Qß replicase contains the protein biosynthesis elongation factorss EF Tu and EF Ts.Proc. Natl. Acad. Sci. USA 69:1313-1317.

Blumenthal, T. and Carmichael, G. 1979. RNA replicaiton: function and structure of the Qß RNA replicase. Ann. Rev. Biochem. 48:525-548.

Bonnet, J. and Ebel, J. P. 1972. Interpretation of incomplete reactions in tRNA amnioacylation. Aminoacylation of yeast $tRNA^{Val}$ with yeast valyl-tRNA synthetase. Eur. J. Biochem. 31:335-344.

Bos, L. 1983. Introduction to plant virology. Longman, London and New York.

Bové, J. M. and Bové, C. 1985. Turnip yellow mosaic virus RNA replication on the chloroplast envelop. Physiologie Vegetale 23:741-748.

Boykov, S. V., Taliansky, M. E., Malyshenko, S. I., Kozlov, Yu. V. and Atabekov, J. G. 1981. Homology in the 3′-terminal regions of different barley stripe mosaic virus RNA species. Virology 113:168-173.

Bozarth, C. S., Weiland, J. J. and Dreher, T. W. 1992. Expression of ORF-69 of turnip yellow mosaic virus is necessary for viral spread in plants. Virology 187:124-130.

Bransom, K. L., Weiland, J. J. and Dreher, T. W. 1991. Proteolytic maturation of the 206-kDa nonstructural protein encoded by turnip yellow mosaic virus RNA. Virology 184:351-358.

Briand, J. -P., Jonard, G., Guilley, H., Richards, K. and Hirth, L. 1977. Nucleotide sequence (n=159) of the amino-acid-accepting 3′-OH extremity of turnip-yellow-mosaic-virus RNA and the last portion of its coat protein cistron. Eur. J. Biochem. 72:453-463.

Briand, J. -P., Keith, G. and Guilley, H. 1978. Nucleotide sequence at the 5′ extremity of turnip yellow mosaic virus genome RNA. Proc. Natl. Acad. Sci. USA 75:3168-3172.

Brierley, I., Boursnell, M. E. G., Binns, M. M., Bilimoria, B., Bolk, V. C., Brown, T. D. K. and Inglis, S. C. 1987. An efficient ribosomal frame-shifting signal in the polymerase-encoding region of the coronavirus IBV. EMBO J. 6:3779-3785.

Brierley, I., Digard, P. and Inglis, S. C. 1989. Characterization of an efficient coronavirus ribosomal frameshifting signal: requirement for an RNA pseudoknot. Cell 57:537-547.

Brisco, M. J., Hull, R. and Wilson, T. M. A. 1985. Southern bean mosaic virus-specific proteins are synthesized in an *in vitro* system supplemented with intact, treated virions. Virology 143:392-398.

Brisco, M. J., Hull, R. and Wilson, T. M. A. 1986. Swelling of isometric and of bacilliform plant virus nucleocapsids is required for virus-specific protein synthesis *in vitro*. Virology 148:210-217.

Bruce, A. G. and Uhlenbeck, O. C. 1982a. Enzymatic replacement of the anticodon of yeast phenylalanine transfer ribonucleic acid. Biochemistry 21:855-861.

Bruce, A. G. and Uhlenbeck, O. C. 1982b. Specific interaction of anticodon loop residues with yeast phenylalanyl-tRNA synthetase. Biochemistry 21:3921-3926.

Candresse, T., Mouches, C. and Bove, J. M. 1986. Characterization of the virus encoded subunit of turnip yellow mosaic virus RNA replicase. Virology 152:322-330.

Carriquiry, E. and Litvak, S. 1974. Further studies on the enzymatic aminoacylation of TMV-RNA by histidine. FEBS Letters 38:287-291.

Carter, P. J., Winter, G., Wilkinson, A. J. and Fersht, A. R. 1984. The use of double mutants to detect structural changes in the active site of the tyrosyl-tRAN synthetase (*Bacillus stearothermophilus*). Cell 38:835-840.

Cavener, D. R. and Ray, S. C. 1991. Eukaryotic start and stop translation sites. Nucleic Acids Res. 19:3185-3192.

Cech, T. R. 1983. RNA splicing: three themes with variations. Cell 34:713-716.

Chamorro, M., Parkin, N. and Varmus, H. E. 1992. An RNA pseudoknot and an optimal heptameric shift site are required for highly efficient ribosomal frameshifting on a retroviral messenger RNA. Proc. Natl. Acad. Sci. USA 89:713-717.

Chattapadhyay, R., Pelka, H. and Schulman, L. H. 1990. Initiation of *in vivo* protien synthesis with non-methionine amino acids. Biochemistry 29:4263-4268.

Chen, C. C. and Somberg, E. W. 1980. Purification and characterization of histidyl-transfer RNA synthetase form *Neurospora crassa*. Biochem. Biophy. Acta 613:514

Chen, E. Y. and Seeburg, P. 1985. Supercoil sequencing: A fast and simple method for sequencing plasmid DNA. DNA 4:165-170.

Chen, J. M. and Hall, T. C. 1973. Comparison of tyrosyl transfer ribonucleic acid and brome mosaic virus tyrosyl ribonucleic acid as amino acid donors in protein synthesis. Biochemistry 12:4570-4574.

Chu, W. -C. and Horowitz, J. 1991. Recognition of *Escherichia coli* valine transfer RNA by its cognate synthetase: a fluorine-19 NMR study. Biochemistry 30:1655-1663.

Cohen, S. S. and Greenberg, M. L. 1981. Spermidine, an intrinsic component of turnip yellow mosaic virus. Proc. Natl. Acad. Sci. USA 78:5470-5474.

Cohen, S. S., Balint, R. and Sindhu, R. K. 1981. The synthesis of polyamines from methionine in intact and disrupted leaf protoplasts of virus infected Chinese cabbage. Plant Physiol. 68:1150-1155.

Cohen, S. S., Sindhu, R. K., Greenberg, M., Yamanoha, B., Balint, R. and McCarthy, K. 1985. Cellular systems for the study of the biosynthesis of polyamines and ethylene, as well as of virus multiplicaiton. Plant Growth Regul. 3:227-238.

Daubert, S. 1988. Sequence determinants of symptoms in the genomes of plant viruses, viroids, and satellites. Mol. Plant-Microbe. Interact. 1:317-325.

Davanloo, P., Rosenberg, A. H., Dunn, J. J. and Studier, F. W. 1984. Cloning and expression of the gene for bacteriophage T7 RNA polymerase. Proc. Natl. Acad. Sci. USA 81:2035-2039.

Deckman, I. C. and Draper, D. E. 1987. S4-α mRNA translation regulation complex. II. Secondary structures of the RNA regulatory site in the presence and absence of S4. J. Mol. Biol. 196:323-332.

Deutscher, M. P. 1982. in The enzymes (Boyer, P. D., ed.) vol. 15, pp. 267-279. Academic Press, New York.

Ding, S. -W., Keese, P. and Gibbs, A. 1989. Nucleotide sequence of the ononis yellow mosaic tymovirus genome. Virology 172:547-554.

Ding, S. -W., Keese, P. and Gibbs, A. 1990a. The nucleotide sequence of the gemonic RNA of kennedya yellow mosaic tymovirus-Jervis Bay isolate: relationships with potex- and carlaviruses. J. Gen. Virol. 71:925-931.

Ding, S. -W., Howe, J., Keese, P., MacKenzie, A., Meek, D., Osorio-Keese, M., Skotnicki, M., Srifah, P., Torronen, M. and Gibbs, A. 1990b. The tymobox, a sequence shared by most tymoviruses: its use in molecular studies of tymoviruses. Nucleic Acid Res. 18:1181-1187.

Dinman, J. D., Icho, T. and Wickner, R. B. 1991. A -1 ribosomal frameshift in a double-stranded RNA virus of yeast forms a gag-pol fusion protein. Proc. Natl. Acad. Sci. USA 88:174-178.

Domingo, E. and Holland, J. J. 1988. High error rates, population equilibrium and evolution of RNA replication systems, p. 3-36. In E. Domingo, J. J. Holland and P. Ahlquist (ed.), RNA Genetics Vol. III. CRC Press, Boca Raton, Fla.

Dreher, T. W., Bujarski, J. J. and Hall, T. C. 1984. Mutant viral RNAs synthesized *in vitro* show altered aminoacylation and replicase template acitvities. Nature 311:171-175.

Dreher, T. W. and Hall, T. C. 1988a. RNA replication in brome mosaic virus and related viruses. In RNA Genetics. CRC Press. Boca Raton, Fl.

Dreher, T. W. and Hall, T. C. 1988b. Mutational analysis of the sequence and structural requirements in brome mosaic virus RNA for minus strand promoter activity. J. Mol. Biol. 201:31-40.

Dreher, T. W. and Hall, T. C. 1988c. Mutational analysis of the tRNA mimicry of brome mosaic virus RNA: sequence and structural requirements for aminoacylation and 3'-adenylation. J. Mol. Biol. 201:41-55.

Dreher, T. W., Florentz, C. and Giegé, R. 1988. Valylation of tRNA-like transcripts from cloned cDNA of turnip yellow mosaic virus RNA demonstrate that the L-shaped region at the 3' end of the viral RNA is not sufficient for optimal aminoacylation. Biochimie 70:1719-1727.

Dreher, T. W., Rao, A. L. N. and Hall, T. C. 1989. Replication *in vivo* of mutant brome mosaic virus RNAs defective in aminoacylation. J. Mol. Biol. 206:425-438.

Dreher, T. W. and Bransom, K. L. 1992. Genomic RNA sequence of turnip yellow mosaic virus isolate TYMC, a cDNA-based clone with verified infectivity. 1992. Plant Mol. Biol. 18:403-406.

Dumas, P., Moras, D., Florentz, C., Giegé, R., Verlaan, P., van Belkum, A. and Pleij, C. W. A. 1987. 3D graphics modelling of the tRNA-like 3'-end of turnip yellow mosaic virus RNA: structural and functional implications. J. Biomol. Struct. Dyn. 4:707-728.

Feldmann, H. and Zachau, H. G. 1977 Charging of a yeast methionine tRNA with phenylalanine and its implication for the synthetase recognition problem. Hoppe Seylers Z. Physiol. Chem. 358:891-896.

Finch, J. T. and Klug, A. 1966. Arrangement of protein subunits and the distribution of nucleic acids in turnip yellow mosaic virus. J. Mol. Biol. 15:344-356

Florentz, C., Briand, J. P., Romby, P., Hirth, L., Ebel, J. P. and Giegé, R. 1982. The tRNA-like structure of turnip yellow mosaic virus RNA: structural organization of the last 159 nucleotides from the 3' OH terminus. EMBO J. 1:269-276.

Florentz, C., Briand, J. P. and Giegé, R. 1984. Possible functional role of viral tRNA-like structures. FEBS Lett. 176:295-300.

Florentz, C. and Giegé, R. 1986. Contact areas of the turnip yellow mosaic virus tRNA-like structure interacting with yeast valyl-tRNA synthetase. J. Mol. Biol. 191:117-130.

Florentz, C., Dreher, T. W., Rudinger, J. and Giegé, R. 1991. Specific valylation identity of turnip yellow mosaic virus RNA by yeast valyl-tRNA synthetase is directed by the anticodon in a kinetic rather than affinity-based discrimination. Eur. J. Biochem. 195:229-234.

Florentz, C. and Giegé, R. 1993. tRNA-like structures in viral RNAs. In: Transfer RNA. (D. Söll and U. L. RajBhandary, eds.). American Society for Microbiology.

Fox, G. E. and Woese, C. R. 1975. 5S RNA secondary structure. Nature 256:505-507.

Francki, R. I. B., Milne, R. G. and Hatta, T. 1985. Altas of Plant Viruses. CRC Press. Boca Raton, Fl.

Francki, R. I. B. 1987. Responses of plant cells to virus infection with special reference to the sites of RNA replication. In: Positive Strand RNA Viruses (M. A. Brinton and R. R. Rueckert, eds), pp. 423-436. Alan R. Liss, Inc., New York.

Francklyn, C. and Schimmel, P. 1989. Aminoacylation of RNA minihelices with alanine. Nature 337:478-481.

Francklyn, C. and Schimmel, P. 1990. Enzymatic aminoacylation of an eight-base-pair microhelix with histidine. Proc. Natl. Acad. Sci. USA 87:8655-8659.

French, R. and Ahlquist, P. 1987. Intercistronic as well as terminal sequences are required for efficient amplification of brome mosaic virus RNA 3. J. Virol. 61:1457-1465.

French, R. and Ahlquist, P. 1988. Characterization and engineering of sequences controlling *in vivo* synthesis of brome mosaic virus subgenomic RNA. J. Virol. 62:2411-2420.

Frugier, M., Florentz, C. and Giegé, R. 1992. Anticodon-independent aminoacylation of an RNA minihelix with valine. Proc. Natl. Acad. Sci. USA 89:3990-3994.

Fulton, J. P., Scott, H. A. and Gamez, R. 1980. Beetles, in: Vectors of Plant Pathogens (K. F. Harris and K. Maramorosch, eds.), pp. 115-132, Academic Press, New York.

Gallie, D. R. and Walbot, V. 1990. RNA pseudoknot domain of tobacco mosaic virus can functionally substitute for poly(A) tail in plant and animal cells. Genes & Develop. 4:1149-1157.

Gallie, D. R., Feder, J. N., Schimke, R. J. and Walbot, V. 1991. Functional analysis of the tobacco mosaic virus tRNA-like structure in cytoplasmic gene regulation. Nucleic Acids Res. 19:5031-5036.

García-Arenal, F. 1988. Sequence and structure at the genome 3′ end of the U2-strain of tobacco mosaic virus, a histidine-accepting tobamovirus. Virology 167:201-206.

Gargouri-Bouzid, R., David, C. and Haenni, A. -L. 1991. The 3′ promoter region involved in RNA synthesis directed by the turnip yellow mosaic virus genome *in vitro*. FEBS letter 294:56-58.

Garnier, M., Mamoun, R. and Bove, J. M. 1980. TYMV RNA replication *in vivo*: replicative intermediate is mainly single-stranded. Virology 104:357-365.

Garnier, M., Candresse, T. and Bove, J. M. 1986. Immunocytochemical localization of TYMV coded structural and nonstructural proteins by the protien A-gold technique. Virolgy 151:100-109.

Geiduschek, E. P. and Tocchini-Valentini, G. P. 1988. Transcription by RNA polymerase III. 57:873-914.

Ghosh, G., Pelka, H., and Schulman, L. H. 1990. Identification of the tRNA anticodon recognition site of *Escherichia coli* methionyl-tRNA synthetase. Biochemistry 29:2220-2225.

Giegé, R., Kern, D. and Ebel, J. P. 1972. Incorrect aminoacylations catalysed by *E. coli* valyl-tRNA synthetase (*). Biochimie 54:1245-1255.

Giegé, R., Briand, J. -P., Mengual, R., Ebel, J. -P. and Hirth, L. 1978. Valylation of the two RNA components of turnip yellow mosaic virus and specificity of the tRNA aminoacylation reaction. Eur. J. Biochem. 84:251-256.

Gokhman, I. and Zamir, A. 1990. Nucleotide sequence of $tRNA^{Val}$ (GUU) from *Arabidopsis thaliana*. Nucleic Acids Res. 18:6729.

Gold, L. 1988. Posttranscriptional regulatory mechanisms in *Escherichia coli*. Ann. Rev. Biochem. 57:199-233.

Goldbach, R. 1987. Genome similarities between plant and animal RNA viruses. Microbiol. Sci. 4:197-202.

Goldbach, R., Lomonossoff, G. P. and Ryan, M. D. 1991. Alpha-like viruses in plants. Semi. Virol. 2:19-25.

Gorbalenya, A. E. and Koonin, E. V. 1989. Viral proteins containing the purine NTP-binding sequence pattern. Nucl. Acids Res. 17:8413-8440.

Grange, D. K., Gottesman, G. S., Lewis, M. B. and Marini, J. C. 1990. Detection of point mutations in type I collagen by RNase digestion of RNA/RNA hybrids. Nucl. Acids Res. 18:4227-4236.

Grodberg, J. and Dunn, J. J. 1988. *ompT* encodes the *Escherichia coli* outer membrane protease that cleaves T7 RNA polymerase during purification. J. Bacterio. 170:1245-1253.

Grosjean, H., Cedergren, R. J. and McKay. W. 1982. Structure in tRNA data. Biochimie 64:387-397.

Guerrier-Takada, C., Dardiner, K., Marsh, T., Pace, N. and Altman, S. 1983. The RNA moiety of ribonuclease P is the catalytic subunit of the enzyme. Cell 35:849-857.

Gurevich, V. V., Pokrovskaya, I. D., Obukhova, T. A. and Zozulya, S. A. 1991. Preparative *in vitro* mRNA synthesis using SP6 and T7 RNA polymerases. Anal. Biochem. 195:207-213.

Habili, N. and Symons, R. H. 1989. Evolutionary relationship between luteoviruses and other RNA plant viruses based on sequence motifs in their putative RNA polymerases and nucleic acid helicases. Nucl. Acids Res. 17:9543-9555.

Haenni, A. -L., Joshi, S. and Chapeville, F. 1982. tRNA-like structures in the genomes of RNA viruses. Prog. Nucl. Acid Res. Mol. Biol. 27:85-104.

Hall, T. C. 1979. Transfer RNA-like structures in viral genomes. Int. Rev. Cytol. 60:1-26.

Hatta, T. and Matthews, R. E. F. 1974. The sequence of early cytological changes in Chinese cabbage leaf cells following systemic infection with turnip yellow mosaic virus. Virology 59:383-396.

Hayes, R. J. and Buck, K. W. 1990. Complete replication of a eukaryotic virus RNA *in vitro* by a purified RNA-dependent RNA polymerase. Cell 63:363-368.

Hayes, R. J., Tousch, D., Jacquemond, M., Pereira, V. C., Buck, K. W. and Tepfer, M. 1992. Complete replicaiton of a satellite RNA *in vitro* by a purified RNA-dependent RNA polymerase. J. Gen. Virol. 73:1597-1600.

Hegg, L. A., Kou, M. and Thurlow, D. L. 1990. Recognition of the tRNA-like structure in tobacco mosaic viral RNA by ATP/CTP:tRNA nucleotidyltransferases from *Escherichia coli* and *Saccharomyces cereviseae*. J. Biol. Chem. 265:17441-17445.

Himeno, H., Hasegawa, T., Ueda, T., Watanabe, K., Miura, K. and Shimizu, M. 1989. Role of the extra G-C pair at the end of acceptor stem of $tRNA^{His}$ in aminoacylation. Nucleic Acids Res. 17:7855-7863.

Hirth, L. and Givord, L. 1988. Tymovirus. In: The Plant Virus (R. Koenig, eds.), vol. 3. pp.163-212. Plunem Press, NY.

Hou, Y. -M. and Schimmel, P. 1988. A simple structural feature is a major determinant of the identity of a transfer RNA. Nature 333:140-145.

Hou, Y. -M., Francklyn, C. and Schimmel, P. 1989. Molecular dissection of a transfer RNA and the basis for its identity. TIBS 14:233-237.

Hou, Y. -M. and Schimmel, P. 1989. Evidence that a major determinant for the identity of a transfer RNA is conserved in evolution. Biochemistry 28:6800-6804.

Hunter, A. R., Farrell, P. J., Jackson, R. J. and Hunt, T. 1977. The role of polyamines in cell-free protein synthesis in the wheat-gern system. Eur. J. Biochem. 75:149-157.

Igarashi, K., Watanabe,Y., Matsumoto, E., Kogo, A., Yabuki, M. and Hirose, S. 1977. Responsibility of 16S RNA for the stimulation of polypeptide synthesis by spermidine. Biochem. Biophys. Res. Commun. 76:18-25.

Ishikawa, M., Meshi, T., Watanabe, Y. and Okada, Y. 1988. Replication of chimeric tobacco mosaic

viruses which carry heterologous combinations of replicase genes and 3′ noncoding regions. Virology 164:290-293.

Ishikawa, M., Kroner, P., Ahlquist, P. and Meshi, T. 1991. Biological activities of hybrid RNAs generated by 3′-end exchanges between tobacco mosaic and brome mosaic viruses. J. Virol. 65:3451-3459.

Jablonski, S. A., Luo, M. and Morrow, C. D. 1991. Enzymatic activity of poliovirus RNA polymerase mutants with single amino acid changes in the conserved YGDD amino acid motif. J. Virol. 65:4565-4572.

Jacks, T., Madhani, H. D., Masiarz, F. R. and Varmus, H. E. 1988. Signals for ribosomal frameshifting in the Rous sarcoma virus *gag-pol* region. Cell 55:447-458.

Jahn, M., Rogers, M. J. and Söll, D. 1991. Anticodon and acceptor stem nucleotides in $tRNA^{Gln}$ are major recognition elements for *E. coli* glutaminyl-tRNA synthetase. Nature 352:258-260.

Johnson, M. W. and Markham, R. 1962. Nature of the polyamine in plant viruses. Virology 17:276-281.

Jonard, G. Witz, J. and Hirth, L. 1972. Formation of nucleoprotein complexes from dissociated turnip yellow mosaic virus RNA and capsids at low pH [hydrgen-ion concentration]: preliminary observation. J. Mol. Biol. 67:165-169.

Joshi, S., Haenni, A. -L., Hubert, E., Huez, G. and Marbaix, G. 1978. *In vivo* aminoacylation and 'processing' of turnip yellow mosaic virus RNA in *Xenopus laevis* oocytes. Nature 275:339-341.

Joshi, S., Chapeville, F. and Haenni, A. -L. 1982a. Turnip yellow mosaic virus RNA is aminoacylated *in vivo* in Chinese cabbage leaves. EMBO J. 1:935-938.

Joshi, S., Chapeville, F. and Haenni, A. L. 1982b. Length requirements for tRNA-specific enzymes and cleavage specificity at the 3′ end of turnip yellow mosaic virus RNA. Nucl. Acids Res. 10:1947-1962.

Joshi, R. L., Joshi, S., Chapeville, F. and Haenni, A. -L. 1983. tRNA-like structures of plant viral RNAs: conformational requirements for adenylation and aminoacylation. EMBO J. 2:1123-1127.

Joshi, R. L., Faulhammer, H., Chapeville, F., Sprinzl, M. and Haenni, A. -L. 1984. Aminoacyl RNA domain of turnip yellow mosaic virus Val-RNA interacting with elongation factor Tu. Nucleic Acids Res. 12:7467-7478.

Joshi, R. L. and Haenni, A. -L. 1986. Search for tRNA-like properties in tomato aspermy virus RNA. FEBS Letters 194:157-160.

Joshi, R. L., Ravel, J. M. and Haenni, A. -L. 1986. Interaction of turnip yellow mosaic virus Val-RNA with eukaryotic elongation factor EF-1α. Search for a function. EMBO J. 5:1143-1148.

Kamer, G. and Argos, P. 1984. Primary structural comparison of RNA-dependent polymerases from plant, animal and bacterial viruses. Nucl. Acids Res. 12:7269-7282.

Katouzian-Safadi, M. and Berthet-Colominas, C. 1983. Evidence for the presence of a hole in the capsid of turnip yellow mosaic virus after RNA release by freezing and thawing. Eur. J. Biochem. 137:47-55.

Katouzian-Safadi, M. and Haenni, A. -L. 1986. Studies on the phenomenon of turnip yellow mosaic virus RNA release by freezing and thawing. J. Gen. Virol. 67:557-565.

Kawasaki, E. S. 1990. Amplification of RNA, p.21-27. *In* M. A. Innis, D. H. Gelfand, J. J. Sninsky and T. J. White (ed.), PCR protocols: a guide to methods and applications. Academic Press, Inc., San Diego, Cal.

Keese, P., Mackenzie, A. and Gibbs, A.1989. Nucleotide sequence of the genome of an Australian isolate of turnip yellow mosaic tymovirus. Virology 172:536-546.

Kohl, R. J. and Hall, T. C. 1974. Aminoacylation of RNA from several viruses. Amino acid specificity and differential activity of plant, yeast and bacterial synthetases. J. Gen. Virol. 25:257-261.

Koonin, E. V. 1991. The phylogeny of RNA-dependent RNA polymerases of positive-strand RNA viruses. J. Gen. Virol. 72:2197-2206.

Kozak, M. 1987. At least six nucleotides preceding the AUG initiator codon enhance translation in mammalian cells. J. Mol. Biol. 196:947-950.

Kozlov, Yu. V., Rupasov, V. V., Adyshev, D. M., Belgelarskaya, S. N., Agranovsky, A. A., Mankin, A. S., Morozov, S. Yu., Dolja, V. V. and Atabekov, J. G. 1984. Nucleotide sequence of the 3'-terminal tRNA-like structure in barley stripe mosaic virus genome. Nucleic Acids Res. 12:4001-4009.

Kuiper, M. T. R. and Lambowitz, A. M. 1988. A novel reverse transcriptase activity associated with mitochondrial plasmids of Neurospora. Cell 55:693-704.

Kunkel, T.A., Roberts, J. D. and Zakour, R. A. 1987. Rapid and efficient site-specific mutagenesis without phenotypic selection. Meth. Enzymol. 154:367-382.

Laín, S., Riechmann, J. L. and García, J. A. 1990. RNA helicase: a novel activity associated with a protein encoded by a positive strand RNA virus. Nucleic Acids Res. 18:7003-7006.

Laín, S., Martín, M. T., Riechmann, J. L. and García, J. A. 1991. Novel catalytic activity associated with positive-strand RNA virus infection: nucleic acid-stimulated ATPase activity of the plum pox potyvirus helicaselike protein. J. Virol. 65:1-6.

Lane, L. 1986. Propagation and purification of RNA plant viruses. Meth. Enzymol. 118:87-696.

Leipold, B. 1977. Effect of spermidine on the RNA-A protein complex isolated from the RNA bacteriophage MS2. 21:445-450.

Levis, R., Schlesinger, S. and Huang, H. V. 1990. Promoter for sindbis virus RNA-dependent subgenomic RNA transcription. J. Virol. 64:1726-1733.

Litvak, S., Tarrago, A., Tarrago-Litvak, L. and Allende, J. E. 1973. Elongation factor-viral genome interaction dependent on the aminoacylation of TYMV and TMV RNAs. Nature, New Biol. 241:88-90.

Loesch-Fries, L.S. and Hall, T. C. 1980. Synthesis, accumulation and encapsidation of individual brome mosaic virus RNA components in barley protoplasts. J. Gen. Virol. 47:323-332.

Loesch-Fries, L. S. and Hall, T. C. 1982. *In vivo* aminoacylation of brome mosaic and barley stripe mosaic virus RNAs. Nature 298:771-773.

Lopez-Galindez, C., J. A. Lopez, J. A. Melero, L. D. L. Fuente, C. Martinez, J. Ortin and M. Perucho. 1988. Analysis of genetic variability and mapping of point mutations in influenza virus by the RNase A mismatch cleavage method. Proc. Natl. Acad. Sci. (USA) 85:3522-3526.

Mans, R. M. W., Verlaan, P. W. G., Pleij, C. W. A. and Bosch, L. 1990. Aminoacylation of 3' terminal tRNA-like fragments of turnip yellow mosaic virus RNA: the influence of 5' nonviral sequences. Biochem. Biophys. Acta 1050:186-192.

Mans, R. M. W. 1991. Thesis: Functional properties fo plant viral RNA pseudoknots. Classification, site-directed mutagenesis, aminoacylation, RNA replication and recombination.

Mans, R. M. W., Pleij, C. W. A. and Bosch, L. 1991. tRNA-like structures. Eur. J. Biochem. 201:303-324.

Mans, R. M. W., van Steeg, M. H., Verlaan, P. W. G., Pleij, C. W. A. and Bosch, L. 1992. Mutational analysis of the pseudoknot in the tRNA-like structure of turnip yellow mosaic virus RNA. Aminoacylation efficiency and RNA pseudoknot stability. J. Mol. Biol. 223:221-232.

Markham, R. and Smith, K. M. 1946. A new crystalline plant virus. Nature 157:300.

Markham, R. and Smith, K. M. 1949. Studies on the virus of turnip yellow mosaic. Parasitology 39:330-342.

Marsh, L. E. and Hall, T. C. 1987. Evidence implicating a tRNA heritage for the promoters of positive-strand RNA synthesis in brome mosaic and related viruses. Cold Spring Harbor Symp. Quant. Biol. 52:331-341.

Marsh, L. E., Dreher, T. W. and Hall, T. C. 1988. Mutational analysis of the core and modulator sequences of the BMV RNA3 subgenomic promoter. Nucleic Acids Res. 16:981-995.

Marsh, L. E., Pogue, G. P. and Hall, T. C. 1989. Similarities among plant virus (+) and (-) RNA termini imply a common ancestry with promoters of eukaryotic tRNAs. Virology 172:415-427.

Matthews, R. E. F. 1980. Turnip yellow mosaic virus. CMI/AAB Description of Plant Viruses. No. 230.

Matthews, R. E. F. 1981. Plant Virology. 2rd edition, Academic Press, New York.

Matthews, R. E. F. and Witz, T. 1985. Uncoating of turnip yellow mosaic virus RNA *in vivo*. Virology 144:318-327.

Matthews, R. E. F. 1991. Plant Virology. 3rd edition, Academic Press, New York.

McClain, W. H. and Foss, K. 1988. Changing the identity of a tRNA by introducing a G-U wobble pair near the 3' acceptor end. Science 240:793-796.

McClain, W. H., Chen, Y. -M., Foss, K. and Schneider, J. 1988. Association of transfer RNA acceptor identity with a helical irregularity. Science 242:1681-1684.

McClain, W. H., Foss, K., Jenkins, R. A. and Schneider, J. 1991. Four sites in the acceptor helix and one site in the variable pocket of $tRNA^{Ala}$ determine the molecule's acceptor identity. Proc. Natl. Acad. Sci. USA 88:9272-9276.

McPheeters, D. S., Stormo, G. D. and Gold, L. 1988. Autogenous regulatory site on the bacteriophage T4 gene 32 messenger RNA. J. Mol. Biol. 201:517-535.

Mellema, J. -R., Benicourt, C., Haenni, A. -L.,Noort, A., Pleij, C. W. A. and Bosch, L. 1979. Translational Studies with turnip yellow mosaic virus RNAs isolated from major and minor virus particles. Virology 96:38-46.

Meshi, T., Ohno, T., Iba, H. and Okada, Y. 1981. Nucleotide sequence of a cloned cDNA copy of TMV (cowpea strain) RNA, including the assembly origin, the coat protein cistron, and the 3' non-coding region. Mol. Gen. Genet. 184:20-25.

Mi, S. and Stollar, V. 1991. Expression of Sindbis virus nsP1 and methyltransferase activity in *E. coli*. Virology 184:423-427.

Miller, W. A., Dreher, T. W. and Hall, T. C. 1985. Synthesis of brome mosaic virus subgenomic RNA *in vitro* by internal initiation on (-)-sense genomic RNA. Nature 313:68-70.

Miller, W. A., Bujarski, J. J., Dreher, T. W. and Hall, T. C. 1986. Minus-strand initiation by brome mosaic virus replicase within the 3' tRNA-like structure of native and modified RNA templates. J. Mol. Biol. 187:537-546.

Mitra, S. and Kaesberg, P. 1965. Biophysical properties of RNA from turnip yellow mosaic virus. J. Mol. Biol. 14:558-571.

Monore, S. S. and Schlesinger, S. 1983. RNAs from two independently isolated defective-interfering particles of sindbis virus contain a cellular tRNA at their 5'-ends. Proc. Natl. Acad. Sci. USA 80:3279-3283.

Morch, M. -D. and Benicourt, C. 1980. Polyamines stimulate suppression of amber termination codons *in vitro* by normal tRNAs. Eur. J. Biochem. 105:445-451.

Morch, M. -D., Joshi, R. L., Denial, T. M. and Haenni, A. -L. 1987. A new "sense" RNA approach to block viral RNA replication *in vitro*. Nucleic Acids Res. 15:4123-4130.

Morch, M. -D., Boyer, J. -C. and Haenni, A. -L. 1988. Overlapping open reading frames revealed by complete nucleotide sequencing of turnip yellow mosaic virus genomic RNA. Nucl. Acids Res. 15:6157-6173.

Mouches, C., Bove, C. and Bove, J. M. 1974. Turnip yellow mosaic virus RNA replicase:partial purification of the enzyme from the solubilized enzyme-template complex. Virology 58:409-423.

Mouches, C., Candresse, T. and Bove, J. M. 1984. Turnip yellow mosaic virus RNA replicase contains host and virus encoded subunits. Virology 134:78-90.

Munishkin, A. V., Voronin, L. A. and Chetverin, A. B. 1988. An *in vivo* recombinant RNA capable of autocatalytic synthesis by Qß replicase. Nature 333:473-475.

Muramatsu, T., Nishikawa, K., Nemoto, F., Kuchino, Y., Nishimura, S., Miyazawa, T. and Yokoyama, S. 1988. Codon and amino-acid specificities of a transfer RNA are both converted by a single post-transcriptional modification. Nature 336:179-181.

Musier-Forsyth, K., Scaringe, S., Usman, N. and Schimmel, P. 1991. Enzymatic amionacylation of single-stranded RNA with an RNA cofactor. Proc. Natl. Acad. Sci. USA 88:209-213.

Myers, R. M., Larin, Z. and Maniatis, T. 1985. Detection of single base substitutions by ribonuclease cleavage at mismatches in RNA:DNA duplexes. Science 230:1242-1246.

Nazarenko, I. A., Peterson, E. T., Zakharova, O. D., Lavrik, O. I. and Uhlenbeck, O. C. 1992. Recognition nucleotides for human phenylalanyl-tRNA synthetase. Nucleic Acids Res. 20:475-478.

Nishiguchi, M., Kikuchi, S., Kiho, Y., Ohno, T., Meshi, T. and Okada, Y. 1985. Molecular basis of plant viral virulence: The complete nucleotide sequence of an attenuated strain of tobacco mosaic virus. Nucleic Acids Res. 13:5585-5590.

Noort, A., Van Den Dries, C. L. A. M., Pleij, C. W. A., Jaspars, E. M. J. and Bosch, L. 1982. Properies of turnip yellow mosaic virus in cesium chloride solutions: The formation of high-density componenets. Virology 120:412-421.

Normanly, J., Ogden, R. C., Horvath, S. J. and Abelson, J. 1986. Charging the identity of a transfer RNA. Nature 321:213-219.

Normanly, J. and Abelson, J. 1989. tRNA identity. Annu. Rev. Biochem. 58;1029-1049.

Normanly, J., Ollick, T. and Abelson, J. 1992. Eight base changes are sufficient to convert a leucine-inserting tRNA into a serine-inserting tRNA. Proc. Natl. Acad. Sci. USA 89:5680-5684.

Öberg, B. and Philipson, L. 1972. Binding of histidine to tobacco mosaic virus RNA. Biochem. Biophys. Res. Comm. 48:927-932.

Osorio-Keese, M. E., Keese, P. and Gibbs, A. 1989. Nucleotide sequence of the genome of eggplant mosaic tymovirus. Virology 172:547-554.

Pace, N. R. and Smith, D. 1990. Ribonuclease P: function and variation. J. Biol. Chem. 265:3587-3590.

Pallanck, L. and Schulman, L. H. 1991. Anticodon-dependent aminoacylation of a noncognate tRNA with isoleucine, valine, and phenylalanine *in vivo*. Proc. Natl. Acad. Sci. USA 88:3872-3876.

Park, S. J. and Schimmel, P. 1988. Evidence for interaction of an aminoacyl transfer RNA synthetase with a region important for the identity of its cognate transfer RNA. J. Biol. Chem. 263:16527-16530.

Perret, V., Florentz, C., Dreher, T. W. and Giegé, R. 1989. Structural analogies between the 3' tRNA-like structure of brome mosaic virus RNA and yeast $tRNA^{Tyr}$ revealed by protection studies with yeast tyrosyl-tRNA synthetase. Eur. J. Biochem. 185:331-339.

Perret, V., Garcia, A., Grosjean, H., Ebel, J. -P., Florentz, C. and Giegé, R. 1990. Relaxation of a transfer RNA specificity by removal of modified nucleotides. Nature 344:787-789.

Peter, R., Stehelin, D., Reinbolt, J., Collot, D. and Duranton, H. 1972. Primary structure of turnip yellow mosaic virus coat protein. Virology 49:615-617.

Philippe, C., Portier, C., Mougel, M., Grunberg-Manago, M., Ebel, J. P., Ehresmann, B. and Ehresmann, C. 1990. Target site of *Escherichia coli* ribosomal protein S15 on its messenger RNA. Conformation and interaction with the protein. J. Mol. Biol. 211:415-426.

Pinck, M., Yot, P., Chapeville, F. and Duranton, H. M. 1970. Enzymatic binding of valine to the 3' termini of some plant viral RNAs. Nature 226:954-956.

Pleij, C. W. A., Neeleman, A., Van Vloten-Doting, L. and Bosch, L. 1976. Translation of turnip yellow mosaic virus RNA *in vitro*: A closed and an open coat protein cistron. Proc. Natl. Acad. Sci. USA 73:4437-4441.

Pleij, C. W. A., Rietveld, K. and Bosch, L. 1985. A new principle of folding based on pseudoknotting. Nucleic Acids Res. 13:1717-1731.

Pleij, C. W. A., Abrahams, J. P., van Belkum, A., Rietveld, K. and Bosch, L. 1987. The spatial folding of the 3′ noncoding region of aminoacylatable plant viral RNAs. In: Positive Strand RNA Viruses (M. A. Brinton and R. R. Rueckert, eds), pp. 299-316. Alan R. Liss, Inc., New York.

Pleij, C. W. A., Bosch, L. 1989. RNA pseudoknots: structure, detection, and prediction. Methods in Enzymology. 180:289-303

Pleij, C. W. A. 1990. Pseudoknots: a new motif in the RNA game. TIBS 15:143-147.

Pogue, G. P. Marsh, L. E. and Hall, T. C. 1990. Point mutations in the ICR2 motif of brome mosaic virus RNAs debilitate (+)-strand replication. Virology 178:152-160.

Pogue, G. P. and Hall, T. C. 1992. The requirement of a 5′ stem-loop structure in brome mosaic virus replication supports a new model for viral positive-strand RNA initiation. J. Virol. 66:674-684.

Prochiantz, A., Bénicourt, C., Carré, D. and Haenni, A. -L. 1975. tRNA nucleotidyltransferase-catalyzed incorporation of CMP and AMP into RNA-bacteriophage genome fragments. Eur. J. Biochem. 52:17-23.

Pulikowska, J., Wojtaszek, P., Korcz, A., Michalski, Z., Candresse, T. and Twardowski, T. 1988. Immunochemical properties of elongation factors 1 of plant origin. Eur. J. Biochem. 171:131-136.

Pütz, J., Puglisi, J. D., Florentz, C. and Giegé, R. 1991. Identity elements for specific aminoacylation of yeast $tRNA^{Asp}$ by cognate aspartyl-tRNA synthetase. Science 252:1696-1699.

RajBhandary, U. L. 1988. Modified bases and aminoacylation. Nature 336:112-113.

Rao, A. L. N. and Francki, R. I. B. 1981. Comparative studies on tomato aspermy and cucumber mosaic viruses. VI. partial compatibility of genome segments from the two viurses. Virology 114:573-575.

Rao, A. L. N., Dreher, T. W., Marsh, L. E. and Hall, T. C. 1989. Telomeric function of the tRNA-like structure of brome mosaic virus RNA. Proc. Natl. Acad. Sci. USA 86:5335-5339.

Rao, A. L. N. and Hall, T. C. 1991. Interference *in trans* with brome mosaic virus replication by RNA-2 bearing aminoacylation-deficient mutants. Virology 180:16-22.

Rietveld, K., van Poelgeest, R., Pleij, C. W. A., van Boom, J. H. and Bosch, L. 1982. The tRNA-like structure at the 3′ terminus of turnip yellow mosaic virus RNA. Differences and similarities with canonical tRNA. Nucleic Acids Res. 10:1929-1946.

Rietveld, K., Pleij, C. W. A. and Bosch, L. 1983. Three-dimensional models of the tRNA-like 3′ termini of some plant viral RNAs. EMBO J. 2:1079-1085.

Rietveld, K. 1984. Ph.D. thesis, State University of Leiden, p. 118.

Rietveld, K., Linschooten, K., Pleij, C. W. A. and Bosch, L. 1984. The three-dimensional folding of the tRNA-like structure of tobacco mosaic virus RNA. A new building principle applied twice. EMBO J. 3:2613-2619.

Rogers, M. J. and Söll, D.1988. Discrimination between glutaminyl-tRNA synthetase and seryl-tRNA synthetase involves nucleotides in the acceptor helix of tRNA. Proc. Natl. Acad. Sci. USA 85:6627-6631.

Rould, M. A., Perona, J. J and Steitz, T. A. 1991. Structural basis of anticodon loop recognition by glutaminyl-tRNA synthetase. Nature 352:213-218.

Rozanov, M. N., Koonin, E. V. and Gorbalenya, A. E. 1992. Conservation of the putative methyltransferase domain: a hallmark of the 'Sindbis-like' supergroup of positive strand RNA viruses. J. Gen. Virol. 73:2129-2134.

Rudinger, J., Puglisi, J. D., Pütz, J., Schatz, D., Eckstein, F., Florentz, C. and Giegé, R. 1992a. Determinant nucleotides of yeast $tRNA^{Asp}$ interact directly with aspartyl-tRNA synthetase. Proc. Natl. Acad. Sci. USA 89:5882-5886.

Rudinger, J., Florentz, C., Dreher, T. W. and Giegé, R. 1992b. Efficient mischarging of a viral tRNA-like structure and aminoacylation of a minihelix containing a pseudoknot: histidinylation of turnip yellow mosaic virus RNA. Nucleic Acids Res. 20:1865-1870.

Ruff, M., Krishnaswamy, S., Boeglin, M., Poterszman, A., Mitschler, A., Podjarny, A., Rees, B., Thierry, J. C. and Moras, D. 1991. Class II aminoacyl transfer RNA synthetases: crystal structure of yeast aspartyl-tRNA synthetase complexed with $tRNA^{Asp}$. Science 252:1682-1689.

Sakai, T. T. and Cohen, S. S. 1976. Effects of polyamines on the structure and reactivity of tRNA. Progr. Nucleic Acid Res. Mol. Biol. 17:15-42.

Sampson, J. R. and Uhlenbeck, O. C. 1988. Biochemical and physical characterization of an unmodified yeast phenylalanine transfer RNA transcribed *in vitro*. Proc. Natl. Acad. Sci. USA 85:1033-1037.

Sampson, J. R., DiRenzo, A. B., Behlen, L. S. and Uhlenbeck, O. C. 1989. Nucleotides in yeast $tRNA^{Phe}$ required for the specific recognition by its cognate synthetase. Science 243:1363-1366.

Samuelsson, T. and Olsson, M. 1990. Transfer RNA pseudouridine synthases in *Saccharomyces cerevisiae*. J. Biol. Chem. 265:8782-8787.

Santos, M., Colthurst, D. R., Wills, N., McLaughlin, C. S. and Tuite, M. F. 1990. Efficient translation of the UAG termination codon in *Candia* species. Curr. Genet. 17:487-491.

Savithri, H. S., Munshi, S. K., Suryanarayana, S., Divakar, S. and Murthy, M. R. N. 1987. Stability of belladonna mottle virus particles: the role of polyamines and calcium. J. Gen. Virol. 68:1533-1542.

Schatz, D, Leberman, R. and Eckstein, F. 1991. Interaction of *Escherichia coli* $tRNA^{Ser}$ with its cognate amioacyl-tRNA synthetase as determined by footprinting with phosphorothioate-containing tRNA transcripts. Proc. Natl. Acad. Sci. USA 88:6132-6136.

Schimmel, P. 1989. RNA pseudoknots that interact with components of the translation apparatus. Cell 58:9-12.

Schulman, L. H. and Pelka, H. 1983. Anticodon loop size and sequence requirements for recognition of formylmethionine tRNA by methionyl-tRNA synthetase. Proc. Natl. Acad. Sci. USA 80:6755-6759.

Schulman, L. H. and Pelka, H. 1984. Recognition of tRNAs by amnoacyl-tRNA synthetases: *Escherichia coli* $tRNA^{Met}$ and *E. coli* methionyl-tRNA synthetase. FASEB 43:2977-2980.

Schulman, L. H. and Pelka, H. 1988. Anticodon switching changes the identity of methionine and valine transfer RNAs. Science 242:765-768.

Schulman, L. H. and Pelka, H. 1989. The anticodon contains a major element of the identity of arginine transfer RNAs. Science 246:1595-1597.

Schulman, L. H. and Pelka, H. 1990. An anticodon change switches the identity of *E. coli* $tRNA^{Met}$ from methionine to threonine. Nucleic Acids Res. 18:285-289.

Schulman, L. H. 1991. Recognition of tRNAs by aminoacyl-tRNA synthetases. Prog. Nucl. Acid Mole. Biol. 41:23-87.

Shaw, J. G., Plaskitt, K. A. and Wilson, T. M. A. 1986. Evidence that tobacco mosaic virus particles disassemble cotranslationally *in vivo*. Virology 148:326-336.

Shi, J. -P., Francklyn, C., Hill, K. and Schimmel, P. 1990. A nucleotide that enhances the charging of RNA minihelix sequence variants with alanine. Biochemistry 29;3621-3626.

Shintaku, M. H., Zhang, L. and Palukaitis 1992. A single amino acid substition in the coat protein of cucumber mosaic virus induces chlorosis in tobacco. The Plant Cell 4:751-757.

Silberklang, M., Prochiantz, A., Haenni, A. -L. and RajBhandary, U. L. 1977. Studies on the sequence of the 3'-terminal region of turnip yellow mosaic virus RNA. Eur. J. Biochem. 72:465-478.

Singh, I. and Helenius, A. 1992. Nucleocapsid uncoating during entry of enveloped animal RNA viruses into cells. Semi. Virol. 3:511-518.

Snyder, R. D. and Edwards, M. L. 1991. Effects of polyamine analogs on the extent and fidelity of *in vitro* polypeptide synthesis. Biochem. Biophys. Res. Comm. 176:1383-1392.

Spacciapoli, P., Doviken, L., Mulero, J. J. and Thurlow, D. L. 1989. Recognition of tRNA by the enzyme ATP/CTP:tRNA nucleotidyltransferase. Interference by nucleotides modified with diethyl pyrocarbonate or hydrazine. J. Biol. Chem. 264:3799-3805.

Sprague, K. U. 1992. New twists in class III transcription. Curr. Opin. Cell Biol. 4:475-479.

Sprinzl, M., Dank, N., Nock, S. and Schön, A. 1991. Compilation of tRNA and tRNA gene sequences. Nucleic Acids Res. 19 (supplement):2127-2171.

Srifah, P., Keese, P., Weiller, G. and Gibbs, A. 1992. Comparisons of the genomic sequences of erysimum latent virus and other tymoviruses: a search for the molecular basis of their host specificities. J. Gen. Virol. 73:1437-1447.

Steinmetz, A and Weil, J.-H. 1986. Isolation and characterization of chloroplast and cytoplasmic transfer RNAs. Methods Enzymol. 118:212-231.

Stratford, R. and Covey, S. N. 1989. Segregation of cauliflower mosaic virus symptom genetic determinants. Virology 172:451-459.

Strazielle, C., Benoit, H. and Hirth, L. 1965. J. Mol. Biol. 13:735-748.

Struck, J. C. and Erdmann, V. A. 1990. Phylogenetic and biochemical evidence for a secondary structure model of a small cytoplasmic RNA from *Bacilli*. Eur. J. Biochem. 192:17-24.

Studnicka, G. M., Rahn, G. M., Cummings, I. W. and Salser, W. A. 1978. Computer method for predicting the secondary structure of single-stranded RNA. Nucleic Acids Res. 5:3365-3387.

Takamatsu, N., Watanabe, Y., Meshi, T. and Okada, Y. 1990. Mutational analysis of the pseudoknot region in the 3' noncoding region of tobacco mosaic virus RNA. J. Virol. 64:3686-3693.

Tamura, K., Himeno, H., Asahara, H., Hasegawa, T. and Shimizu, M. 1991. Identity determinants of *E. coli* $tRNA^{Val}$. Biochem. Biophys. Res. Comm. 177:619-623.

Tang, C. K. and Draper, D. E. 1989. Unusual mRNA pseudoknot structure is recognized by a protein translational repressor. Cell 57:531-536.

Thang, M. N., Dondon, L. and Mohier, E. 1976. Translation of alfalfa mosaic virus RNA effect of polyamines. FEBS Lett. 61:85-90.

Torget, R., Lapi, L. and Cohen, S. S. 1979. Synthesis and accumulation of polyamines and S-adenosylmethionine in Chinese cabbage infected by turnip yellow mosaic virus. Biochem. Biophys. Res. Commuun. 87:1132-1139.

Tuerk, C., MacDougal, S. and Gold, L. 1992. RNA pseudoknots that inhibit human immunodeficiency virus type 1 reverse transcriptase. Proc. Natl. Acad. Sci. USA 89:6988-6992.

Turner, P. C., Watkins, P. A. C., Zaitlin, M. and Wilson, T. M. A. 1987. Tobacco mosaic virus particles uncoat and express their RNA in *Xenopus laevis* oocytes: Implications for early interactions between plant cells and viruses. Virology 160:515-517.

Tzeng, T. -H., Tu, C. -L. and Bruenn, J. A. 1992. Ribosomal frameshifting requires a pseudoknot in the *Saccharomyces cerevisiae* double-stranded RNA virus. J. Virol. 66:999-1006.

Van Belkum, A., Abrahams, J. B., Pleij, C. W. A. and Bosch, L. 1985. Five pseudoknots are present at the 204 nucleotides long 3' noncoding region of tobacco mosaic virus RNA. Nucleic Acids Res. 13:7673-7686.

Van Belkum, A., Cornelissen, B., Linthorst, H., Bol, J., Pley, C. and Bosch, L. 1987a. tRNA-like properties of tobacco rattle virus RNA. Nucleic Acids Res. 15:2837-2850.

Van Belkum, A., Bingkun, J., Rietveld, K., Pleij, C. W. A. and Bosch, L. 1987b. Structural similarities among valine-accepting tRNA-like structures in tymoviral RNAs and elongator tRNAs. Biochemistry 26:1144-1151.

Van Regenmortel, M. H. V. 1989. Applying the species concept to plant viruses. Arch. Virol. 104:1-17.

Varmus, H. E. 1988. Retroviruses. Science 240:1427-1435.

Waldrop, M. M. 1989. Did life really start out in an RNA world? Science 246:1248-1249.

Watanabe, Y., Morita, N., Nishiguchi, M. and Okada, Y. 1987. Attenuated strains of tobacco mosaic virus reduces synthesis of a viral protein with a cell-to-cell movement function. J. Mol. Biol. 194:699-704.

Waterson, A. P. and Wilkinson, L. 1978. An introduction to the history of virology. Cambridge University Press.

Weiland, J. J. and Dreher, T. W. 1989. Infectious TYMV RNA from cloned cDNA: effects *in vitro* and *in vivo* of point substitutions in the initiation codons of two extensively overlapping ORFs. Nucleic Acids Res. 17:4675-4687.

Weiland, J. J. 1992. Ph. D. Dissertation. Oregon State University.

Weiland, J. J. and Dreher, T. W. 1993. *Cis*-preferential replication of the turnip yellow mosaic virus RNA genome. Proc. Natl. Acad. Sci. USA (in press).

Weiner, A. M. and Maizels, N. 1987. tRNA-like structures tag the 3' ends of genomic RNA molecules for replication: implications for the origin of protein synthesis. Proc. Natl. Acad. Sci. USA 84:7383-7387.

Weiner, A. M. 1988. Eukaryotic nuclear telomeres: molecular fossils of the RNP world? Cell 52:155-157.

Wells, J. A. 1990. Additivity of mutational effects in proteins. Biochemistry 29:8509-8517.

Wills, N. M., Gesteland, R. F. and Atkins, J. F. 1991. Evidence that a downstream pseudoknot is required for translational read-through of the Moloney murine leukemia virus *gag* stop codon. Proc. Natl. Acad. Sci. USA 88:6991-6995.

Wilson, T. M. A. 1984. Cotranslational disassembly increases the efficiency of expression of TMV RNA in wheat germ cell-free extracts. Virology 138:353-356.

Wilson, W., Braddock, M., Adams, S. E., Rathjen, P. D., Kingsman, S. M. and Kingsman, A. J. 1988. HIV expression strategies: ribosomal frameshifting is directed by a short sequence in both mammalian an yeast systems. Cell 55:1159-1169.

Winship, P. P. 1989. An improved method for directly sequencing PCR-amplified material using dimethyl sulfoxide. Nucl. Acids Res. 17:1266.

Wyatt, J. R., Puglisi, J. D. and Tinoco, I. Jr. 1990. RNA pseudoknots. Stability and loop size requirements. J. Mol. Biol. 214:455-470.

Yot, P., Pinck, M., Haenni, A. -L., Duranton, H. M. and Chapeville, F. 1970. Valine-specific tRNA-like structure in turnip yellow mosaic virus RNA. Proc. Natl. Acad. Sci. USA 67:1345-1352.

Zawadzki, V. and Gross, H. J. 1991. Rapid and simple purification of T7 RNA polymerase. Nucleic Acids Res. 19:1948.

ABBREVIATIONS

ORF	open reading frame
ICR	intragenic control region
nt	nucleotide
bp	basepair
kb	kilobase
kDa	kilodalton
BMV	brome mosaic bromovirus
BBMV	broad bean mottle bromovirus
BSMV	barley stripe mosaic hordeivirus
CcTMV	cowpea strain tobacco mosaic tobamovirus
CGMMV	cucumber green mottle mosaic tobamovirus
CMV	cucumber mosaic cucumovirus
HIV	human immunodeficiency virus
IBV	infectious bronchitis coronavirus
TAV	tomato aspermy cucumovirus
TMV	tobacco mosaic tobamovirus
TRV	tobacco rattle tobravirus
TYMV	turnip yellow mosaic tymovirus
TYMC	turnip yellow mosaic tymovirus-Corvallis strain
aaRS	aminoacyl-tRNA synthetase
AlaRS	alanyl-tRNA synthetase
AspRS	aspartyl-tRNA synthetase
GlnRS	glutarmyl-tRNA synthetase
HisRS	histidyl-tRNA synthetase
IleRS	isoleucyl-tRNA synthetase
MetRS	methionyl-tRNA synthetase
TyrRS	tyrosyl-tRNA synthetase
ValRS	valyl-tRNA synthetase
NTase	(CTP, ATP):tRNA nucleotidyltransferase
RNase	ribonuclease
PCR	polymerase chain reaction
SELEX	systematic evolution of ligands by exponential enrichment

APPENDICES

APPENDIX I

In vitro transcription of RNAs with defined 3′ termini from PCR-generated templates

Abstract

We demonstrate the feasibility of using PCR to economically amplify sufficient template to permit the transcription by T7 RNA polymerase of preparative amounts of RNAs for biochemical analyses. We show that a standard 100 μl PCR amplification of a fragment from the 3′ end of the genomic CDNA of turnip yellow mosaic virus yields enough template to support the synthesis of about 50 μg of a 264 nucleotide-long transcript. The choice of the 3′ primer defines the 3′ terminus of the transcripts, although, as with transcription from DNA linearized by restriction digestion, a subpopulation of transcripts with one or two additional 3′ nucleotides is present. This PCR-based approach can be adapted to the rapid generation of RNAs with different 3′ termini and with mutations near the 3′ end.

Introduction

In vitro transcription using purified bacteriophage RNA polymerases such as T7 RNA polymerase has become an indispensable technique in the study of RNA structure and function (Krieg and Melton, 1987; Milligan and Uhlenbeck, 1989). Typically, a cDNA is cloned adjacent to a T7, T3 or SP6 promoter in an appropriate plasmid or M13 vector, which must be linearized by cleavage with a restriction enzyme prior to transcription. We and others have described the application of this approach to the synthesis of RNAs with defined 3′ termini, permitting studies on the aminoacylation of tRNA-like viral RNAs (Dreher *et al.*, 1984; Dreher *et al.*, 1988) and tRNAs (Sampson and Uhlenbeck, 1988), reactions that are strictly dependent on the presence of 3′-CCA termini.

The requirement for an accurately positioned 3′ restriction site for linearization prior to transcription can impose limitations on the 3′ sequences of transcripts. This limitation can be overcome by transcription directly from a synthetic deoxyoligonucleotide template annealed to a shorter oligomer in order to provide a double-stranded promoter (Milligan *et al.*, 1987). The 3′ terminus of a transcript produced in this way is determined by the 5′ end of the synthetic template antisense strand, and there is thus great flexibility with regard to 3′ sequence. This approach is limited, however, to transcripts less than 50 or so nucleotides in length due to the low quality of long synthetic oligomers.

We describe here a technique, in which the transcriptional template is synthesized by PCR, that complements the above techniques. The upstream primer provides the T7 promoter and defines the 5′ end of the transcript, while the downstream primer defines the 3′ end of the amplified DNA and of the transcript made from it. There are no limitations on the 3′ end sequence, and RNAs of any length compatible with the PCR amplification can be made. Large amounts of transcripts can be economically made by this approach, which we have used to study the valylation kinetics of plant viral tRNA-like molecules 264 nucleotides in length.

Materials and Methods

Transcription from linearized cloned DNA. CsCl-purified replicative form (RF) DNA from mpT7YSma (derived from pT7YSma; Dreher *et al.*, 1988) and its mutant derivative mpTY-U56 were digested with *BstN*I restriction enzyme (New England Biolabs, Beverly, MA) and transcribed in 150 μl reactions containing 20 μg of DNA and 300 units of T7 RNA polymerase (United States Biochemical, Cleveland, OH) in 40 mM Tris-HCl (pH 8.0), 25 mM NaCl, 8 mM $MgCl_2$, 2 mM spermidine and 2 mM of each ribonucleoside triphosphate (including [α-^{32}P]UTP at 2.3 Ci/mole), that were incubated at 37°C for 4 h. The transcripts were purified by denaturing PAGE in order to remove short degradation or abortion products, followed by electroelution and dialysis. The presence of radiolabel permitted accurate determination of RNA concentrations.

PCR amplification of DNA templates for transcription. The following oligomers were made by automated synthesis using phosphoramidite chemistry: (a) the upstream primer d(TAATACGACTCACTATAGGGAGAGGGTCAAAGATTCG), which comprises the T7 promoter (including the 6 nucleotides GGGAGA that are present at the 5′ of transcripts) adjacent to the sequence corresponding to nucleotides 258-245 from the 3′ end of turnip yellow mosaic virus (TYMV) RNA; (b) the downstream primer d(TGGTTCCGATGACCCTCG), which is complementary to nucleotides 1-18 from the 3′ end of the 3′-adenylated form of TYMV RNA.

*BstN*I-linearized RF DNA (0.1 μg) and 100 pmoles of each primer were mixed in 100 μl PCR reactions containing 10 mM Tris-HCl (pH 9.0 at 25°C), 50 mM KCl, 1.5 mM $MgCl_2$, 0.1% Triton X-100, 0.01% gelatin (w/v), 0.2 mM of each deoxyribonucleoside triphosphate and 1 unit of *Taq* DNA polymerase (Promega, Madison, WI). DNA amplification occurred during 30 cycles of 1 min at 94°C, 0.5 min at 55°C and 0.5 min at 72°C, programmed on a Perkin-Elmer DNA Thermal Cycler (Perkin-Elmer, Norwalk, CT). Reactions were terminated by the addition of excess EDTA followed by phenol/chloroform extraction. After ethanol precipitation, the entire samples of amplified products were used as templates in transcription reactions as described above. In some cases, the amplified DNA was sequenced according to Winship (1989) to verify the absence of fortuitous mutations.

Characterization of the transcripts. The 3′ termini of transcripts were studied after 3′ terminal labelling as described (Dreher *et al.*, 1988) to estimate the proportion of transcripts with 3′-CCA ends (average values for more than 10 determinations involving different transcription reactions are given in the Results section). The valylation properties of transcripts were studied by incubation with an enriched wheat germ valyl-tRNA synthetase in 25 mM Tris-HCl (pH 8.0), 2 mM $MgCl_2$, 1 mM ATP, 0.1 mM spermine and 10 μM [^{3}H]valine (12 Ci/mmol) at 30°C. Bound valine was determined by liquid scintillation counting after precipitation of RNA with trichloroacetic acid on Whatman 3MM paper filters.

Results and Discussion

The virion RNA of turnip yellow mosaic virus (TYMV) has a 3′ tRNA-like structure terminating in -CC that becomes adenylated upon inoculation into plant cells; the resultant 3′-CCA terminus is an efficient substrate for valylation (Joshi *et al.*, 1982). We have described the preparative *in vitro* transcription of 3′ fragments of TYMV RNA that can be valylated *in vitro* with valyl-tRNA synthetase (Dreher *et al.*, 1988). In order to determine the feasibility of a PCR-based method for making 50-100 μg amounts of RNAs with specific 3′ termini, we compared the properties of transcripts made from PCR-generated templates with those made in the conventional way from linearized cloned DNA. The comparison included (a) transcripts with wild-type valylation activity derived from clone mpT7YSma, which contains the 3′ 258 nucleotides of the genomic cDNA of TYMV cloned adjacent to a T7 promoter in bacteriophage M13, and (b) transcripts from the mutant clone mpTY-U56, in which the A→U substitution in the middle of the anticodon results in extremely poor valylation. The yield of transcripts and the proportion of the desired 3′-CCA termini were determined in each case. The valylation of transcripts by wheat germ valyl-tRNA synthetase was characterized by determining the plateau levels of valine charging (mol val/ mol RNA; Table A-1) and apparent K_M and V_{max} values, estimated by Lineweaver-Burk analysis of initial valylation rates (Table A-1).

Transcripts made after linearization of the above RF DNAs by digestion with *BstN*I restriction enzyme are 264 nucleotides long and have 6 non-viral nucleotides (GGGAGA) at their 5′ ends. Most terminate at the 3′ end with the desired -CCA, although a consistent proportion of transcripts have one or two additional 3′ nucleotides that are inserted in a template independent reaction (Melton *et al.*, 1984; Dreher *et al.*, 1988). In the present studies, 75 ± 5% of transcripts made from *BstN*I-linearized templates terminated with 3′-CCA. Those RNAs were appropriate substrates for valylation studies using wheat germ valyl-tRNA synthetase. We have previously shown that the non-3′-CCA-terminating RNAs present after transcription do not interfere with the determination of kinetic parameters for valylation (Dreher *et al.*, 1988). Although the transcripts made in this study are too long to permit purification of the 3′-CCA-containing RNAs, such purification to single nucleotide resolution is possible by denaturing PAGE for RNAs less than c. 100 nucleotides long (e.g. tRNAs; Sampson and Uhlenbeck, 1988). Typical yields were 30-50 μg of RNA transcripts from 20 μg of linearized cloned DNA. Table A-1A presents the kinetic parameters determined for the valylation of wild-type RNA and of mutant TY-U56 RNA.

When *BstN*I-linearized RF DNAs from mpT7YSma and mpTY-U56 were used as templates in PCR amplification reactions, about 1.5-2.5 μg of the specific 281 nucleotide-long DNA fragment were typically made in 100 μl reactions containing 0.1 μg of template DNA after 30 cycles using 1 unit of *Taq* DNA polymerase (not shown). The entire PCR product was then used as template DNA in T7 transcription reactions identical to those using linearized cloned DNA as template. Typical yields were

40-60 μg of RNA transcripts, identical in sequence and length to those made directly from *BstN*I-linearized cloned DNA. Analysis of the 3' ends of these transcripts showed that 63 $\pm$ 5% of molecules ended in the desired 3'-CCA. Apparently, the end-structure of the PCR-generated DNA template (blunt or with an unpaired 3' dA residue) results in a slightly lower proportion of the expected transcript compared with the *BstN*I-linearized template DNA. The valylation properties of transcripts derived from PCR-generated templates (Table A-1B) were not significantly different from those derived from transcripts made directly from linearized cloned DNA (Table A-1A). This was true both for wild-type RNAs, which are efficiently valylated, and mutant TY-U56 RNAs, which are very inefficiently valylated.

These results demonstrate that sufficiently large amounts of transcripts with accurate 3' ends can be economically generated for biochemical studies using the PCR-based approach described here. [The cost of *Taq* DNA polymerase consumed in making 1 mg of RNA transcript is currently less than $10]. The main advantage of this approach is the limitless flexibility in determining the 3' end of the transcripts synthesized *in vitro*, dependent only on the synthesis of a specific deoxyoligonucleotide primer. For instance, in our studies on the role of the tRNA-like properties and replication of plant viral RNAs, we have prepared RNAs that either lacked one or more 3' nucleotides or had short additional 3' sequences (Miller *et al.*, 1986; Dreher and Hall, 1988). In another instance, comparative *in vitro* valylation and *in vivo* replication studies demanded the generation of the same set of mutations in the context of two different 3' restriction sites (Chapter III in this thesis). The use of the PCR-based method described in this paper would have greatly simplified the preparation of RNAs for those studies. We believe that many other applications are possible in studies of RNA structure and function, including the facile introduction of mutations close to either end of the transcript by using an appropriate mutant primer. In these applications, it will be necessary to avoid contaminating the amplified transcription template with the input PCR template, e.g. by purifying the amplified DNA, or by linearizing the PCR template at a site that will yield inactive 3'-extended transcripts that can easily be removed during RNA purification.

Although we have not observed the amplification of unplanned mutated sequences generated as a result of the relatively low fidelity of *Taq* DNA polymerase (Higuchi, 1989), the procedure we have described in this paper will clearly benefit from the use of higher fidelity thermostable DNA polymerases as they become more available.

Table AI-1: Valylation of TYMV transcripts with wheat germ valyl-tRNA synthetase					
	Mutant	**mol val/ mol RNA[a]**	**K_M (nM)[b]**	**V_{max}[c]**	**V_{max}/K_M**
A Transcripts from *BstN*I-linearized cloned DNA	wild type	1.01	28	988	36
	TY-U56	$<10^{-3}$	3100	15	1.0×10^{-4}
B Transcripts from PCR-generated templates	wild type	0.99	35	972	28
	TY-U56	$<10^{-3}$	3600	16	9.4×10^{-5}

a. Extent of valylation after 60 min at 0.6 μM RNA (3'-CCA species).

b. Concentrations refer to the 3'-CCA species. Error, 15-20%.

c. Arbitrary units. Error, 15-20%.

References

Dreher, T.W., Bujarski, J.J. and Hall, T.C. 1984. Mutant viral RNAs synthesized *in vitro* show altered aminoacylation and replicase template activities. Nature 311:171-175.

Dreher, T.W., Florentz, C. and Giegé, R. 1988. Valylation of tRNA-like transcripts from cloned cDNA of turnip yellow mosaic virus RNA demonstrate that the L-shaped region at the 3' end of the viral RNA is not sufficient for optimal aminoacylation. Biochimie 70:1719-1727.

Dreher, T.W. and Hall, T.C. 1988. Mutational analysis of the tRNA mimicry of brome mosaic virus RNA. Sequence and structural requirements for aminoacylation and 3'-adenylation. J. Mol. Biol. 201:41-55.

Higuchi, R. 1989. Using PCR to engineer DNA, p.61-70. In H.A. Erlich (Ed.), PCR Technology: Principles and applications for DNA amplification. Stockton Press, New York.

Joshi, S., Chapeville, F. and Haenni, A.L. 1982. Turnip yellow mosaic virus RNA is aminoacylated *in vivo* in Chinese cabbage leaves. EMBO J. 1:935-938.

Krieg, P.A. and Melton, D.A. 1987. *In vitro* RNA synthesis with SP6 RNA polymerase. Methods Enzymol. 155:397-415.

Melton, D.A., Krieg, P.A., Rebagliati, M.R., Maniatis, T., Zinn, K. and Green, M.R. 1984. Nucl. Acids Res. 12:7035-7056.

Miller, W.A., Bujarski, J.J., Dreher, T.W. and Hall, T.C. 1986. Minus-strand initiation by brome mosaic virus replicase within the 3' tRNA-like structure of native and modified RNA templates. J. Mol. Biol. 187:537-546.

Milligan, J.F., Groebe, D. R., Witherell, G.W. and Uhlenbeck, O.C. 1987. Oligoribonucleotide synthesis using T7 RNA polymerase and synthetic DNA templates. Nucl. Acids Res. 15:8783-8798.

Milligan, J.F. and Uhlenbeck, O.C. 1989. Synthesis of small RNAs using T7 RNA polymerase. Methods Enzymol. 180:51-62.

Sampson, J.R. and Uhlenbeck, O.C. 1988. Biochemical and physical characterization of an unmodified yeast phenylalanine transfer RNA transcribed *in vitro*. Proc. Natl. Acad. Sci. (USA) 85:1033-1037.

Winship, P.R. 1989. An improved method for directly sequencing PCR amplified material using dimethyl sulphoxide. Nucl. Acids Res. 17:1266.

APPENDIX II

Increased Viral Yield and Symptom Severity Result from a Single Amino Acid Substitution in the Turnip Yellow Mosaic Virus Movement Protein

Abstract

Turnip yellow mosaic virus is a positive-strand RNA virus that produces light green or yellow-green mosaic symptoms in Chinese cabbage plants. We have characterized a strain that produces nearly uniform yellow-green chlorosis in systemically infected Chinese cabbage leaves. The increased symptom severity is due to the single nucleotide substitution U+1888→C, which results in a tyrosine to histidine substitution in the movement protein encoded by ORF-69. Coding by the overlapping ORF-206 is not affected. The mutation results in four-fold higher accumulations of viral products in systemically infected Chinese cabbage leaves, but does not affect viral replication in isolated protoplasts. These results suggest that the increased viral yield and symptom severity result from improved viral spread in the host plant. These effects were specific to Chinese cabbage, since neither viral yield nor symptoms in turnips were affected by the U+1888→C mutation.

Introduction

Turnip yellow mosaic virus (TYMV), the type member of the tymovirus group of monopartite positive- strand RNA viruses, was first described by Markham and Smith in 1946. Strains that differ in symptom severity, ranging in Chinese cabbage from mild mosaic involving pale green islands to brilliant white mottling, have been recognized (Matthews, 1980), but no investigations of the viral genetic element(s) responsible for symptom variations have been reported to date.

In the course of our studies with TYMV, we observed the spontaneous generation of a strain that produced more severe, almost uniformly chlorotic symptoms in the systemically infected leaves of Chinese cabbage plants. The severe symptoms accompanied increased yields of virus in infected tissue. Since the use of a virus strain that produced higher accumulations of viral products would improve the sensitivity of our studies on TYMV gene expression and replication, we determined the genetic alteration responsible for the severe chlorosis. We report that the severe symptoms result from a single nucleotide substitution in the 6.3 kb genome of TYMC, the Corvallis isolate of TYMV-type that was cloned from a turnip-adapted type strain of TYMV obtained from Strasbourg, France (Weiland and Dreher, 1989). The substitution alters one amino acid in the protein encoded by ORF-69, which is dispensable for RNA replication in single cells, but is required for virus spread in the plant (Bozarth *et al.*, 1992). The coding potential was not changed in the overlapping ORF-206, whose expression is essential for RNA replication.

Materials and Methods

Materials. Chinese cabbage (*Brassica pekinensis* cv. Spring A-1) and turnip (*Brassica rapa* cv. Just Right) plants were grown in a growth chamber under 16 hr day-length at 21°C. Plasmid pTYMC (Weiland and Dreher, 1989), a cDNA clone from which infectious TYMC (TYMV-Corvallis strain) genomic RNA can be transcribed with T7 RNA polymerase, was the original source of all viral RNAs used. Enzymes and reagents were from the sources described in Chapter IV of this thesis.

Virion RNA extraction and characterization. Virus was isolated from infected plants by polyethylene glycol precipitation according to Lane (1986) and quantitated spectrophotometrically. Virion RNA was prepared from virus by two phenol/chloroform extractions and one chloroform/isoamyl alcohol extraction, followed by ethanol precipitation. The concentration of RNA was determined spectrophotometrically, and its quality was assessed by agarose gel electrophoresis. Ribonuclease protection experiments were performed as described (Chapter IV in this thesis). Virion RNAs (2 μg) were probed with minus-strand RNAs representing TYMC sequences between the following restriction sites: *Hind*III$^{3'}$-*Eco*RI$^{5'}$ (full-length), *Hind*III$^{3'}$-*Bam*HI^{1755}, and *Hind*III$^{3'}$-*Sst*I^{3286}.

The partial sequences of virion RNAs were derived after reverse transcription and amplification by polymerase chain reaction (PCR). This involved PCR amplification using d(GCGGAGAGAAGACAATTCAAGGTG) as 3′ oligomer to prime opposite nucleotide 2431, in combination with d(CCTGAGGCAACATTGG) to prime at nucleotide 1255 or d(CCTTTTACTCCCACGACTTC) to prime at nucleotide 1836. Amplified fragments were either cloned into pUC18 or sequenced directly (Winship, 1989).

Cloning and transcription. Since our previous studies with TYMV have focused on the 3′-noncoding region, we have adopted the convention of numbering nucleotides from the 5′ beginning with G+1, and those in the 3′ noncoding region beginning at the 3′-terminus with A-1 (Chapter IV in this thesis).

The double mutant TYMC+A92-U57 was constructed by fusing the mutant sequences from two previously reported mutant clones, pTYMC-U57 (Chapter III in this thesis) and pTYMC+A92 (Chapter IV in this thesis). Fragments between the unique *Eco*RI$^{5'}$ and *Bam*HI^{1755} sites were exchanged. In preparation of the mutant pTYMC+C1888, double-stranded cDNA was synthesized by using the (-)-sense oligomer d(AAGGCGTCGGAAAACATGGCGGAAGAGC) to prime at nucleotide 3738 for first strand synthesis, and a 59-mer oligomer corresponding to a 5′ *Eco*RI site and the T7 promoter fused to nucleotides 1-35 of the TYMV genome for second strand synthesis. The double-stranded cDNA was digested with *Bam*HI^{1755} and *Sst*I^{3286} to generate a 1.5 kb fragment that was cloned into pUC18. A 0.6 kbp *Bam*HI^{1755}-*Kpn*I^{2366} cDNA fragment containing the C+1888 mutation was then subcloned into pTYMC to create pTYMC+C1888. The triple mutant TYMC+A92+C1888-U57 was

constructed by subcloning the 1.5 kb *Bam*HI[1755] to *Sst*I[3286] from pTYMC+C1888 into pTYMC+A92-U57.

Plasmid DNAs were prepared from 50 ml bacterial cultures, and the mutant sequences were confirmed by double-stranded DNA sequencing (Chen and Seeburg, 1985). Capped genomic transcripts labelled with [α-^{32}P]UTP (0.1 Ci/mmol) were prepared with T7 RNA polymerase from DNA templates linearized with *Hind*III, and were analyzed as described previously (Weiland and Dreher, 1989) prior to inoculation.

RNA inoculations and analysis of viral products. Protoplasts were prepared from Chinese cabbage plants and inoculated as previously described (Chapter IV in this thesis). Inoculated protoplasts were incubated under constant light at 25°C for 48 hr prior to harvest. Three-week-old Chinese cabbage plants with two true leaves were used for inoculations of whole plants (Chapter IV in this thesis).

The levels of coat protein in harvested protoplasts were analyzed in western blots using horseradish peroxidase-labelled secondary antibody and the chromogenic substrate 4-chloro-1-naphthol as described (Weiland and Dreher, 1989). RNA was extracted from protoplasts, glyoxalated, electrophoresed through 1% agarose and transferred to nylon membranes as described (Weiland and Dreher, 1989). The hybridization probe was a ^{32}P-labelled RNA transcript complementary to 0.9 kb at the 3′ end of TYMV RNA (*Pst*I-*Hind*III fragment, see Fig. AII-2A), permitting the detection of both genomic and subgenomic RNAs (Chapter III in this thesis). The results of western and northern blots were quantitated by scanning laser densitometry (Chapter III in this thesis).

Results

Characterization of a TYMV isolate that causes severe symptoms on Chinese cabbage plants. During a series of studies on TYMV replication in Chinese cabbage, one plant inoculated with TYMC RNA (i.e. RNA derived from pTYMC; referred to as wild-type) and another inoculated with TYMC+A1460 RNA (which has a wild-type phenotype; Chapter IV in this thesis) developed unusually severe symptoms on systemically infected leaves (Fig. AII-1). Infections in Chinese cabbage derived either from a cloned source (TYMC transcripts) or from our original TYMV-type stock (Strasbourg, France) consistently present vein clearing, followed by the development of a pale green/dark green mosaic on systemically infected leaves. By contrast, the two plants with severe symptoms displayed an almost uniform yellow-green chlorosis on systemically infected leaves, although dark green flecks appeared on later emerging leaves. There were no distinct differences compared with wild-type infections in the appearance of chlorotic lesions on the inoculated leaves, nor in the timing or appearance of the systemic symptoms. Virus from the plants with severe symptoms were passaged onto healthy plants, which developed the same severe symptoms, indicating that the novel symptoms resulted from an alteration of the viral genome, rather than host plant variability. The new isolates are referred to as TYMC(s) and TYMC+A1460(s), reflecting the original T7 transcript from which the severe symptoms arose.

To characterize the genetic alterations in the severe TYMC(s) and TYMC+A1460(s) isolates, we probed their genomes by ribonuclease (RNase) protection analysis. Three minus-sense probes derived from pTYMC (Fig. AII-2A) were hybridized to virion RNA of each isolate, and to TYMC as control, and the hybrids were treated with a mixture of RNases T1 and A. The full-length 6.3 kb-long *Hind*III$^{3'}$-*Eco*RI$^{5'}$ probe fully protected a portion of the TYMC RNA from RNase cleavage, but three bands were produced when probing the TYMC(s) genome (Fig. AII-2B). Two bands of 5 kb and 2 kb represented complementary fragments resulting from a single cleavage of the hybridized duplex RNA, while the 7 kb fully protected band indicated that RNase cleavage did not go to completion. This result suggests the presence of a mismatch between the TYMC and TYMC(s) sequences about 2 kb from one end of the genome.

The 3′, 3 kb-long *Hind*III$^{3'}$ -*Sst*I^{3286} probe protected both TYMC(s) and TYMC genomes fully (Fig. AII-2B), suggesting that the mutation in TYMC(s) was located 2 kb from the 5′ end of the genome. Probing with the 4.5 kb probe corresponding to sequences between *BamH*I^{1755} and the 3′ end (*Hind*III) verified this conclusion, and mapped the mutation more accurately to a position about 130 nucleotides downstream of the *BamH*I^{1755} site, i.e. about 1900 nucleotides from the 5′ end of the genome. This was indicated by a 130 bp fragment arising from RNase protection analysis of the TYMC(s), but not the TYMC, genome (Fig. AII-2C). No other differences between the digestion patterns of the TYMC(s) and TYMC genomes were observed.

RNase protection analysis of the TYMC+A1460(s) genome (not shown) indicated the presence of a similarly positioned mismatch, in addition to the expected mismatch at nucleotide +1460.

One nucleotide change in TYMC is responsible for causing severe symptoms in Chinese cabbage plants. To determine the nucleotide change(s) in the severe-symptom isolates, and to verify that the mutations indicated by the RNase protection assays were indeed responsible for the development of severe symptoms, we cloned the 1.2 kb cDNA fragment corresponding to nucleotides 1240 to 2440 of the TYMC(s) and TYMC+A1460(s) genomes. This was accomplished by PCR amplification in the case of TYMC+A1460(s) RNA, but with TYMC(s) RNA, amplification failed repeatedly, perhaps due to interference by nucleic acid secondary structure. Double-stranded cDNA corresponding to the 5′ half of TYMC(s) RNA was synthesized without amplification, and the *BamH*I[1755] to *Sst*I[3286] fragment was cloned into pUC18 (Material and Methods). The sequences between *BamH*I[1755] and *Kpn*I[2366] were determined for the clones derived from both TYMC(s) and TYMC+A1460(s). The only mutation found relative to TYMC was U+1888→C, and this same mutation was present in both TYMC(s) and TYMC+A1460(s).

Because RNase protection analysis overlooks some mismatches (Myers *et al.*, 1985), it was necessary to verify that the U+1888→C mutation alone was responsible for the severe symptom phenotype. The 0.6 kbp *BamH*I[1755] - *Kpn*I[2366] fragment derived from TYMC(s) was subcloned into pTYMC (see Materials and Methods), creating pTYMC+C1888. The entire subcloned fragment was resequenced to ensure the presence of only the desired mutation. Inoculation of Chinese cabbage plants with capped TYMC+C1888 transcripts yielded severe systemic symptoms identical to those of TYMC(s) developed on systemically infected leaves. Virion RNA extracted from the infected leaves was subjected to RNase protection analysis, revealing the same digestion pattern observed for TYMC(s) RNA (Fig. AII-2B,C). The partial sequence of the progeny RNA was also determined after reverse transcription and PCR amplification between nucleotides 1817 and 2324. The U+1888→C substitution was the only mutation found (not shown).

These experiments firmly establish that the severe symptoms observed in Chinese cabbage were due to the U+1888→C transition. This substitution alters the coding of ORF-69, resulting in a tyrosine to histidine substitution in the ORF-69 product, but does not alter the coding of ORF-206.

Severe symptoms are associated with more efficient viral movement in plants rather than enhanced replication in cells. We have previously shown that ORF-69 expression is dispensable for viral replication in isolated protoplasts (Bozarth *et al.*, 1992). It would thus be expected that the U+1888→C mutation, which affects only the coding of ORF-69, does not affect RNA replication in protoplasts. The replication of TYMC+C1888 was studied in Chinese cabbage protoplasts and in plants, and compared with that of other mutants, which from previous studies were shown (or were expected) to replicate more efficiently than TYMC. TYMC-U57 and TYMC+A92 have been studied previously (Chapters III and IV in this thesis) and the combined mutants TYMC+A92-U57 and

TYMC+A92+C1888-U57 were constructed by subcloning. The additional mutants were studied in order to screen for a variant that replicated to higher levels than TYMC, since such a variant would facilitate our further studies on the molecular biology of TYMV. Because virion RNAs have a higher specific infectivity than *in vitro* transcripts (Weiland and Dreher, 1989), virion RNAs were freshly prepared from plants systemically infected with TYMC and each of the above mutants.

Chinese cabbage protoplasts ($4x10^5$) were inoculated with each of the virion RNAs (3 μg) and were harvested after incubating for 48 hr at 25°C. The accumulations of coat protein, and of genomic and subgenomic RNAs were determined in western and northern blots, respectively (Fig. AII-3), and bands were quantified by laser scanning densitometry (Table AII-1). Two Chinese cabbage plants were inoculated with each virion RNA, and fully formed systemically infected leaves were harvested 3 weeks after inoculation. Virions were prepared from each plant. Protoplasts infected with mutants TYMC+C1888 and TYMC+A92+C1888-U57 accumulated viral products to levels 1.2 to 1.6 relative to TYMC (Fig. AII-3; Table AII-1). However, the accumulations of mutant virus in plants were 3- to 4-fold higher than for TYMC (Table AII-1). The accumulations of viral products in protoplasts infected with the other mutants (TYMC+A92, TYMC-U57 and TYMC+A92-U57) ranged between 1.0 and 2.0 relative to TYMC, and the yields in plants were 1.2 to 1.4 relative to TYMC (Table AII-1). Thus, the mutants carrying the C+1888 mutation were distinguished by an increased accumulation relative to TYMC in plants that was not matched by increased replication in protoplasts. For the other mutants, the slightly enhanced accumulations were similar in protoplasts and plants. These results support the conclusion that improved virus spread due to the mutation in the ORF-69 product underlies the enhanced yield and more severe symptoms associated with the U+1888→C mutation. The increased area of chlorosis clearly indicates that the mutant infections spread to a higher proportion of leaf cells. It is uncertain whether the increased severity of chlorosis (yellow green cf. pale green) is a consequence of diminished amounts of healthy tissue surrounding chlorotic areas, or a direct effect of some interaction between the mutant ORF-69 product and the host cell. The data of Table 1 indicate, however, that the intensified symptoms are unlikely to result from increased levels of virus within infected cells.

The infection of TYMC+C1888 was compared with TYMC in turnip plants (cv. Just Right). We had previously found that TYMC replicated faster in turnip than in Chinese cabbage protoplasts (Weiland and Dreher, unpublished). We found both the symptoms and yield resulting from infection of turnip plants with TYMC and TYMC+C1888 to be similar. The yields were comparable to those produced by TYMC+C1888 in Chinese cabbage, while the symptoms were intermediate in severity between those caused by the two virus strains in Chinese cabbage: vein clearing, and distinct yellow-green mosaic, but no uniform yellow-green chlorosis.

Figure AII-1. Symptomatology of TYMV isolates on Chinese cabbage. Equivalent non-inoculated leaves are shown from a mock-inoculated plant (left), and from systemically infected plants inoculated with TYMC (middle) and TYMC+C1888 (right).

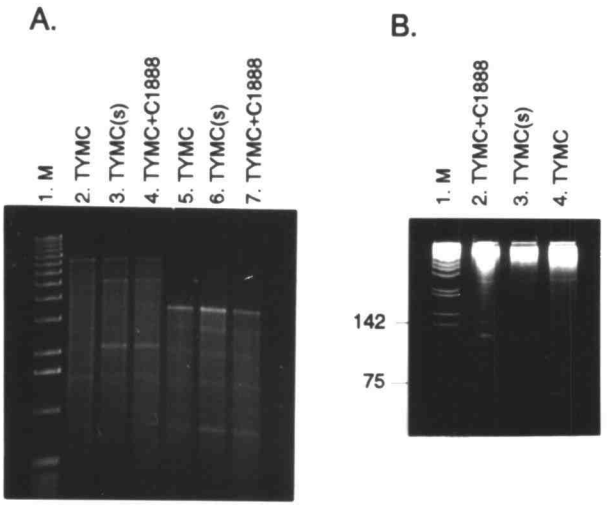

Figure AII-2. Localization of the mutation responsible for severe symptoms by RNase protection analysis. A. Diagram of the insert of pTYMC (Weiland and Dreher 1989), the genomic cDNA clone from which infectious transcripts can be generated with T7 RNA polymerase. The major open reading frames (ORFs) and relevant restriction sites are indicated. The sequences represented in the three minus-sense RNA probes used for RNase protection analysis are indicated by the open boxes: *Hind*III$^{3'}$-*Sst*I^{3286}; full-length, *Hind*III$^{3'}$-*Eco*RI$^{5'}$; *Hind*III$^{3'}$-*Bam*HI^{1755}. B. Examples of ribonuclease protection analysis. The virion RNAs indicated were hybridized to the full-length probe (lanes 2-4) or to the *Hind*III$^{3'}$-*Sst*I^{3286} probe (lanes 5-7) and subjected to RNase digestion. Note that TYMC(s) is RNA derived from the original plant that had developed severe symptoms, while TYMC+C1888 is reconstructed mutant RNA derived from the mutated cDNA. The digestion products were separated on a 1% agarose gel and visualized by staining with ethidium bromide. M, 1 kb ladder DNA markers (Gibco-BRL). C. Example of RNase protection analysis. The indicated virion RNAs were probed with the *Hind*III$^{3'}$-*Bam*HI^{1755} probe and the digestion products were separated by electrophoresis on a 5% polyacrylamide gel.

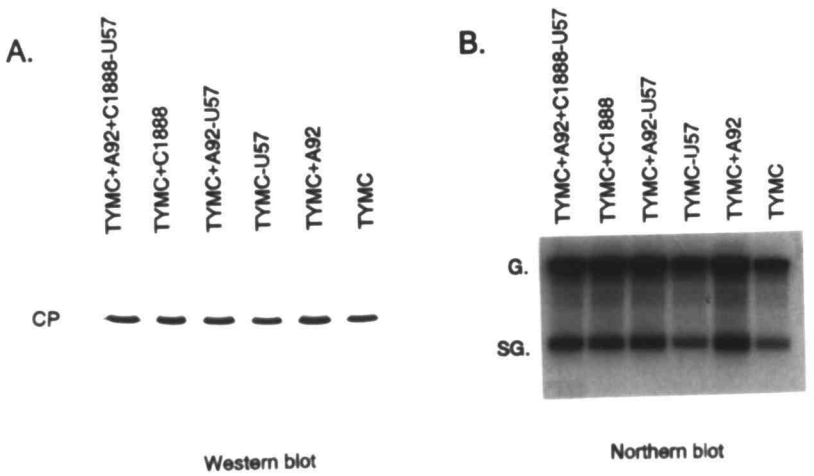

Figure AII-3. Replication of TYMC and derivatives in Chinese cabbage protoplasts. Representative experiments related to Table 1 are shown. Protoplasts ($4x10^5$) were inoculated with 3 μg of TYMC or mutant virion RNAs, as indicated, and harvested 48 hpi. A. Detection of coat protein in a western blot made after separation of proteins from $5x10^4$ protoplasts by 14% SDS-PAGE. The blot was probed with anti-TYMV antiserum, and developed using horseradish peroxidase-linked second antibody and 4-chloro-1-naphthol color reagent. B. Detection of viral genomic (G, 6.3 kb) and subgenomic (SG, 0.7 kb) RNAs in a northern blot. RNAs from $4x10^4$ protoplasts were separated on a 1% agarose gel, blotted and probed with a ^{32}P-labelled transcript complementary to 0.9 kb at the 3′ end of the genomic RNA. TYMC mutants are named with a "+" to denote a nucleotide substitution at a position numbered conventionally from the 5′ end, and a "-" to denote a substitution in the 3′ noncoding region, numbered from the 3′ end.

Table AII-1. Replication of TYMC mutants in Chinese cabbage				
Mutant	Protoplasts[a]			Plants[b]
	Relative coat protein	Relative genomic RNA	Relative subgenomic RNA	Relative virus yield
TYMC (wild type)	1.0	1.0	1.0	1.0
TYMC+A92	1.14	1.57	1.94	1.23
TYMC-U57	1.02	1.20	1.04	1.41
TYMC+A92-U57	1.24	1.60	1.95	1.19
TYMC+C1888	1.18	1.64	1.37	4.03
TYMC+A92+C1888-U57	1.20	1.26	1.40	3.32

a. Protoplasts were harvested 48 hpi and analyzed as shown in Fig. AII-3. The results were derived from 4 separate experiments and were quantified by laser densitometric scanning.

b. Virions were purified from at least 2 systemically infected leaves harvested 3 weeks after inoculation.

Discussion

Uniformly chlorotic phenotypes have been described for a several viruses. For cucumber mosaic virus infecting tobacco, the chlorotic phenotype has been associated with a single amino acid substitution in the coat protein (Shintaku *et al.*, 1992), while for cauliflower mosaic virus infecting turnip, chlorosis has been associated with uncharacterized sequences from gene VI (involved in the regulation of viral gene expression) and from an intergenic region (Stratford and Covey, 1989). Our studies with TYMV infecting Chinese cabbage have now shown that chlorotic symptoms can result from a mutation in the movement protein encoded by ORF-69. The development of chlorosis can thus be influenced by a variety of viral genetic elements, presumably reflecting a variety of interactions between a replicating virus and the host that affect chloroplast health. The genetic makeup of the host clearly also influences the development of chlorosis (also noted by Shintaku *et al.*, 1992), as demonstrated by the lack of differential symptoms between TYMC and TYMC+C1888 in turnips.

The severe symptoms induced by TYMC+C1888 in Chinese cabbage were found to correlate with a higher accumulation of virus in systemically infected leaves (Table AII-1). The L_{11} and $L_{11}A$ attenuated strains of TMV provide a similar example where both viral yield and symptom severity are decreased as a result of impaired cell-to-cell movement. The L_{11} and $L_{11}A$ strains produce mild symptoms and accumulate to yields about 10-20% those of the L strain. The altered phenotype is due to mutations in the essential nonstructural gene encoding p126/p183 (Nishiguchi *et al.*, 1985) that have no influence on the accumulation of genomic and coat protein subgenomic RNAs in isolated protoplasts, but do decrease the levels of subgenomic RNA encoding the p30 movement protein (Watanabe *et al.*, 1987). Symptom severity and virus accumulation in turnips infected with cauliflower mosaic virus were also found to be co-ordinately influenced by sequence variations in the movement protein (gene I), although gene VI sequences were additionally implicated (Anderson *et al.*, 1991).

The movement protein encoded by TYMC+C1888 has a tyrosine to histidine substitution relative to TYMC (Dreher and Bransom, 1992) at position 601 of the 628 amino acid-long protein. Interestingly, histidine is present at this position in the reported sequences of both the Paris (France) holding of TYMV-type (also originally obtained from Strasbourg, France, but apparently maintained in Chinese cabbage; Morch *et al.*, 1988) and an Australian isolate of TYMV (Keese *et al.*, 1989). Our studies indicate that our cloned TYMV isolate, TYMC, produces relatively mild symptoms in Chinese cabbage, and that TYMC+C1888 is more representative on this host of the TYMV strains described by Markham and Smith (1946; 1949) and Matthews (1980). However, TYMC and TYMC+C1888 are indistinguishable on turnip, perhaps reflecting the fact that TYMC was cloned from a turnip-adapted type strain of TYMV (Weiland and Dreher, 1989).

Symptom development in viral infections is clearly a complex process that is influenced by various viral elements (Daubert, 1988; Stratford and Covey, 1989). Our studies with TYMV

emphasize the importance of virus movement in symptom development, and point to the potential for controlling viral infections by impairing cell-to-cell movement.

References

Anderson, E. J., Qiu, S. G. and Schoelz, J. E. 1991. Genetic analysis of determinants of disease severity and virus concentration in cauliflower mosaic virus. Virology 181:647-655.

Bozarth, C. S., Weiland, J. J. and Dreher, T. W. 1992. Expression of ORF-69 of turnip yellow mosaic virus is necessary for viral spread in plants. Virology 187:124-130.

Chen, E. Y. and Seeburg, P. 1985. Supercoil sequencing: A fast and simple method for sequencing plasmid DNA. DNA 4:165-170.

Daubert, S. 1988. Sequence determinants of symptoms in the genomes of plant viruses, viroids, and satellites. Mol. Plant-Microbe. Interact. 1:317-325.

Dreher, T. W. and Bransom, K. L. 1992. Genomic RNA sequence of turnip yellow mosaic virus isolate TYMC, a cDNA-based clone with verified infectivity. Plant Mol. Biol. 18:403-406.

Keese, P., MacKenzie, A. and Gibbs, A. 1989. Nucleotide sequence of the genome of an Australian isolate of turnip yellow mosaic tymovirus. Virology 172:536-546.

Lane, L. 1986. Propagation and purification of RNA plant viruses. Meth. Enzymol. 118:87-696.

Markham, R. and Smith, K. M. 1946. A new crystalline plant virus. Nature 157:300

Markham, R. and Smith, K. M. 1949. Studies on the virus of turnip yellow mosaic. Parasitology 39:330-342.

Matthews, R. E. F. 1980. Turnip yellow mosaic virus. CMI/AAB Descriptions of Plant Viruses, No. 230.

Matthews, R. E. F. 1991. Plant Virology. 3rd edition, Academic Press, New York.

Morch, M.-D., Boyer, J.-C. and Haenni, A. L. 1988. Overlapping open reading frames revealed by complete nucleotide sequencing of turnip yellow mosaic virus genomic RNA. Nucleic Acids Res. 15:6157-6173.

Myers, R. M. Larin, Z., and Maniatis, T. 1985. Detection of single base substitutions by ribonuclease cleavage at mismatches in RNA:DNA duplexes. Science 230:1242-1246.

Nishiguchi, M., Kikuchi, S., Kiho, Y., Ohno, T., Meshi, T. and Okada, Y. Molecular basis of plant viral virulence: The complete nucleotide sequence of an attenuated strain of tobacco mosaic virus. Nucl. Acids Res. 13:5585-5590.

Shintaku, M. H., Zhang, L. and Palukaitis 1992. A single amino acid substitution in the coat protein of cucumber mosaic virus induces chlorosis in tobacco. The Plant Cell 4:751-757.

Stratford, R. and Covey, S. N. 1989. Segregation of cauliflower mosaic virus symptom genetic determinants. Virology 172:451-459.

Watanabe, Y., Morita, N., Nishiguchi, M. and Okada, Y. 1987. Attenuated strains of tobacco mosaic virus reduces synthesis of a viral protein with a cell-to-cell movement function. J. Mol. Biol. 194:699-704.

Weiland, J. J. and Dreher, T. W. 1989. Infectious TYMV RNA from cloned cDNA: effects *in vitro* and *in vivo* of point substitutions in the initiation codons of two extensively overlapping ORFs. Nucl. Acids Res. 17:4675-4687.

Winship, P. P. 1989. An improved method for directly sequencing PCR-amplified material using dimethyl sulfoxide. Nucl. Acids Res. 17:1266.